New developments in orthogonality catastrophe physics (Redacted version)

Conor George Jackson

A thesis submitted for the degree of PhD
at the
University of St Andrews

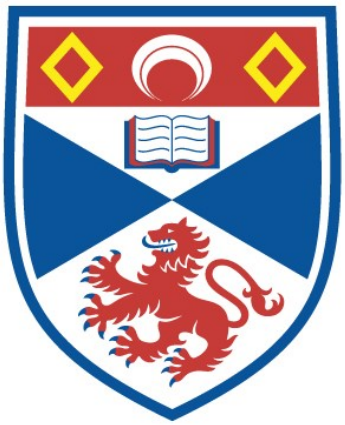

2023

Identifier to use to cite or link to this thesis:
DOI: https://doi.org/10.17630/sta/339

Abstract

The Fermi edge singularity, and related Anderson's orthogonality catastrophe, has been a touchstone of many body quantum physics for over 50 years. There are, however, a number of facets of this phenomenon that have, up until now, been left largely unexplored in the scientific literature. In this thesis we investigate two of these. Firstly we explore how the orthogonality catastrophe spatially spreads through a system, with particular considerations for the implications for quantum information processing implementations. We find that there is a propagating signal carrying the information about the Fermi edge singularity, but at long times the orthogonality catastrophe reasserts itself, posing a significant obstacle to the transmission of quantum information. We also found an "echo" formed by the interference of multiple Fermi edge singularities at different locations. Secondly we consider the effect of band structure on the Fermi edge singularity. Here we make significant progress in analytically understanding the effect of having a finite band bottom and of band curvature on the Fermi edge singularity. In the course of this we clarify some subtle points about the relationship between energy and time in non-relativistic quantum mechanics, which had been glossed over in the previous literature.

Candidate's declaration

I, Conor George Jackson, do hereby certify that this thesis, submitted for the degree of PhD, which is approximately 32,300 words in length, has been written by me, and that it is the record of work carried out by me, or principally by myself in collaboration with others as acknowledged, and that it has not been submitted in any previous application for any degree. I confirm that any appendices included in my thesis contain only material permitted by the 'Assessment of Postgraduate Research Students' policy.

I was admitted as a research student at the University of St Andrews in August 2016.

I received funding from an organisation or institution and have acknowledged the funder(s) in the full text of my thesis.

Date 17/05/22 Signature of candidate

Supervisor's declaration

I hereby certify that the candidate has fulfilled the conditions of the Resolution and Regulations appropriate for the degree of PhD in the University of St Andrews and that the candidate is qualified to submit this thesis in application for that degree. I confirm that any appendices included in the thesis contain only material permitted by the 'Assessment of Postgraduate Research Students' policy.

Date 17.5.2022 Signature of supervisor

Permission for publication

In submitting this thesis to the University of St Andrews we understand that we are giving permission for it to be made available for use in accordance with the regulations of the University Library for the time being in force, subject to any copyright vested in the work not being affected thereby. We also understand, unless exempt by an award of an embargo as requested below, that the title and the abstract will be published, and that a copy of the work may be made and supplied to any bona fide library or research worker, that this thesis will be electronically accessible for personal or research use and that the library has the right to migrate this thesis into new electronic forms as required to ensure continued access to the thesis.

I, Conor George Jackson, confirm that my thesis does not contain any third-party material that requires copyright clearance.

The following is an agreed request by candidate and supervisor regarding the publication of this thesis:

Printed copy

Embargo on part (Chapter 5 and the Conclusion) of print copy for a period of 2 years on the following ground(s):

- Publication would preclude future publication

Supporting statement for printed embargo request

Publication of these parts would preclude future publication

Electronic copy

Embargo on part (Chapter 5 and the Conclusion) of electronic copy for a period of 2 years on the following ground(s):

- Publication would preclude future publication

Supporting statement for electronic embargo request

Further publications are being prepared based on the content of these chapters

Title and Abstract

- I agree to the title and abstract being published.

Date 17/05/22 Signature of candidate

Date 17/5/2022 Signature of supervisor

Underpinning Research Data or Digital Outputs

Candidate's declaration

I, Conor George Jackson, hereby certify that no requirements to deposit original research data or digital outputs apply to this thesis and that, where appropriate, secondary data used have been referenced in the full text of my thesis.

Date 17/05/22 Signature of candidate

Contents

Chapter 1

Introduction

One of the major questions of modern condensed matter physics is the behaviour of many-body quantum systems far from thermodynamic equilibrium. Whilst the statistical physics of equilibrium systems has a well established theoretical framework, the non-equilibrium case is far less developed.

Non-equilibrium quantum systems arise in a wide range of contexts, from relatively mundane settings such as a system with an imposed temperature gradient or with a driving force applied, to the practically important cases of quantum devices, laser physics or implementations of quantum computers, right through to more exotic situations such as the very early universe.

In recent decades our understanding of many-body systems out of equilibrium has advanced on many fronts. Developments in statistical and quantum thermodynamics have given us new tools to study the statistical properties of these systems. There is growing interest in the possibility of new phases of matter such as many-body localised or time crystal phases that can exist without the constraints of equilibrium. The theory of open quantum systems developing rapidly, pushing beyond the Markovian approximation that inevitably pulls systems to thermalize and new techniques with cold atom gases are giving us tools to probe these systems experimentally in detail.

One important class of non-equilibrium phenomena is the response of a system to an abrupt change of the Hamiltonian, on time scales much shorter than any internal time scale of the system, known as a quench. Quenches are both of practical significance for device physics but also theoretical interest as the separation of timescales can offer significant simplifications. Furthermore the Kibble-Zurek [1, 2] mechanism suggests that quenches describe the universal physics of systems driven across a phase boundary. Furthering our understanding of quench physics, therefore, represents a significant challenge in modern condensed matter physics.

Possibly the paradigmatic example of a non-equilibrium, non-perturbative phenomenon in a many-body quantum system is the Fermi edge singularity (FES). It is a rare example of an exactly solvable [3] non-equilibrium effect in a many-body system and so has provided both a conceptual touchstone to understand

more complex many-body physics as well as a test bed for new theoretical tools.

The FES describes the fact that the frequency spectrum to introduce a local impurity into a metallic Fermi system generally approaches the threshold minimum energy for the process as a (normally non-integer) power law, leading to a singularity at the threshold. It is closely related to Anderson's orthogonality catastrophe (OC) [4]; at long times the overlap between the final state of the system and its initial state before the introduction of the impurity tends to zero, again with a non-integer power law. This vanishing of the overlap leads to a failure of conventional perturbation theory, hence the "catastrophe". These phenomena are the result of the creation of a large number of low energy excitation by the quench, known as Fermi sea shake up [5–8].

There are however a number of aspects of the FES that have received little to no attention in the scientific literature up to this point. In this thesis we will aim to address two of these. Firstly, in chapter 4, we will examine how the OC spreads out from the impurity in space. This is a natural, physical question to ask about the introduction of a local impurity by a quench, but it has only received very limited consideration in the literature [8–10]. There are also practical motivations to consider this question. There have been proposals for quantum computing implementations with gates implemented using metallic leads to mediate an effective interaction between qubits [11]. It is important for these implementations to understand the dynamics taking place in the leads. We therefore examine the possibility of the OC occurring in a toy model of such a lead and investigate what this means for the transmission of quantum information.

Secondly we will consider how band structure influences the FES, in chapter **??**. Much of the literature on the FES assumes an infinite linear band, which is a reasonable approximation for weak impurity potentials when the Fermi level is far from the band edge. For strong impurity potentials and in systems where the chemical potential is comparatively low, for example in cold atom gases, this approximation breaks down and we must take account of the band curvature and the fact that the band does not extend indefinitely. There has been notable interest in this area in the past 10 years, motivated by the possibility of studying the FES in cold atom experiments, but much of the work has been numerical [6]. We will aim, by contrast, to develop an analytical treatment of the FES in a non-trivial band structure and make significant progress in this direction. By generalising a method known as the Riemann-Hilbert approach to account for the more complex band structure we were able obtain an explicit integral representation of the decaying OC overlap in a finite band with a variable density of states, although the evaluation of this integral remains open. This expression, however, already provides physical insight into the interplay of the physics of the FES with a complex band structure.

During our investigation into the FES in a finite band we clarified some subtleties about the role of time in non-relativistic quantum mechanics, which had been glossed over in the previous literature, but which proved to be crucial in the current case.

By pushing the study of the FES in new directions, we may further its use

as springboard to study more complex phenomena and as a test bed for new tools for the study of many-body physics. For example we have developed the extensions to the Riemann-Hilbert approach discussed above and, in chapter 4, we will consider the FES as mediating a time delayed interaction, which gives a new perspective for considering the temporal structure of effective interactions mediated by a Fermi sea, such as the RKKY interaction.

The thesis is structured as follows: In chapter 2 we review the existing literature on the FES. In chapter 3we review the key theoretical tools that were used in carrying out our research. In chapter 4 we will explore the spatial aspects of the FES. In chapter **??** we will investigate the effect of band structure on the FES. We will briefly summarise our findings in chapter **??**. Throughout the thesis we will work in units such that $\hbar = 1$.

Chapter 2

Background and Literature Review

2.1 Setting up the catastrophe

In the past 60 years the Fermi edge singularity (FES) has been studied with a wide range of approaches and has built up an extensive literature. As a rare example of an exactly solvable quantum many body phenomenon it has provided a key conceptual touchstone for understanding more complex systems as well as providing a benchmark for theoretical and numerical techniques. Here we will review some of the key ideas in the existing literature on the FES and orthogonality catastrophe (OC).

Historically the FES and orthogonality catastrophe were first considered in the context of X-ray absorption and emission in metals [4, 12, 13], but the phenomenon was quickly seen to be more general and the FES has been observed in wide range of systems including quantum dot tunnelling current [14–21] and, more recently, in ultracold gases of fermionic atoms [6, 22, 23].

For the essential setup of the FES we will consider a metallic system, described by fermionic creation operators $c^\dagger_{\mathbf{k}}$ coupled to a localised impurity with two states $|+\rangle$ and $|-\rangle$. The Hamiltonian for this system is given as

$$H = \sum_{\mathbf{k}} \varepsilon_{\mathbf{k}} c^\dagger_{\mathbf{k}} c_{\mathbf{k}} + E_0 |+\rangle\langle+| + \sum_{\mathbf{k}\mathbf{k}'} V_{\mathbf{k}\mathbf{k}'}\, c^\dagger_{\mathbf{k}} c_{\mathbf{k}'} |+\rangle\langle+| \,. \tag{2.1}$$

The continuum states are coupled to the impurity state via the potential $V_{\mathbf{k}\mathbf{k}'}$. This potential is "turned on" only when the impurity is in the $|+\rangle$ state.

We consider what happens to the system when the state of the impurity is rapidly changed. How this is done will depend on the physical setup, for example in the original X-ray absorption scenario the absorption of a photon excites a core electron leading a positive hole, creating the impurity potential. This can be represented by a perturbation of the form

$$H_{\text{pert}} = W e^{-\imath\omega t} \psi^\dagger(0) d \,+\, \text{h.c.} \tag{2.2}$$

where $d = |+\rangle\langle -|$ and the $\psi^\dagger$ represents the addition of the excited electron to the Fermi sea. In other cases, such as in cold atom setups where the impurity is introduced by tuning the system to a Feshbach resonance [6], this additional particle may be absent.

The FES problem has two key simplifying features:

1. The Hamiltonian in eq. (2.1) has a block diagonal structure, with blocks defined by the state of the impurity. This means that the impurity dynamics are trivial and the problem effectively reduces from a many-body problem of a large number of fermions interacting with an impurity to a single particle problem with an external potential.

2. It turns out that the long time dynamics after changing the impurity state (that is the decay in the overlap with the initial state that characterises the OC) are entirely controlled by the behaviour of the system close to the Fermi surface. This means, in particular that the exact form of the potential away from the Fermi level does not matter and it can be approximated by a constant potential in momentum space, that is a Dirac delta function in real space.

These two properties are at the heart of the FES physics and will be explored more fully below.

In order to calculate observables of interest the quantities most often considered in the literature [3, 6, 24] are the Green's function for the impurity state, $G_{\rm imp}(t)$, and the time dependent correlation function for the perturbing Hamiltonian, F(t).

$$G_{\rm imp}(t) = \langle T\, d^\dagger(t) d(0)\rangle \tag{2.3}$$

$$F(t) = \langle T\, H_{\rm pert}(t) H_{\rm pert}(0)\rangle \tag{2.4}$$

where the operators are taken in the Heisenberg picture, time evolved under the Hamiltonian in eq.(2.1), and T is the time ordering operator. With these quantities many measurable quantities of interest can be calculated, such as emission and absorption rates in X-ray spectra, quantum dot tunnelling currents and transition rates in cold atom gases.

As an exactly solvable problem the FES has been used as a benchmark for a wide range of theoretical techniques, including most of the traditional workhorses of condensed matter physics. The earliest works on the FES typically employed diagrammatic perturbation theory and the linked cluster theorem, resumming the series to all orders to obtain the result [3, 12, 25, 26]. Taking inspiration from these diagramatic approaches Nozières and De Dominicis were able to exactly solve the problem by solving the associated Dyson equation, obtaining the key results that, in the long time limit

$$G_{\rm imp} \sim \theta(t) t^{-2\sum_l (2l+1)\frac{\delta_l^2}{\pi^2}}\ , \tag{2.5}$$

$$F(t) \sim \theta(t) \sum_{l,m} |W_{lm}|^2 t^{-1+2\frac{\delta_l}{\pi}-2\sum_{l'}(2l'+1)\frac{\delta_{l'}^2}{\pi^2}}\ , \tag{2.6}$$

where δ is the scattering phase shift of the impurity potential at the Fermi level, and W_{lm} are the matrix coupling constants in H_{pert} in the angular momentum basis. From these we can find the frequency space Green's function $G_{\text{imp}}(\omega)$ and the transition rate, $\Gamma(\omega)$ by taking Fourier transforms of $G_{\text{imp}}(t)$ and $F(t)$ respectively

$$G_{\text{imp}}(\omega) \sim (\omega - E_0)^{-1+2\sum_l (2l+1)\frac{\delta_l^2}{\pi^2}} , \tag{2.7}$$

$$\Gamma(\omega) \sim \sum_{l,m} |W_{lm}|^2 (\omega - E_0)^{-2\frac{\delta_l}{\pi}+2\sum_{l'}(2l'+1)\frac{\delta_{l'}^2}{\pi^2}} . \tag{2.8}$$

Note that the asymptotic relations in eq. (2.5) and eq. (2.6) are taken in the long time limit, relative to inverse of the smallest energy scale in the band structure, whilst in eq. (2.7) and eq. (2.8) they are taken in the corresponding small $\omega - E_0$ limit.

Subsequently many other central methods on many-body physics have been applied to the FES such as directly solving equations of motion for G_{imp} and F [27, 28], conformal field theory methods [29] or renormalisation group approaches [30].

With a finite temperature initial state these long time limits are ultimately cut off by an exponential decay on a time scale of $\frac{1}{k_B T}$, as thermal fluctuations scramble excitations.

2.2 Experimental setups

The FES has been studied in a wide variety of experimental contexts. The first considerations of the problem dealt with the absorption and emission X-rays by deep core orbitals. The predicted frequency spectra were observed in a range of metals over the subsequent decades [13, 31–37].

The absorption problem, where an impurity is suddenly introduced, and the emission problem, where an impurity is removed, are straightforwardly related to each other. As the system is assumed to have been able to relax before the start of the experiment the impurity potential can be assumed to have been screened by the Fermi sea in the emission case. Removing the impurity then can be thought of as introducing an impurity with a potential $-V$ [3]. To transform between the emission and absorption problems we, therefore, simply make the substitution $V \to -V$ and shift the ground state energy by the screening energy, ΔE, given by Fumi's theorem [38]

$$\Delta E = -\sum_l \int_0^{E_F} \mathrm{d}E \, \frac{\delta_l(E)}{\pi} \tag{2.9}$$

where E_F is the scattering phase shift.

Later experiments considered optical frequency absorption and emission edges in semiconductor systems and heterostructures, which allowed greater

flexibility in types of system considered, allowing experiments on the FES in low dimensional systems such as quantum wires to be studied [39–41]. In particular it allowed the FES to be studied in the context of one dimensional Luttinger liquids, discussed in section 2.4.2 [42, 43].

The realisation that FES physics could be observed in tunnelling onto quantum dots allowed for experiments with greater control of the experimental design as parameters such as the excitation energy and the tunnelling coupling could be tuned by engineering the structure of the dot. Here the key measured quantity was the tunnelling current. An electron tunnelling into or out of the dot changed the field around it due to the Coulomb interaction, creating the impurity [14–21, 44, 45].

More recently the prospect of studying the FES in gases of ultracold atoms has been the focus of growing attention. These systems allow an exquisite level of control over the parameters in the Hamiltonian but also raise new challenges not encountered in solid state implementations. These systems typically have a much lower density and so the impurity potential may be significant compared to the Fermi energy, or at least with an energy scale over which the band shows significant non-linearity, this means more attention must be paid to the effect of band structure than had been previously. Cold atom experiments also inevitably lose particles over time through a variety of processes. This means they are inherently non-equilibrium setups (although the approximation of equilibrium may be adequate, depending on the length of the experiment). This raises questions about the nature of the FES in systems initially out of equilibrium, which have attracted an increasing level of attention from theorists. The smaller energy scales in ultracold atoms also lead to longer timescales, opening the possibility of directly observing the OC in the time domain [6, 22, 23].

2.3 Reduction to the single particle problem

The fact that the Hamiltonian in eq. (2.1) is block diagonal in the impurity degree of freedom leads to an essential simplification of the problem. As the block diagonal Hamiltonian cannot cause transitions in the impurity, the potential term can be treated as a fixed external field during evolution under H. The potential only changes when a perturbation causes transitions in the impurity state. This can be viewed as giving the potential seen by the fermions a time dependence, turning it on or off.

Treating the impurity potential as a time dependent external potential in this way reduces the problem to an effective single particle model, which is responsible, to a significant extent, for the solvability of the FES problem [3]. Many-body effects only enter into the calculation through Fermi statistics.

When the system is reduced the system in this manner we arrive at a single particle version of the Hamiltonian eq. (2.1)

$$h = \sum_{\mathbf{k}} \varepsilon_{\mathbf{k}} c^\dagger_{\mathbf{k}} c_{\mathbf{k}} + \sum_{\mathbf{k}\mathbf{k}'} V_{\mathbf{k}\mathbf{k}'}(t) c^\dagger_{\mathbf{k}} c_{\mathbf{k}'} \tag{2.10}$$

$$= h_0 + V(t) \tag{2.11}$$

up to a time dependent c-number term which can, for the moment, be ignored.

The quantities of interest $G_{\text{imp}}(t)$ and $F(t)$ can similarly be written in terms of the single particle representation. The impurity Green's function, in particular, can be written as [3, 24]

$$G_{\text{imp}}(t) = \theta(t) e^{-\imath E_0 t} \left\langle e^{\imath h_0 t} e^{-\imath (h_0 + V) t} \right\rangle \ . \tag{2.12}$$

That is G_{imp} is given by the overlap of the state of system time evolved in the impurity present and the state of the system time evolved with the impurity absent. This quantity is known as the Loschmidt amplitude and its square modulus, $|\left\langle e^{\imath h_0 t} e^{-\imath (h_0 + V) t} \right\rangle|^2$, is known as the Loschmidt echo [46].

2.3.1 Quench physics

The single particle formulation of the problem makes the central role of quench physics in the FES explicit. Applying standard perturbative methods to H_{pert} allows us to consider transitions of the impurity as happening at discrete times, which translates in the single particle picture to the impurity potential turning on and off instantaneously, quenching the system. We then observe the non-equilibrium response of the Fermi sea to the quench.

2.3.2 The form of the impurity

The requirements that the Hamiltonian be block diagonal in the state of the impurity and that the potential be local pose severe limitations for the possibilities for physical realisations of the impurity. Indeed the only practical possibilities are impurities with a small number of possible states, often only the two considered here. For this reason the FES is often described as dealing with a *structureless* impurity in the literature [3, 47].

If this requirement for a structureless impurity is relaxed, that is the Hamiltonian is no longer required to be fully block diagonal in the impurity degree of freedom, then the full complexity of a typical many-body system rapidly returns. One physically natural case is to replace the fixed impurity with a finite mass impurity. Here it is found that the FES [48] and the orthogonality catastrophe [49] are cut off by the mass of the impurity. This can be attributed to the effect of recoil energy. When particles in the Fermi sea scatter off a finite mass impurity, they transfer some of their energy to the impurity, reducing the energy available to create particle-hole excitations and suppressing the Fermi sea shake up [22]. This reduced Fermi sea shake up around the mobile impurity results in the formation of a quasiparticle known as a Fermi polaron.

Another natural way to break the block diagonal structure of the Hamiltonian is to allow interactions with the Fermi sea to change the state of the impurity, for example a spinful impurity which can exchange angular momentum with the surrounding metal. This is the Kondo model, which has its own extensive literature, which we will not discuss in detail here [50–57].

The connection between the Kondo model and FES was explored thoroughly by Anderson Yuval and Hamann [52, 54, 58, 59]. They expressed the evolution of the Kondo system as an infinite series of FES like events. This approach amounts to explicitly evaluating the path integral by summing over all possible sequences of flips of the Kondo spin. The propagation between these flips is governed by the solvable FES propagator. Whilst this approach to the Kondo problem is cumbersome compared to more modern methods, it provides important conceptual insights and allows developments in FES physics to be carried over immediately into the more complex many-body physics of the Kondo problem.

2.3.3 The return of many-body physics: Fermi statistics and functional determinants

Whilst the FES problem can in many respects be reduced to single particle physics, there is one important aspect of many-body physics that still plays an important role and that is Fermi statistics.

Reconstructing the behaviour of many-fermion systems in terms of single particle behaviour is often considered in terms of evaluating Slater determinants and quite generally, since the determinant can be characterised up to a constant by being linear and totally antisymmetric in the rows of the input matrix, it is almost inevitable that a wide range of problems in the physics of fermionic quantum systems can be cast in terms of evaluating some form of determinant. There are, therefore, a wide range of techniques for modelling many-fermion systems based around functional determinants, which have been applied to studying the FES.

Direct Slater determinant methods have been applied to the FES. Indeed Anderson's original OC paper took this approach [4]. Slater determinant methods were further developed by Combescot and Nozières [47] to reproduce the Nozières De Dominicis result and by Ohtaka and Tanabe to obtain the prefactors to the characteristic FES power laws [60]. The Slater determinant based approach is, however cumbersome to work with and difficult to extend.

A more flexible and direct approach to express observables in terms of functional determinants in non-interacting fermion problems is offered via the Klich formula [61]

$$\left\langle e^{A} e^{B} \dots e^{C} \right\rangle = \det \left[1 - n + n e^{a} e^{b} \dots e^{c} \right] \tag{2.13}$$

where n is the fermion occupation number operator, A, B, C, etc. are single particle operators (i.e. quadratic in the fermionic operators) in the many particle Fock space and a, b, c, etc. are the corresponding operators on the single particle space. Correspondingly the expectation and determinant are taken over the Fock and single particle Hilbert spaces respectively.

The Klich formula makes the dependence on the fermion occupation in the many-body state explicit without placing any constraint upon it. This makes it a good starting point for methods that aim to study finite temperature or non-equilibrium physics, a number of examples of which will be discussed below.

Another key tool in these methods has been the Szegö theorem and the Fisher-Hartwig conjecture [62], allowing the asymptotic behaviour of the determinants of large Toeplitz matrices to be determined. If we focus on the slow, long, but finite, time dynamics the key physics will happen at the Fermi surface, far from the band edge. In this case the frequency space representation of the problem can be safely be folded around and treated as being periodic, with a large period given by the band width, as nothing happens at the band top and bottom where the system is "glued together" to form a circle. (Formally this is achieved through the use of exponential regulators to remove any contribution from the band edges.) This puts the desired determinant into Toeplitz form and so allows the above theorems to be used to extract the long time behaviour [63, 64].

Functional determinants can also be evaluated numerically. This allows the examination of systems that are too complex for analytical treatment, for example those with a non-trivial band structure, as well as offering a method to investigate the short time dynamics before the universal FES physics has set in [6, 22].

2.4 Low Energy Excitations and Fermi Surface Physics

The physics of the FES is dominated by the behaviour close to the Fermi surface [3]. This second key simplifying feature of the problem means that the details of the band structure and the exact form of the impurity potential, provided it is sufficiently local, play little role. This insensitivity to the details of the system results in the universal physics at long times and, correspondingly, frequencies close to the excitation edge.

As the potential in eq. (2.1) is assumed to be local it couples modes with widely separated momenta, and so when the impurity is introduced it creates particle-hole excitations with a wide range of energies. The high energy excitations rapidly dephase and so do not contribute to the coherent response of the system except at very short times. As the system is metallic, however, there exist modes with energies arbitrarily close to the Fermi surface. Particle-hole excitations in these modes can have an arbitrarily low energy and so can take an arbitrarily long time to dephase. This is the Fermi sea shake up mentioned above.

This slow dephasing of the low energy modes gives rise to slow dynamics at long times in the form of power laws. The Fourier transform of this power law at long times leads to a corresponding power law in the frequency spectrum close to threshold [3, 12, 65]. In particular as modes dephase the overlap of the final state with the initial state of the system, that is the Loschmidt amplitude of eq. (2.12) decays with a non-integer power law.

Since it is only the low energy modes arbitrarily close to the Fermi surface that control the long time behaviour of the system, it is only the properties

of the system at the Fermi surface that are important, resulting in universal physics. In particular the details of the band structure of the material are largely unimportant, with only the density of states at the Fermi level contributing to the universal physics. Similarly, the structure of the impurity away from the Fermi level has little impact. Since the impurity is local in real space and so should be broad and slowly varying in momentum space, it should not have any dramatic features at the Fermi energy and so the universal physics is given by a constant potential in momentum space, with its value given by the strength of the potential at the Fermi surface. This corresponds to a δ-potential in real space.

2.4.1 The Loschmidt Echo

The term Loschmidt echo was first coined in the field of quantum chaos [46]. The idea was to compare two states evolving under slightly perturbed variants of a classically chaotic Hamiltonian [66]. The decay of the overlap could be related to the Lyapunov exponent of the classical system [46], which can been seen as a quantum manifestation of the classical butterfly effect. The name is in reference to Loschmidt's paradox [67]: How can reversible microscopic dynamics give rise to irreversible thermodynamics? The Loschmidt echo can been seen as measuring a type of reversibility in the dynamics, forward time evolving with one Hamiltonian and backward time evolving with a modified one.

As with many simple quantities, the Loschmidt echo arises in a wide variety of contexts in physics. In quantum information it can be seen as the fidelity between the initial and final states, in the special case that both these states are pure [68]. It gives the probability that a measurement of the final state energy with respect to the initial Hamiltonian will find it in the ground state. In quantum thermodynamics the Loschmidt echo between the initial and final Hamiltonians of a process gives the characteristic function of the work distribution [69]. For example, if we consider our impurity quench in the FES as a thermodynamic process, we find that the work distribution is proportional to the energy space Green's function $G_{\text{imp}}(\omega)$ in eq. (2.7).

For our purposes the most useful way to view the Loschmidt echo is as a measure of the coherence in a many-body system [70]. Its slow algebraic decay at long times in the FES is indicative that there are degrees of freedom, specifically the low energy modes, that are dephasing arbitrarily slowly. This is in contrast to its typical exponential decay in an ergodic system noted above.

2.4.2 Bosonization

The key role of these low energy excitations in the FES is possibly best illustrated by treatments based around bosonization techniques. Bosonization maps a 1D fermionic model onto a bosonic one, with the bosonic excitations representing charge density waves in the Fermionic model. The mathematical details of bosonization will be discussed in section 3.1. Remarkably for fermionic models with a linear dispersion, which includes the low energy regime of a broad class of

metallic systems, bosonization allows the Hamiltonian to be diagonalised even in the presence of interactions, resulting in what is known as the Luttinger Liquid model [24, 71, 72].

In the bosonized model the Fermi sea shake up can be seen directly and the key role of the low energy modes can be explicitly tracked [65, 73]. The FES has proved a particularly useful model to test and develop new methods in Luttinger Liquid physics.

Whilst the Luttinger liquid model can easily accommodate fermion-fermion interactions, a fixed impurity with the capacity to backscatter particles from one Fermi point to the other turns out to be more complex, resulting in transcendental functions of the boson fields [24]. Due to the 1D nature of the system such and impurity, or 'weak link', can profoundly influence the physics, with an arbitrarily weak backscatterer blocking transmission in the presence of repulsive interactions [74, 75]. Using a range of innovative techniques it is found that if such an impurity is suddenly introduced into a Luttinger liquid the backscattering term contributes a factor of $t^{-1/8}$ to the decay of $G_{\mathrm{imp}}(t)$ [76–78].

Extensions of bosonization techniques has allowed the FES to be studied in new contexts. In recent decades there has been great strides in applying bosonization techniques to non-equilibrium situations [63, 64]. The bosonization procedure is, in principle, an exact mapping of Hilbert spaces, so, with many aspects of the bosonization procedure, there are no approximations that might depend on the equilibrium case. The construction of the Hilbert space, formulating the Hamiltonian and finding expressions for the operators of interest are unchanged by departing from equilibrium. The complication does enter in at two points:

1. Non-linearities in the fermion dispersion relation manifest as interactions in the bosonic representation. In equilibrium at low energies we can linearise the dispersion around the Fermi level. Out of equilibrium this may not be possible.

2. Ultimately, in order to calculate observables we must represent the non-equilibrium state of the fermionic system in terms of the bosonic degrees of freedom.

The second point has been addressed by Gutman, Gefen and Mirlin [63, 64] in a path integral formulation. They find that the generating function for the non-equilibrium Luttinger Liquid can be expressed in terms of a functional determinant, of the same form as those discussed in section 2.3.3. This can be evaluated by the methods discussed above and allows an arbitrary fermion distribution to be inserted. They retain, however, the ability to incorporate fermion interactions, one of the key advantages of the bosonization approach.

Applying this formalism to the FES, Gutman *et al.* , find that, for the example non-equilibrium fermion distribution of a 'double step' distribution,

$$n(E) = a\theta((1-a)eV - E) + (1-a)\theta(-aeV - E) \tag{2.14}$$

the overlap is suppressed in the time domain by an exponential with a decay length

$$\tau_{\text{split}} = \frac{eV}{2\pi} \ln\left(1 - 4a(1-a)\sin^2\delta\right) \ . \tag{2.15}$$

This can be interpreted as being due to the rapid dephasing of excitations at the two, finitely separated, Fermi surfaces, exponentially fast in the separation of the discontinuities. In the energy domain this results in a smearing out of the FES.

There has also been progress in moving beyond the linear dispersion of the Luttinger liquid. On this front the physics of the FES has proved an essential inspiration. In a 1D metal with non-zero band curvature, in order to excite a fermion from below the Fermi level to above it energy and momentum conservation require the creation of a large number of particle hole pairs, in addition to the originally excited fermion. This creates a Fermi sea shake up similar to the FES and so results in power laws in the spectral function, reminiscent of eq. (2.7). [79–81]

2.4.3 Singular integral equations

A different perspective on the key role played by the Fermi surface in the FES can be seen by mapping the problem fully into the time domain. Given the representation in terms of a time dependent potential discussed above it is natural to consider the problem this way. This leads us to consider the Fourier transform of the particle distribution function, which for the zero temperature Fermi function is a Cauchy kernel [82]. The sharp discontinuity in the energy representation leads to singular behaviour in the time domain. This singular behaviour profoundly influences the mathematical character of of the problem, in particular allowing powerful techniques from the theory of singular integral equations to be brought to bare [83].

The exact solutions Nozières and De Dominicis' a key step in resumming the diagramtic series is forming the Dyson equations for the Green's functions, which have the form of singular integral equations and can be solved [3].

One notable singular integral equation based method is the known as the Riemann-Hilbert approach (RHA). This approach allows the calculating of observables in time dependent impurity problems in many-fermion problems [5, 82]. This method uses the Klich formula eq. (2.13) to express the observable of interest as a functional determinant. This can then be converted into the problem of finding the inverse of the argument of the determinant via trace-determinant formula

$$\ln\left[\det A\right] = \operatorname{tr}\left[\ln A\right], \tag{2.16}$$

and the fact that the logarithm of a bounded operator can be expressed in terms of the integral of its inverse. The problem of finding the inverse of an operator M can be viewed as an integral equation

$$\int \mathrm{d}t\, M(t_1, t) M^{-1}(t, t_2) = \delta(t_1 - t_2) \ . \tag{2.17}$$

The RHA solves this equation by mapping it onto an auxiliary Riemann-Hilbert boundary value problem, exploiting the singular nature of $M = 1 - n + nR$, where n is the particle number operator, in the time basis. This problem involves finding a complex analytic function, $Y(z)$, with a discontinuity on the real axis given by $Y_+ Y_-^{-1} = R$. From this Y the inverse M^{-1} can be found. In the Abelian case, that is R commutes with itself at all times, the general solution for $Y(z)$ is known [83].

We will give a more rigorous treatment of the RHA in section 3.2. In Chapter **??** we will extend the RHA to the case where the bandwidth is not infinite and the density of states is not constant. Using this we will consider the effect of band structure, and in particular the effect of a finite band width of the FES.

It is possible to extend the RHA to finite temperatures [84] by considering a Riemann-Hilbert problem on a finite width strip of width $\frac{1}{k_B T}$ in the imaginary time direction. The Klich formula makes introducing finite temperature fermion distributions straightforward. Despite the fact that the fermion distribution is continuous the underlying integral equations are still singular. This is because in an infinite band we can always consider energies $|E - E_F| \gg k_B T$ much greater or much less than the Fermi energy, relative to T. At these energies the particle distribution will look like a zero temperature Fermi function. Correspondingly in the time representation, at short times the Fourier transform of the Fermi function resembles a Cauchy kernel, that is it has a simple pole. Non-equilibrium situations, considering a tunnelling junction with a different chemical potential each side have also been considered [85].

It is also possible to formulate the FES in terms of singular integral equations in the energy representation [28]. Here the singular behaviour is the result of the quench physics. The discontinuity in the potential, as a function of time, when the quench occurs results in singularities in its Fourier transformed energy representation. This again allows the use of tools based on singular integral equations.

It may be surprising that the same structures arise in both the time and frequency domains, rather than Fourier transformed versions of each other. It is important to bear in mind that in non-relativistic quantum mechanics energy and time are treated on a fundamentally different footing. Energy is a true observable. It is obtained as eigenvalues of the Hamiltonian and can be used to label the corresponding basis of eigenstates, whereas time is a parameter in the time dependent Shrödginger equation that labels the evolution of a state. Eigenstates of the Hamiltonian evolve as $|E\rangle \to e^{-\imath Et}|E\rangle$, and so the evolution of a general state has the form

$$|\psi(t)\rangle = \sum_i a_i e^{-\imath E_i t}|E_i\rangle, \tag{2.18}$$

which resembles a Fourier transform. The energy spectrum of a physical system is necessarily bounded from below (although we may approximate it by an unbounded spectrum, as we do in the case of a linear dispersion). This implies that there can be no group of energy translation operators, which act for all

energy states $|E\rangle$ as

$$U(\Delta E)|E\rangle = |E + \Delta E\rangle \tag{2.19}$$

as applying this to the ground state with a negative value of ΔE, would result in a state with an energy below the ground state, a contradiction. There can, in turn, be no operator $\hat{t}$ such that

$$U(\Delta E) = e^{-\imath \Delta E \hat{t}} \tag{2.20}$$

that is, there is no time operator in quantum mechanics. This result is known as Pauli's Theorem [86].

Furthermore, the evolution in eq. (2.18) assumes that the Hamiltonian is time independent. If the Hamiltonian is time dependent, however, this no longer holds. In the case of quench, for example, there is, in general, no reason for any particular relationship to exist between the pre and post quench energy spectra, and so the only way to write relate the instantaneous energy and the time evolution is to fully keep track when particular a Hamiltonian was applied via time-ordering.

In problems where we have to deal with bounded spectra, time dependent Hamiltonians or both, such as in the case of the FES, it is important to distinguish between physical time and the 'time' obtained by Fourier transforming the energy spectrum of an instantaneous Hamiltonian, which we will refer to as a *formal time*. Similarly we must distinguish between physical energy and the *formal energy* obtained from Fourier transforming a physical time. This distinction will be particularly significant in Chapter **??**.

It is also possible to formulate a RHA based on a real time/formal energy formulation [87]. This has been used to examine the non-equilibrium double step particle distributions that were later examined with non-equilibrium bosonization in [63, 64] which confirmed the results obtained via the RHA.

2.4.4 Dependence on particle number: deep and shallow Fermi seas

The significance of the Fermi surface raises questions about the dependence of the FES on particle number. Anderson's original paper on the orthogonality catastrophe [4] calculated the overlap in the long time, large particle number (N) limit, finding that it decayed as a power law in particle number, with the long time overlap only vanishing in the thermodynamic limit. This result was then confirmed and refined in later work that built on the full solution by Nozières and De Dominicis [26, 88].

More recently attempts have been made to understand the small N case, where the impurity potential is comparable to Fermi energy. This has been motivated by the desire to investigate the FES in the exquisitely controllable setting of cold atom gases, where the Fermi level is often far lower than in traditional solid state contexts. Much of this work has relied on numerical methods. Functional determinant methods have been used to calculate the FES decay in both the time and frequency domains, finding that the power law behaviour is

augmented by oscillations at the Fermi frequency [6]. These are attributed to exciting particles from the band bottom [6, 22]. These phenomena have been modelled analytically via a variational approach [89]. We will investigate this case using an extension of the RHA in Section **??**.

Bosonization techniques have been extended to take account of the band curvature and investigate the effect of the band bottom on the FES, by using a formal time basis. Within the linear dispersion of the Luttinger liquid moving between energy and momentum bases amount to a trivial relabelling and so position eigenstates can just as well be thought of as eigenstates of a time operator $\hat{t} = \frac{1}{v_F}\hat{x}$. Moving beyond the linear regime, energy and momentum states no longer coincide but, in 1D, states can typically be separated into branches where the relationship is ordered and monotonic. It is still possible, therefore, to map momentum states onto the energy states

$$c_E = \sqrt{2\pi g(E)} c_{k(E)} \tag{2.21}$$

where c_k are the standard fermionic annihilation operators. As the Hamiltonian clearly has the form of a linear dispersion in terms of these new operators, we can bosonize the system in the standard manner.

If the system has only a finite bandwidth, fictional spectator states can be added to the Hilbert space of the system, extending the dispersion to $\pm\infty$. Provided the Hamiltonian is block diagonal in the real and spectator modes, they will remain separate and the contribution from the fictional states can be removed later. As the mapping between energy and momentum states is no longer a simple relabelling, the Fourier transformed fields as a function of respectively formal time and position no longer coincide either. This means, in particular, that a local impurity potential in real space will typically have a non-trivial representation in terms of formal time. A Hamiltonian can be obtained in the bosonic formal time representation which exactly accounts for the band structure and can act as a starting point for a range of treatments of the FES in a non-linear band structure, for example in a cold atom system, as will be discussed further below, where the impurity potential may be comparable to the Fermi energy [90].

We will employ the same broad approach of using a formal time representation of the system, with spectator states to extend the dispersion to infinity, in Chapter **??** to consider the FES in a non-trivial band structure, but employ the Riemann-Hilbert approach, discussed below, rather than bosonization.

2.5 Spatial spread of the FES

One area in which there has been comparatively little research is the real space phenomenology of the FES.

Studies of the structure of ground state of quantum wires coupled to a dynamic impurity (with a separation of impurity levels much greater than the coupling between them, so the system is far from the Kondo regime) show signatures of the FES. The probability of finding the impurity in a given energy

level in the global ground state show a power law dependence on the difference of the energy level from the impurity ground state energy, depending on the impurity scattering phase shift. This in turn leaves a signature in the spatial correlation functions, specifically the current-current correlator and the fermion Green's function [91].

Further work has found more evidence of the FES in the dynamic correlations above the ground state of these systems. The generating functional for correlation in the charge density in the wire was directly related to the generating functional for correlation in the impurity state, leading to a corresponding relationship between the respective Green's functions and susceptibilities. In particular

$$\chi_{\nu,\nu'}(x,y,t) \propto G''_{\mathrm{Imp}}(t-y+x), \tag{2.22}$$

Where $\chi_{\nu,\nu'}(x,y,t)$ is the susceptibility of the system to a perturbation coupling to charge. The impurity Green's function displays the FES, so this carries over onto the dynamic response of the system [8].

An alternative method to introduce spatial considerations into the FES problem is to consider a semi-infinite wire, with the impurity some distance from the end. In this case it is found that the transition rate, $\Gamma(\omega)$, shows, in addition to the standard power law edge singularity, oscillations corresponding to the frequency of resonant charge density waves in the space between the impurity and the end of the wire [9]. This demonstrates that the transition rate is sensitive to the spatial structure of the environment through the Fermi sea shake up taking place.

Studies using exact diagonalisation techniques have been performed on impurity quench systems. Zhang and Liu [10] found a wavefront spreading out from the impurity separating two distinct regions. The outer region resembled the undisturbed system before the quench, whilst the region inside the wavefront showed oscillations in the particle density. These regions, with a sharp propagating boundary can be seen at both the single and many particle level.

Campbell *et al.*, also using exact diagonalisation methods, have claimed to see precursors to the OC is systems of just two fermions in a harmonic trap with an impurity. This study also shows oscillations in the spatial density distribution after the quench [92]. It is not clear, however, how straightforward interpolating from this to the full many-body case is.

There is still significant room to explore the manifestations of the FES in position space. We take steps in the direction in Chapter 4, considering the correlations between a pair of impurities coupled to a Luttinger liquid as different spatial positions.

Chapter 3

Methods in Non-Equilibrium 1D Quantum Systems

3.1 Bosonization

Bosonization is an extremely powerful method for understanding the behaviour of Fermi systems in 1D. It is particularly noteworthy due to its ability to tackle systems of interacting fermions without recourse to perturbation theory.

Physically bosonization maps the fermionic Fock space onto a space of density wave excitations of the Fermi-sea, described by bosonic statistics. These density waves turn out to be the elementary excitations of the many-fermion system, as apposed to the quasi-particle excitations in $d \geq 2$.

We will give only a brief overview of the method here, which will skim over some technical details, which are, for the most part unimportant. A more thorough treatment can be found in [24, 71, 72, 93] among others. We will focus on the case of spinless fermions, with only a few comments on the phenomenology of the spinful case; For our purposes explicitly considering spin will largely result in added mathematical complication without adding much conceptually. Bosonization has historically suffered from a lack of consistent notation in the community; we will aim to use notation consistent with [24] where possible.

We consider a 1D fermionic system with periodic boundary conditions. Let the field operators be $\psi(x)$ and let the size of the system be L. The momentum space fermionic operators c_k are defined in the usual way. Let $|0\rangle$ be the ground state of the system, which for non-interacting fermions has $\langle 0|c_k^\dagger c_k|0\rangle = 1$ for $|k| < k_F$ and $\langle 0|c_k^\dagger c_k|0\rangle = 0$ for $|k| > k_F$. We define normal ordered product by subtracting the operator product's ground state expectation.

$$: AB := AB - \langle 0|AB|0\rangle \tag{3.1}$$

This ground state expectation may be divergent, in particular when considering infinite bands, which will be needed below.

The Fermi surface of the system consists of 2 disconnected points at $\pm k_F$. This property is unique to the 1D problem; in higher dimensions the Fermi surface is consists of a (number of) extended manifold(s) in k-space. When considering low energy phenomena, therefore, it is convenient to split the dispersion into disconnected branches around each Fermi-point. We refer to these 2 branches of the dispersion as the left moving and right moving branches for $k < 0$ and $k > 0$ respectively. We write the creation operators for these branches as $c_{\nu,k}$ and can define the left and right moving field operators by taking the Fourier transform of the creation operators in each branch. (Note this means that there is a non-local relationship between the left/right moving field operators and the full field operators.)

$$\psi_{L/R}(x) = \sum_k e^{-\imath kx} c_{L/R,k} \ , \tag{3.2}$$

$$\psi(x) = \psi_L(x) + \psi_R(x) \ . \tag{3.3}$$

It will generally be convenient to label right movers with $\nu = +1$ and left movers with $\nu = -1$.

In order to bosonize the system we define the left/right-moving fermion density operators by

$$\rho_{\nu,k} = \sum_q c^\dagger_{\nu,q} c_{\nu,q+k} \ . \tag{3.4}$$

Some care must be taken when considering the $k = 0$ case. Naively applying $\rho_{\nu,k}$ to the ground state would give a divergent result in the case of an infinite band, due to the infinite number of particles in the ground state, so it is important only to consider the normal ordered product in this case.

$$: \rho_{\nu,0} := \sum_q \left(c^\dagger_{\nu,q} c_{\nu,q} - \langle 0 | c^\dagger_{\nu,q} c_{\nu,q} | 0 \rangle \right) \ . \tag{3.5}$$

These operators are the Fourier components of the left/right moving fermion density operator

$$: \rho_\nu(x) : = \sum_k e^{\imath kx} : \rho_{\nu,k} : \tag{3.6}$$

$$= \sum_{k,q} e^{\imath kx} : c^\dagger_{\nu,q} c_{\nu,k+q} : \tag{3.7}$$

$$= \sum_{p,q} e^{\imath (p-q)x} : c^\dagger_{\nu,q} c_{\nu,p} : \tag{3.8}$$

$$=: \psi^\dagger_\nu(x) \psi_\nu(x) : \tag{3.9}$$

and so represent fluctuations in the fermion density.

The commutators for the $\rho_{\nu,k}$ can be calculated straightforwardly

$$[\rho_{\nu,k},\rho_{\nu',k'}] = \sum_{q,q'}[c^\dagger_{\nu,q}c_{\nu,q+k},c^\dagger_{\nu',q'}c_{\nu',q'+k'}]^\dagger \tag{3.10}$$

$$\begin{aligned}=&\delta_{\nu,\nu'}\sum_{q,q'}\Big(c^\dagger_{\nu,q'}c^\dagger_{\nu,q}\{c_{\nu,q+k},c_{\nu,q'+k'}\}-c^\dagger_{\nu,q'}\{c^\dagger_{\nu,q},c_{\nu,q'+k'}\}c_{\nu,q+k}\\&+c^\dagger_{\nu,q}\{c_{\nu,q+k},c^\dagger_{\nu,q'}\}c_{\nu,q'+k'}-\{c^\dagger_{\nu,q},c^\dagger_{\nu,q'}\}c_{\nu,q+k}c_{\nu,q'+k'}\Big)\end{aligned} \tag{3.11}$$

$$=\delta_{\nu,\nu'}\sum_q\Big(c^\dagger_{\nu,q}c_{\nu,q+k'+k}-c^\dagger_{\nu,q-k'}c_{\nu,q+k}\Big) \tag{3.12}$$

$$\begin{aligned}=&\delta_{\nu,\nu'}\sum_q\Big(:c^\dagger_{\nu,q}c_{\nu,q+k'+k}:+\langle 0|c^\dagger_{\nu,q}c_{\nu,q+k'+k}|0\rangle\\&-:c^\dagger_{\nu,q-k'}c_{\nu,q+k}:-\langle 0|c^\dagger_{\nu,q-k'}c_{\nu,q+k}|0\rangle\Big)\end{aligned} \tag{3.13}$$

$$=\delta_{\nu,\nu'}\delta_{k,-k'}\sum_q\Big(\langle 0|c^\dagger_{\nu,q}c_{\nu,q}|0\rangle-\langle 0|c^\dagger_{\nu,q+k}c_{\nu,q+k}|0\rangle\Big) \tag{3.14}$$

$$=\delta_{\nu,\nu'}\delta_{k,-k}\frac{\nu kL}{2\pi} \tag{3.15}$$

The difference in eq. (3.14) is non-zero only if one term is above and the other is below the Fermi surface. There are k values of q where this occurs for each of the left/right moving branches, hence the factor of k in eq. (3.15). The normal ordering of operators in eq. (3.13) is critical as it allows us to relabel the indices in one of the terms, reordering the summation, and cancel the two normal ordered operators. Reordering the sum without normal ordering the operators leads to an incorrect result, due to invalid manipulations of divergent terms. This result is highly suggestive and encourages us to define the operators

$$b^\dagger_k=\sqrt{\frac{2\pi}{L|k|}}\sum_\nu\Theta(\nu k)\rho^\dagger_{\nu,k} \tag{3.16}$$

$$b_k=\sqrt{\frac{2\pi}{L|k|}}\sum_\nu\Theta(\nu k)\rho_{\nu,k}\ . \tag{3.17}$$

These operators obey true bosonic commutation relations

$$[b^\dagger_k,b^\dagger_{k'}]=0 \tag{3.18}$$

$$[b_k,b^\dagger_{k'}]=\delta_{k,k'} \tag{3.19}$$

and annihilate the ground state $|0\rangle$.

In order to find an expression for the fermionic operators in terms of the bosonic ones we consider the commutator

$$[\rho_{\nu,k},\psi_{\nu'}(x)]=\sum_q\sum_{k'}e^{-\imath xk'}[c^\dagger_{\nu,q}c_{\nu,k+q},c_{\nu',k'}] \tag{3.20}$$

$$= -\sum_q \sum_{k'} e^{-\imath x k'} \delta_{\nu,\nu'} \delta_{q,k'} c_{\nu,k+q} \tag{3.21}$$

$$= -\delta_{\nu,\nu'} e^{-\imath k x} \psi_\nu(x) \ . \tag{3.22}$$

This shows that $\psi_\nu(x)$ has a coherent state representation in terms of $\rho_{\nu,k}$ (or equivalently b_k), that is

$$\psi_\nu(x) \sim e^{\sum_{k>0} \frac{2\pi\nu}{Lk}(e^{-\imath k x}\rho_{\nu,k} - e^{\imath k x}\rho^\dagger_{\nu,k})} \tag{3.23}$$

$$\sim e^{\nu \sum_{k>0} \sqrt{\frac{2\pi}{Lk}}(e^{-\imath k x} b_{\nu k} - e^{\imath k x} b^\dagger_{\nu k})} \ . \tag{3.24}$$

This cannot be the complete story, as $\psi_\nu(x)$ reduces the fermion number by 1, while b_k contains only pairs of fermionic creation and annihilation operators, and so cannot change the fermion number. There must, therefore, be a prefactor which changes the fermion number. We define the *Klein factor* F_ν to commute with all bosonic operators, reduce the fermion number by 1 and be unitary . It turns out that the Klein factors rarely matter in practice; in most (but not all) cases when a mismatch of fermion number would cause an expectation value to vanish, other factors in the term also vanish. With this we can write

$$[N_\nu, F^\dagger_{\nu'}] = \delta_{\nu,\nu'} F^\dagger_\nu \ , \tag{3.25}$$

$$\psi = F_\nu e^{\nu \sum_{k>0} \sqrt{\frac{2\pi}{Lk}}(e^{-\imath k x} b_{\nu k} - e^{\imath k x} b^\dagger_{\nu k})} \ , \tag{3.26}$$

where N_ν are the number operators for left/right moving fermions respectively.

If we consider a non-interacting Fermi-gas, with Hamiltonian

$$H_0 = \sum_\nu \sum_k \epsilon_{\nu,k} c^\dagger_{\nu,k} c_{\nu,k} \tag{3.27}$$

we find that the density operators have the following algebra

$$[\rho_{\nu,k}, H_0] = \sum_r \sum_{k'} \epsilon_{r,k'} [\rho_{\nu,k}, c^\dagger_{r,k'} c_{r,k'}] \tag{3.28}$$

$$= \sum_r \sum_{k'} \sum_q \epsilon_{r,k'} [c^\dagger_{\nu,q} c_{\nu,k+q}, c^\dagger_{r,k'} c_{r,k'}] \tag{3.29}$$

$$= \sum_{k'} \sum_q \epsilon_{\nu,k'} \left(\delta_{k+q,k'} c^\dagger_{\nu,q} c_{\nu,k'} - \delta_{q,k'} c^\dagger_{\nu,k'} c_{\nu,k+q} \right) \tag{3.30}$$

$$= \sum_q \epsilon_{\nu,k+q} c^\dagger_{\nu,q} c_{\nu,q+k} - \epsilon_{\nu,q} c^\dagger_{\nu,q} c_{\nu,k+q} \tag{3.31}$$

$$= \sum_q (\epsilon_{\nu,k+q} - \epsilon_{\nu,q}) c^\dagger_{\nu,q} c_{\nu,q+k} \tag{3.32}$$

Now if we consider a narrow range around each Fermi-point we may treat the dispersion as being approximately linear, $\epsilon_{\nu,k} \approx v_F \nu (k - k_f)$. In this case $(\epsilon_{\nu,k+q} - \epsilon_{\nu,q}) = \nu v_F k$, independent of q. We can, therefore, write eq. (3.32) as

$$[\rho_{\nu,k}, H_0] = v_F \nu k \rho_{\nu,k} \tag{3.33}$$

which implies that the density wave operators, or equivalently the bosonic operators b_k, act as ladder operators for H_0, and that the Hamiltonian can be written in the form

$$H_0 = E_0 + \frac{2\pi}{L}\sum_{\nu}\sum_{k>0} v_F \rho^\dagger_{\nu,k}\rho_{\nu,k} \tag{3.34}$$

$$= E_0 + \sum_k v_F k b^\dagger_k b_k \tag{3.35}$$

that is the density waves created by the bosonic operators are elementary excitations of the linearised Fermi gas. Here E_0 is the ground state energy. The sum in eq. (3.35) is taken over all k, with $k > 0$ denoting right moving modes and $k < 0$ denoting left moving odes.

We can define bosonic fields by taking the Fourier transforms of the bosonic creation and annihilation operators. In practice it can be advantageous to consider the Fourier transform of a particular combination of bosonic operators, to obtain Hermitian fields that can be related to the physical density and current in eq. (3.41) and eq. (3.42) below.

$$\phi(x) = -\frac{\pi x}{L}\sum_\nu N_\nu - \imath\sqrt{\frac{\pi}{2L}}\sum_p \frac{\sqrt{|p|}}{p} e^{-xp-\alpha|p|/2}(b^\dagger_p + b_{-p}) \tag{3.36}$$

$$\theta(x) = \frac{\pi x}{L}\sum_\nu \nu N_\nu + \imath\sqrt{\frac{\pi}{2L}}\sum_p \frac{1}{\sqrt{|p|}} e^{-xp-\alpha|p|/2}(b^\dagger_p - b_{-p})\ . \tag{3.37}$$

The comutation relations for these fields are given by

$$[\phi(x), \phi(x')] = 0 \tag{3.38}$$

$$[\theta(x), \theta(x')] = 0 \tag{3.39}$$

$$[\phi(x), \theta(x')] = \imath\frac{\pi}{2}\,\mathrm{sgn}(x' - x) \tag{3.40}$$

Differentiating eq. (3.36) and eq. (3.37) we obtain

$$\nabla\phi(x) = -\pi\sum_\nu \rho_\nu(x) \tag{3.41}$$

$$\nabla\theta(x) = \pi\sum_\nu \nu\rho_\nu(x) \tag{3.42}$$

that is the gradient of ϕ tells us the total charge density and the gradient of θ tells us the total current, arising from low momentum sector $k \ll k_F$. The full density and current includes a large momentum contribution that mixes left and right movers

$$\rho(x) =: \psi^\dagger(x)\psi(x) : \tag{3.43}$$

$$= \sum_{\nu,\nu'} : \psi^\dagger_\nu(x)\psi_{\nu'}(x) : \tag{3.44}$$

$$= \sum_{\nu} \left(\rho_\nu(x) + :\psi^\dagger_\nu(x)\psi_{-\nu}(x):\right) \tag{3.45}$$

$$= -\frac{1}{\pi}\nabla\phi(x) + \frac{e^{-2\imath k_F x}}{2\pi} e^{-\imath 2\phi(x)} \tag{3.46}$$

In terms of the bosonic fields, the fermionic operators can be written

$$\psi_\nu(x) = \lim_{\alpha\to 0} \frac{F_\nu}{\sqrt{2\pi\alpha}} e^{\imath k_F i x - \frac{\pi}{L}x} e^{-\imath(r\phi(x)-\theta(x))} \tag{3.47}$$

Substituting eq. (3.41) and eq. (3.42) into the Fourier transform of eq. (3.34) we can write the Hamiltonian as

$$H_0 = \int \frac{\mathrm{d}x}{2\pi} v_F \left[(\nabla\phi(x))^2 + (\nabla\theta(x))^2\right] \tag{3.48}$$

The remarkable power of the bosonization approach becomes apparent when interactions are added to the system. The generic fermion-fermion interaction has the form

$$H_{\text{ee}} = \int \mathrm{d}x\, \mathrm{d}x'\, U(x-x')\rho(x)\rho(x') \tag{3.49}$$

If we decompose this into left and right movers using eq. (3.45) we get three distinct non-zero terms

$$H_{\text{ee}} = \sum_\nu \int \mathrm{d}x\, \mathrm{d}x' \Big[\frac{1}{2} g_4(x-x')\rho_\nu(x)\rho_\nu(x') + g_2(x-x')\rho_\nu(x)\rho_{-\nu}(x') + g_1(x-x')\psi^\dagger_\nu(x)\psi_{-\nu}(x)\psi^\dagger_{-\nu}(x')\psi_\nu(x')\Big] \tag{3.50}$$

where we have allowed generalised our expression slightly by allowing the different terms to have different potentials. The naming of the coefficents g_i has become traditional and is known as the g-ology of 1d interacting Fermi systems [94]. Terms that do not conserve the number of left and right movers separately vanish due to momentum conservation; Converting a left mover to a right mover requires a large momentum transfer $\sim 2k_F$ which cannot be matched a momentum tranfer remaining within a small neighbourhood of the Fermi point.

The g_4 term describes the scattering of two particles close to the same Fermi point, whilst the g_2 term describes the scattering of two fermions on oposite sides of the dispersion realtion. Both processes involve relatively small momentum transfers. The g_1 term, by contrast involves particles close to different Fermi points scattering with a large momentum transfer $\sim 2k_F$, so that they exchange which patch of the dispersion they are residing on. Since we are dealing with spinless fermions here, however, particle indistinguishability means that this term is the same as the the g_2 term, up to a redefinition of the kinetic energy term. For spinful particles, however, this term must be treated separately.

The g_2 term can be written in terms of ϕ and θ as

$$g_2\rho_\nu(x)\rho_{-\nu}(x) = \frac{g_2}{(2\pi)^2}\left[(\nabla\phi(x))^2 - (\nabla\theta(x))^2\right] \tag{3.51}$$

In a similar way we can write the g_4 term for right movers as

$$\frac{g_4}{2}\psi_+^\dagger(x)\psi_+(x)\psi_+^\dagger(x)\psi_+(x) = \frac{g_4}{2(2\pi)^2}(\nabla\phi(x) + \nabla\theta(x))^2 \tag{3.52}$$

which, when combined with the equivilant term for left movers gives

$$\frac{g_4}{(2\pi)^2}\left[(\nabla\phi(x))^2 + (\nabla\theta(x))^2\right] \tag{3.53}$$

We will now limit our attention to a contact interaction, to represent a heavily screened interaction between particles, so that g_2 and g_4 are now constants. Putting this together with eq. (3.48) we obtain

$$H = \int \frac{\mathrm{d}x}{2\pi} u \left[\frac{1}{K}(\nabla\phi(x))^2 + K(\nabla\theta(x))^2\right] \tag{3.54}$$

$$K = \left[\frac{2\pi v_F + g_4 - g_2}{2\pi v_F + g_4 + g_2}\right]^{1/2} \tag{3.55}$$

$$u = v_F\left[\left(1 + \frac{g_4}{2\pi v_F}\right)^2 - \left(\frac{g_2}{2\pi v_F}\right)^2\right]^{1/2} \tag{3.56}$$

It will be convenient in chapter 4 to employ another representation of the bosonized fields. This is in terms of the pure left and right moving normal modes of the Hamiltonians eq. (3.54). We define these fields as

$$\tilde{\varphi}_\nu(x) = \phi(x) - \nu K\theta(x) \tag{3.57}$$

The commutators for these fields are given by

$$[\tilde{\varphi}_\nu(x), \tilde{\varphi}_{\nu'}(x')] = -K\nu'[\phi(x), \theta(x')] - K\nu[\theta(x), \phi(x')] \tag{3.58}$$

$$= \imath\frac{\pi}{2}K\left(-\nu'\,\mathrm{sgn}(x' - x) + \nu\,\mathrm{sgn}(x - x')\right) \tag{3.59}$$

$$= \imath\pi\nu K\delta_{\nu,\nu'}\,\mathrm{sgn}(x - x') \tag{3.60}$$

In terms of the normal mode fields the Hamiltonian in eq. (3.54) can be written as

$$H = u\int \frac{\mathrm{d}x}{2\pi}\frac{1}{K}\left(\frac{\nabla\tilde{\varphi}_-(x) + \nabla\tilde{\varphi}_+(x)}{2}\right)^2 + K\left(\frac{\nabla\tilde{\varphi}_-(x) - \nabla\tilde{\varphi}_+(x)}{2K}\right)^2 \tag{3.61}$$

$$= \frac{u}{2K}\sum_\nu \int \frac{\mathrm{d}x}{2\pi}\left(\nabla\tilde{\varphi}_\nu(x)\right)^2 \ . \tag{3.62}$$

The Heisenberg equation for $\tilde{\varphi}_\nu(x)$ is given by

$$\dot{\tilde{\varphi}}_\nu(x) = \imath[H, \tilde{\varphi}_n u(x)] \tag{3.63}$$

$$= \imath \frac{u}{2K} \int \frac{\mathrm{d}y}{2\pi} 2\nabla\tilde{\varphi}_\nu(y)[\nabla\tilde{\varphi}_\nu(y), \tilde{\varphi}_\nu(x)] \tag{3.64}$$

$$= -\nu u \int \mathrm{d}y\, \delta(y-x)\nabla\tilde{\varphi}_\nu(y) \tag{3.65}$$

$$= -\nu u \nabla\tilde{\varphi}_\nu(x) \tag{3.66}$$

$$\Rightarrow \tilde{\varphi}_\nu(x,t) = \tilde{\varphi}(x-\nu u t)\ . \tag{3.67}$$

That is $\tilde{\varphi}_\nu(x)$ is respectively a purely left or right moving solution to the equations of motion.

The fermionic operators in terms of the normal mode operators are given by

$$\psi_\nu(x) = \lim_{\alpha\to 0} \frac{F_\nu}{\sqrt{2\pi\alpha}} e^{\imath k_F i x - \frac{\pi}{L}x} e^{-\frac{\imath}{2}\sum_\nu (r+\frac{\nu}{K})\tilde{\varphi}_\nu(x)} \tag{3.68}$$

Notice that for $K=1$, ψ_ν depends only on $\tilde{\varphi}_\nu$ and not on $\tilde{\varphi}_{-\nu}$, so that in the absence of backscattering interactions a left(right) moving electron continues to propagate to the left(right) as would be expected. The fact that a physical fermion will in general contain a left and a right moving part, which will typically separate and travel separately, is known as charge fractionalisation [95, 96].

We alo can rewrite eq. (3.41) and eq. (3.42) in terms of the normal modes to obtain

$$\nabla\tilde{\varphi}_\nu = -\pi \sum_r (1 + r\nu K)\, \rho_r(x) \tag{3.69}$$

$$\rho_r(x) = -\frac{1}{4\pi} \sum_\nu \left(1 + \frac{r\nu}{K}\right) \nabla\tilde{\varphi}_\nu(x) \tag{3.70}$$

In order to calculate measurable quantities we must be able to calculate expectation values of the bosonic field operators. We will focus on the zero temperature behaviour of systems, although generalising our results to finite temperature would be a simple matter of substituting the zero temperature expectations for the standard finite temperature results. The zero temperature expectation values can be obtained by a number of methods, either by starting with a representation in terms of the b_k and $b_k^\dagger$ operators and using the standard bosonic operator results, or by using path integral methods, as is done in [24]. This yields

$$\langle T_\mathcal{K}(\tilde{\varphi}_\nu(x,t) - \tilde{\varphi}_{\nu'}(x',t'))^2\rangle = 2K \ln\left(\frac{x-x'-\nu u(t-t') + \imath\nu\,\mathrm{sgn}(t-t')\alpha}{\imath\nu\,\mathrm{sgn}(t-t')\alpha}\right) \tag{3.71}$$

Note that care must be taken to choose expectations such that the result in well defined. Here $T_\mathcal{K}$ denotes ordering along a Keldysh contour and the $\mathrm{sgn}(t-t't)$ should similarly be understood as $+1$ if t is ahead of t' along the contour and -1 if t' is ahead of t. This determines the imaginary shifts, which encode crucial physics of the system. The standard time ordered, anti-time ordered, greater and lesser correlators can be cound by choosing times respectively both on the forward branch, both on the backward branch or on different branches of the contour.

We will mostly be concerned with spinless fermions, as these will demonstrate the physics we are interested in without adding unnecessary complication. We will therefore only briefly describe the qualitative features of spinful Luttinger liquids here, without going into the exact details.

To reintroduce the spin degrees of freedom we initially treat the spin up and spin down fermions separately, bosonizing the spin up fermions $\psi_\uparrow$ to obtain a pair of bosonic fields $\phi_\uparrow$ and $\theta_\uparrow$ and similarly bosonizing the spin down fermions $\psi_\downarrow$ to obtain $\phi_\downarrow$ and $\theta_\downarrow$.

It turns out that the natural thing to do is define a pair of "charge" and "spin" fields

$$\phi_c(x) = \frac{1}{\sqrt{2}}(\phi_\uparrow(x) + \phi_\downarrow(x)) \tag{3.72}$$

$$\phi_s(x) = \frac{1}{\sqrt{2}}(\phi_\uparrow(x) - \phi_\downarrow(x)) \tag{3.73}$$

and similarly for the θ and normal mode fields. The charge field carries electric charge but no spin angular mometum and the spin filed carries spin but no charge, hence the names. Remarkably when expressed in terms of these fields, the Hamiltonian for an interacting system takes the form

$$H = H_c + H_s \tag{3.74}$$

where H_c and H_s depend only on the charge or spin fields respectively. This implies that the spin and charge degrees of freedom completely decouple and can be considered independently. Excitations of the spin and charge fields, however, propagate with different spin and charge velocities. That is if an electron is injected into a spinful Luttinger liquid its spin and charge will separate and travel independently through the system.

3.1.1 The Fermi-Edge Singularity in bosonization

The language of bosonization give a particularly insightful perspective on the FES, first developed by Schotte & Schotte [65]. It shows the origin of the Fermi-edge singularity to be in the large number of low energy density wave excitations created by the introduction of the impurity. As these many low energy excitations slowly dephase this gives rise to slow long time dynamics and the power laws characteristic of the FES.

Introducing and removing a core hole is essentially a zero dimensional process. A central scattering potential cannot alter the angular momentum of a scattering particle, so angular momentum channels decouple. This results in physics that is largely independent of the dimension. We will consider a radial basis set and for simplicity consider only s-wave scattering (higher order angular momentum terms are straightforward to include). With this setup we can, again, limit ourselves to only low energy phenomena and linearise the dispersion around the Fermi level. The s-wave radial basis has one significant difference

from a true 1D system; The radial k vector takes values only of $k > 0$, so there are, in effect "no left movers" in the problem.

We can now bosonize the system as before, with b_k now defined for $k > 0$, reflecting that the lack of left moving fermions.

The deep core potential has the form

$$V = V_+(\rho(0) + \rho^\dagger(0))dd^\dagger, \tag{3.75}$$

$$= \frac{V_+}{L}\sum_{k>0}(\rho_k + \rho_k^\dagger)dd^\dagger \tag{3.76}$$

where $d^\dagger$ creates the deep core state.

Combining eq. (3.76) with eq. (3.35) and the core hole Hamiltonian $H_{\text{Core}} = E_{\text{Core}}dd^\dagger$ we obtain the full Hamiltonian of the system.

$$H = E_0 + E_{\text{Core}}dd^\dagger + \sum_k v_F k b_k^\dagger b_k + \frac{V_+}{\sqrt{2\pi L}}\sum_k \sqrt{k}(b_k + b_k^\dagger)dd^\dagger \tag{3.77}$$

As discussed in Chapter 2, one of the key observation to the solubility of the Fermi-Edge problem is that it can be reduced to single particle physics, by noting that the interaction between the hole and the Fermi sea cannot induce a change in the state of the core hole, and so the interaction can essentially be treated as an external potential, which may be switched on or off by an external perturbation changing the state of the hole. Treating the core hole in this manner gives us a pair of effective Hamiltonians for the Fermi gas, with and without the core hole present.

$$h_0 = E_0 + \sum_{k>0} v_F k b_k^\dagger b \tag{3.78}$$

$$h_1 = E_0 + \sum_{k>0} v_F k b_k^\dagger b + \frac{V_+}{\sqrt{2\pi L}}\sum_{k>0}\sqrt{k}(b_k + b_k^\dagger)\ . \tag{3.79}$$

We can rewrite h_1 as

$$h_1 = E_0 + v_F\sum_{k>0} k\left(b_k + \frac{1}{\sqrt{2\pi L}}\frac{V_+}{v_F\sqrt{k}}\right)^\dagger\left(b_k + \frac{1}{\sqrt{2\pi L}}\frac{V_+}{v_F\sqrt{k}}\right) + const\ . \tag{3.80}$$

We see that the effect of the impurity potential is to apply a shift to each of the bosonic modes. Expressing the eigenfunctions of a shifted harmonic oscillator in terms of the unshifted eigenfunctions requires an infinite number of function to be used. This is why the FES generates an infinite number of excitations; They are required to express the eigenfunctions of the original Hamiltonian in terms of the eigenfunctions of the new Hamiltonian.

With this shifting in mind we define

$$W = e^{\frac{\delta}{\pi}\sum_{k>0}\sqrt{\frac{2\pi}{Lk}}(b_k^\dagger - b_k)} \tag{3.81}$$

as the shift operator. Under the action of W, b_k transforms as

$$W^\dagger b_k W = b_k + \frac{\delta}{\pi}\sqrt{\frac{2\pi}{Lk}}\,. \tag{3.82}$$

We can gain some intuition for the form of W by noting that if b and $b^\dagger$ are the creation and annihilation operators for a harmonic oscillator, the momentum is given by $p \sim b - b^\dagger$ and so $e^{a(b-b^\dagger)}$ is the translation operator for position $x \sim b + b^\dagger$. W then is simply the product of the translation operators for the infinite family of bosonic modes indexed by k.

If we choose $\delta = \frac{V_+}{2v_F}$ then we have that

$$h_1 = W^\dagger h_0 W + const \tag{3.83}$$

With this machinery in place we are in a position to calculate essentially any quantity of interest. The traditional choices are the core hole Green's function, $G_{\text{imp}}(t)$ and the matrix element for a perturbation, $\psi^\dagger(0)d$, exciting core holes to the Fermi sea.

The calculation of $G_{\text{imp}}(t)$ reduces to calculating the Loschmidt amplitude for the Fermi gas, ignoring the impurity state.

$$\begin{aligned} G_{\text{imp}}(t) &= \langle d^\dagger(t) d\rangle & (3.84)\\ &= \langle e^{\imath H t} d^\dagger e^{-\imath H t} d\rangle & (3.85)\end{aligned}$$

When we move to the reduced system with the external impurity potential we find that the first d turns of the impurity potential, while the $d^\dagger$ turns it off again. Therefore

$$\begin{aligned} G_{\text{imp}}(t) &= \langle e^{\imath h_0 t} e^{-\imath h_1 t}\rangle & (3.86)\\ &= \langle e^{\imath h_0 t} W^\dagger e^{-\imath h_0 t} W\rangle & (3.87)\\ &= \langle W^\dagger(t) W(0)\rangle & (3.88)\end{aligned}$$

The calculation of the perturbation matrix element proceeds along similar lines.

$$\begin{aligned} F(t) &= \langle d^\dagger \psi(t)\psi^\dagger(0) d(0)\rangle & (3.89)\\ &= \langle e^{\imath H t} d^\dagger \psi e^{-\imath H t}\psi^\dagger d\rangle & (3.90)\\ &= \langle e^{\imath h_0 t}\psi W^\dagger e^{-\imath h_0 t} W\psi^\dagger\rangle & (3.91)\\ &= \langle \psi(t) W^\dagger(t) W(0)\psi^\dagger(0)\rangle & (3.92)\end{aligned}$$

Expressing ψ and W in terms of the bosonic creation/annihilation operators and using the relation $e^A e^B = e^{A+B+\frac{1}{2}[A,B]}$, valid when $[A,B] \in \mathbb{C}$, we find that

$$G_{\text{imp}}(t) = e^{-\imath\left(\frac{\delta}{\pi}\right)^2 \sum_{k>0} \frac{2\pi}{Lk} e^{-\alpha k}\sin(v_F k t)}$$

$$\times \left\langle e^{\frac{\delta}{\pi}\sum_k e^{-\alpha k/2}\sqrt{\frac{2\pi}{Lk}}\left[\left(e^{\imath v_F kt}-1\right)b_k^\dagger-\left(e^{-\imath v_F kt}-1\right)b_k\right]}\right\rangle \tag{3.93}$$

$$F(t) = e^{-\imath\left(1+\frac{\delta}{\pi}\right)^2\sum_{k>0}\frac{2\pi}{Lk}e^{-\alpha k}\sin(v_F kt)} \times \left\langle e^{\left(1+\frac{\delta}{\pi}\right)\sum_k e^{-\alpha k/2}\sqrt{\frac{2\pi}{Lk}}\left[\left(e^{\imath v_F kt}-1\right)b_k^\dagger-\left(e^{-\imath v_F kt}-1\right)b_k\right]}\right\rangle \tag{3.94}$$

Here we can see explicitly that the introduction of the impurity is creating an infinite number of particle-hole pairs, weighted towards those with long wavelengths; that is towards low energy excitations. This is the Fermi-sea shake up which is the physical root of the FES.

We can now employ the formula

$$\left\langle e^{\sum_i ab_i+cb_i^\dagger}\right\rangle = e^{\frac{1}{2}\left\langle\left(\sum_i ab_i+cb_i^\dagger\right)^2\right\rangle}, \tag{3.95}$$

to find that

$$G_{\text{imp}}(t) = e^{-\imath\left(\frac{\delta}{\pi}\right)^2\sum_{k>0}\frac{2\pi}{Lk}e^{-\alpha k}\sin(v_F kt)} \times \exp\left[-\frac{\delta^2}{\pi^2}\sum_{k>0}\frac{2\pi}{L}e^{-\alpha k}\frac{1-\cos(v_F tk)}{k}\langle b_k^\dagger b_k + b_k b_k^\dagger\rangle\right] \tag{3.96}$$

$$= \exp\left[\frac{\delta^2}{\pi^2}\sum_{k>0}\frac{2\pi}{L}e^{-\alpha k}\frac{e^{\imath v_F tk}-1}{k}\right] \tag{3.97}$$

$$\sim \left(\frac{v_F t}{\alpha}\right)^{-\frac{\delta^2}{\pi^2}} \tag{3.98}$$

$$F(t) = e^{-\imath\left(1+\frac{\delta}{\pi}\right)^2\sum_{k>0}\frac{2\pi}{Lk}e^{-\alpha k}\sin(v_F kt)} \times \exp\left[-\left(1+\frac{\delta}{\pi}\right)^2\sum_{k>0}\frac{2\pi}{L}e^{-\alpha k}\frac{1-\cos(v_f tk)}{k}\langle b_k^\dagger b_k + b_k b_k^\dagger\rangle\right] \tag{3.99}$$

$$= \exp\left[\left(1+\frac{\delta}{\pi}\right)^2\sum_{k>0}\frac{2\pi}{L}e^{-\alpha k}\frac{e^{\imath v_F tk}-1}{k}\right] \tag{3.100}$$

$$\sim \left(\frac{v_F t}{\alpha}\right)^{-\left(1+\frac{\delta}{\pi}\right)^2} \tag{3.101}$$

In eq. (3.96) and eq. (3.99) we can see the generation of particle-hole excitations at all energies and how, at long times the high energy contributions dephase, leaving only the contribution from the divergent weighting of the low energy modes, and that this leads to slow power law decays at long times, as these low energy modes finally dephase from each other.

The value of $\delta = \frac{V_+}{2v_F}$ is equal to the scattering phase shift in the Born-approximation. Comparing the solution in eq. (3.98) and eq. (3.101) to the

exact solution of Nozières and De Dominicis [3], we see that the only difference is that the exact solution has the exact scattering phase shift instead of the Born approximation. This is a result of the approximation of a linear dispersion in the bosonization method.

3.2 The Riemann-Hilbert Approach

The Riemann-Hilbert (RH) approach is a non-perturbative method of calculating observables in scattering problems for non-interacting many-fermion systems [5, 82]. It maps the problem onto an auxiliary Riemann-Hilbert boundary value problem, which, in the Abelian case, where the observable of interest commutes with itself at all times, can be solved exactly.

We will consider a metallic system containing a time dependent scattering potential. We will, for the moment, assume that the Fermi level is somewhere in the middle of the band and that at all times the scattering potential is much less than the bandwidth, so that we may assume the band extends to $\pm\infty$. We will also assume for the moment that we can linearise the dispersion around the Fermi energy, that is that the density of states is constant.

We consider an observable $R(t)$ which can be written as in a form which is no more than quadratic in fermion operators, i.e. it represents a single particle observable in the many body system. As the system is non-interacting, the expectation of the observable can be written as an anti-symmetrised sum over the occupied single particle states, that is as a determinant

$$\chi(t) = \mathrm{Det}_{\mathrm{occupied}}\left[R(t)\right] \ . \tag{3.102}$$

The determinant over occupied states is cumbersome to work with, so it is convenient to extend it to a determinant over all single particle states via the Klich formula[61]. This gives us

$$\chi(t) = \mathrm{Det}\left[1 - n + nR(t)\right] \ , \tag{3.103}$$

where the determinant is now taken over all single particle states and n is the occupation of single-particle states. An intuition for this formula can be gain by considering the case of zero temperature where

$$n(\epsilon, \epsilon') = \Theta(\epsilon_F - \epsilon)\frac{\delta(\epsilon - \epsilon')}{2\pi\nu(\epsilon_F)} \ , \tag{3.104}$$

i.e. it projects onto the states below the Fermi level, in which case it is clear that the determinant factors into a contribution from the occupied states, which is given by eq. (3.102) and a contribution from the unoccupied states which is simply the determinant of the identity, that is 1.

The functional determinants are, in general, non-trivial to calculate. In order to make progress with eq. (3.103) we will consider its logarithm and employ the

Trace-Determinant formula[1]. This gives us

$$\ln \chi(t) = \operatorname{Tr} \ln \left[1 - n + nR(t)\right] \tag{3.109}$$
$$= \operatorname{Tr} \left[n \ln R(t)\right] + \operatorname{Tr} \left[\ln \left(1 - n + nR(t)\right) - n \ln R(t)\right] \tag{3.110}$$
$$= \ln \chi_1(t) + \ln \chi_2(t) \tag{3.111}$$

where we have added and subtracted $\ln \chi_1(t) = \operatorname{Tr} \left[n \ln R(t)\right]$ from the right hand side for eq. (3.109). The reason for doing this is to separate out the, typically divergent, contributions from states deep within the Fermi-Sea from the more physically interesting term χ_2. In the cases we will be interested in R is the scattering matrix, S, and so χ_1 is the sum of the scattering phase shifts. By Fumi's Theorem [38] this gives the shift the ground state energy due to the impurity potential. More generally this term is known as the generalised Fumi contribution [85].

We have, in eq. (3.109), exchanged the problem of calculating a functional determinant for the problem of calculating a functional logarithm. If we now assume that $R(t)$ is a bounded operator for all t, implying that $1 - n + nR$ is also bounded, we may now employ the relation $\ln M(\lambda) = \int \mathrm{d}\lambda \; M^{-1} M'$, valid for bounded operators. To do this we give $R(t) = R(t, \lambda)$ some dependence on a dummy parameter λ. We are largely free to choose the form of the dependence for our own convenience; a common choice is

$$R(t, \lambda) = \exp \left(\lambda \ln R(t)\right) \; . \tag{3.112}$$

We can now write

$$\ln \chi_2(t) = \int_0^1 \mathrm{d}\lambda \; \operatorname{Tr} \left[\left((1 - n + nR(t, \lambda))^{-1} n - nR^{-1}(n, \lambda) \right) \frac{\mathrm{d}R}{\mathrm{d}\lambda} \right] \; . \tag{3.113}$$

The remaining challenge is to calculate the inverse function $(1 - n + nR(t))$. It is for this that we introduce the auxiliary RH problem. Before we can do this

[1] To prove the Trace-Determinant formula

$$\det e^M = e^{\operatorname{tr} M} \tag{3.105}$$

consider a matrix diagonalisable M with a complete set of eigenvalues $\lambda_1, \lambda_2 \ldots$. By definition of the matrix exponential e^M has eigenvalues $e^{\lambda_1}, e^{\lambda_2} \ldots$. The determinant is given by the product of the eigenvalues so we have

$$\det e^M = \prod_i e^{\lambda_i} \; . \tag{3.106}$$

On the other hand the trace of a matrix is given by the sum of its eigenvalues so

$$e^{\operatorname{tr} M} = e^{\sum_i \lambda_i} \; . \tag{3.107}$$

Comparing these two expressions we see that they are equal. Letting $M = \ln A$ and taking logarithms of both sides we have

$$\ln \det A = \operatorname{tr} \ln A \; . \tag{3.108}$$

we will first move to a *formal time basis*, defined to be the Fourier transform of the energy basis

$$|s\rangle = \sqrt{\nu(\epsilon_F)} \int_{-\infty}^{\infty} \mathrm{d}\epsilon \, e^{\imath\epsilon s} |\epsilon\rangle \; . \tag{3.114}$$

Note that we have used the assumption of an infinite band. It is also important to distinguish between the physical time, which appears as a parameter in $R(t)$ and the formal time used to label the basis states. This point will be discussed in more detail in chapter **??**, along with a more detailed account of the argument given below about the form of R.

When transformed into the formal time basis, the Fermi function has the form

$$n(s, s') = \frac{\imath}{2\pi} \frac{1}{s - s' + \imath 0^+} \tag{3.115}$$

that is, it is a Cauchy kernel, with its pole in the upper half plane. This opens up a wide range of powerful analytic methods, which form the heart of the RH approach.

The exact form of $R(s, s')$ will depend on the details of the observable being considered, however it will typically be possible to relate it to the scattering matrix of the impurity in some way. If the scattering potential is slowly varying relative to the typical scattering time (characterised by the Wigner delay time $\tau_{\mathrm{scat}} = -\imath S^\dagger \frac{\partial S}{\partial t}$ [97]), then scattering particles will experience an essentially static potential and further approximations are possible. Explicitly we will assume, if the scattering matrix if viewed as a function of scattering energy, E, and time, t, that [5]

$$S^\dagger \frac{\partial S}{\partial t} S^\dagger \frac{\partial S}{\partial E} \ll 1 \; . \tag{3.116}$$

In this case we expect the scattering to be nearly elastic. With this in mind we express the matrix elements of $R_{\epsilon,\epsilon'}$ as a function of the relative and centre of mass energies

$$\omega = \epsilon_1 - \epsilon_2 \; , \tag{3.117}$$

$$E = \frac{\epsilon_1 + \epsilon_2}{2} \; . \tag{3.118}$$

The expectation that scattering will approximately conserve energy now corresponds to an expectation that $R(\omega, E)$ will be a sharply peaked functions of ω.

With this in mind we consider the Wigner transform of R

$$R(\tau, E) = \frac{\nu(\epsilon_F)}{2\pi} \int_{-\infty}^{\infty} \mathrm{d}\omega \, e^{-\imath\tau\omega} R(\omega, E) \; . \tag{3.119}$$

We can express $R(s', s)$ in terms of $R(\tau, E)$

$$R(s', s) = \frac{1}{(2\pi)^2} \int \mathrm{d}\epsilon_1 \, \mathrm{d}\epsilon_2 \, e^{-\imath\epsilon_1 s' + \imath\epsilon_2 s} \nu(\epsilon_F) \int \mathrm{d}\tau \, \frac{e^{\imath(\epsilon_1 - \epsilon_2)\tau}}{\nu(\epsilon_F)} R(\tau, E) \tag{3.120}$$

We will now make a key approximation. Due to Fermi-Dirac statistics, we do not expect states far from the Fermi surface to contribute significantly to the final result and so we can neglect the dependence of $R(\tau, E)$ and the density of states in eq. (3.120) on E. We will treat the centre of mass energy as a constant parameter fixed at ϵ_F. With this we find that

$$R(s', s) = \frac{1}{(2\pi)^2} \int \mathrm{d}\omega \, \mathrm{d}E \, e^{-\imath E(s'-s) - \imath\omega \frac{(s'+s)}{2}} \int \mathrm{d}\tau \, e^{\imath\omega\tau} R(\tau, \epsilon_F) \tag{3.121}$$

$$= \delta(s - s') \int \mathrm{d}\tau \, \delta(s - \tau) R(\tau, \epsilon_F) \tag{3.122}$$

$$= \delta(s - s') R(s, \epsilon_F) \tag{3.123}$$

that is, within the approximations of eq. (3.116) we have that R is diagonal in the formal time basis.

We are now in a position to setup the auxiliary RH problem. A RH boundary value problem consists of finding the piecewise analytic function, Y, which satisfies given boundary conditions along the contour and at infinity. In our case we will choose the contour to run along the formal time axis from the point at which the scattering potential is introduced to the final time of the experiment (at which point we may assume the scattering potential is removed). Note that this implies we will require $Y(s)$ to be analytic over the upper and lower half planes, with the only nonanalyticity along the real axis. We will require $Y(s)$ to satisfy

$$Y_-(s) Y_+^{-1}(s) = R(s) \tag{3.124}$$

where $Y_\pm(s) = Y(s \pm \imath 0^+)$ is the value of Y immediately above and below the contour respectively. We will further require that

$$|s| \to \infty \Rightarrow Y(s) \to 1 \, . \tag{3.125}$$

We now consider the expressions $nY_\pm n$, where the product here denotes matrix multiplication; for definiteness we will consider the expression with Y_+ first. Explicitly writing out the matrix product reads

$$nY_+ n = \int \mathrm{d}s \, n(s_1, s) Y_+(s) n(s, s_2) \, . \tag{3.126}$$

Now, as Y_+ is analytic in the upper half plane (but not the lower half plane as it has been shifted above the contour), we may close the integration contour in the upper half plane and so pick up the residue for the pole of $n(s_1, s)$ at $s_1 + \imath 0^+$, giving us

$$nY_+ n = Y_+ n \, . \tag{3.127}$$

$$nY_- n = nY_- \, . \tag{3.128}$$

where the second equation was found in an analogous way to the first, closing the contour in the lower half plane, resulting in the change in the ordering of n and Y on the right hand side.

With the identities eq. (3.127) and eq. (3.128) it can be explicitly verified that

$$(1-n+nR)Y_+[(1-n)Y_+^{-1}+nfY_-^{-1}]=1\ , \tag{3.129}$$

that is $(1-n+nR)^{-1}=Y_+[(1-n)Y_+^{-1}+nY_-^{-1}]$. We can now write

$$\ln\chi_2=\int_0^1 \mathrm{d}\lambda\int \mathrm{d}s\ \left(Y_+[(1-n)Y_+^{-1}+nY_-^{-1}]n-nR^{-1}\right)\frac{\mathrm{d}R}{\mathrm{d}\lambda} \tag{3.130}$$

$$=\int_0^1 \mathrm{d}\lambda\int \mathrm{d}s\ \left(1-Y_+nY_+^{-1}n+Y_+nY_-^{-1}n-nR^{-1}\right)\frac{\mathrm{d}R}{\mathrm{d}\lambda} \tag{3.131}$$

$$=\int_0^1 \mathrm{d}\lambda\int \mathrm{d}s\ \left(1-Y_+Y_+^{-1}n+Y_+nY_-^{-1}-nR^{-1}\right)\frac{\mathrm{d}R}{\mathrm{d}\lambda} \tag{3.132}$$

$$=\int_0^1 \mathrm{d}\lambda\int \mathrm{d}s\ \left(1-Y_+Y_+^{-1}n+Y_+nY_-^{-1}-nY_+Y_-^{-1}\right)\frac{\mathrm{d}R}{\mathrm{d}\lambda} \tag{3.133}$$

$$=\int_0^1 \mathrm{d}\lambda\int \mathrm{d}s\,[Y_+,n]Y_-^{-1}\frac{\mathrm{d}R}{\mathrm{d}\lambda}\ . \tag{3.134}$$

The diagonal matrix elements should be viewed as the limit as $s\to s'$, so the commutator becomes

$$[Y_+,n](s,s)=\lim_{s'\to s}\frac{\imath}{2\pi}\frac{Y_+(s)-Y_+(s')}{s-s'+\imath 0^+} \tag{3.135}$$

$$=\frac{\imath}{2\pi}\frac{\mathrm{d}Y_+}{\mathrm{d}s} \tag{3.136}$$

which gives us

$$\ln\chi_2(t)=\frac{\imath}{2\pi}\int \mathrm{d}\lambda\,\mathrm{d}s\ \mathrm{tr}\left[\frac{\mathrm{d}Y_+}{\mathrm{d}s}Y_+^{-1}(s,t)R^{-1}(s,t,\lambda)\frac{\mathrm{d}R}{\mathrm{d}\lambda}\right] \tag{3.137}$$

The only piece now missing needed to calculate $\chi_2(t)$ is now to actually solve the RH problem to obtain an explicit form for $Y(s)$. For the Abelian case, that is where $[R(t),R(t')]=0\ \forall t,t'$ this can be found explicitly[83] as

$$Y(z)=\exp\left[\frac{-\imath}{2\pi}\int \mathrm{d}s\,\frac{\ln R(s)}{z-s}\right]\ . \tag{3.138}$$

3.2.1 The Fermi Edge Singularity from the Riemann-Hilbert Approach

To illustrate the RH approach we will use it to calculate the Loschmidt amplitude for the FES. In this case our observable is given by the forward and reversed time evolution operators, with and without the impurity

$$R(t_f)=e^{\imath Ht_f}e^{-\imath(H+V(t_f))t_f}\ . \tag{3.139}$$

It can be shown the long time limit this tends towards the Wigner transform of the instantaneous scattering matrix, with a more in-depth derivation in chapter **??**.

$$R(\epsilon_1, \epsilon_2) = \frac{1}{2\pi\nu\left(\frac{\epsilon_1+\epsilon_2}{2}\right)} \int \mathrm{d}\tau \, e^{\imath \frac{\epsilon_1-\epsilon_2}{2}\tau} S\left(\frac{\epsilon_1+\epsilon_2}{2}, \tau\right) . \tag{3.140}$$

The formal time domain representation of R for states close to the Fermi level is, therefore, simply

$$R(s_1, s_2) = \delta(s_1 - s_2) S(E_F, s_1) . \tag{3.141}$$

Furthermore, for the FES, the time dependence of the impurity is simply to turn on at $t = 0$ and off again at $t = t_f$. This clearly satisfies the conditions in eq. (3.116) for all times more that the typical quench time away from $t = 0, t_f$. $S(E_f, s_1)$ is explicitly given by

$$S(E, s) = 1 + (e^{2\imath\delta} - 1) \sqcap (0, t_f, s) . \tag{3.142}$$

where

$$\sqcap(x, y, z) = \begin{cases} 1 & x \leq z < y , \\ 0 & \text{otherwise} . \end{cases} \tag{3.143}$$

From this we can explicitly calculate $Y(s)$

$$Y(z) = \exp\left[\frac{-\imath}{2\pi} \int_0^{t_f} \mathrm{d}s \, \frac{2\imath\lambda\delta}{z - s}\right] \tag{3.144}$$

$$= \exp\left[\lambda \frac{\delta}{\pi} \ln\left(\frac{z}{z - t_f}\right)\right] \tag{3.145}$$

$$= \left(\frac{z}{z - t_f}\right)^{\lambda\frac{\delta}{\pi}} , \tag{3.146}$$

$$Y_+(s) = \left(\frac{s}{s - t_f + \imath 0^+}\right)^{\lambda\frac{\delta}{\pi}} , \tag{3.147}$$

$$\frac{\mathrm{d}Y_+}{\mathrm{d}s} Y_+^{-1}(s) = \lambda \frac{\delta}{\pi} \left(\frac{1}{s} - \frac{1}{s - t_f + \imath 0^+}\right) . \tag{3.148}$$

Substituting this into eq. (3.137) we find that

$$\ln \chi_2(t_f) = \frac{\imath}{2\pi} \int_0^1 \mathrm{d}\lambda \int_0^{t_f} \mathrm{d}s \, \lambda \frac{\delta}{\pi} \left(\frac{1}{s} - \frac{1}{s - t_f + \imath 0^+}\right) 2\imath\delta\lambda \tag{3.149}$$

$$= -\frac{\delta^2}{\pi^2} \frac{1}{2} \int_0^{t_f} \mathrm{d}s \left(\frac{1}{s} - \frac{1}{s - t_f + \imath 0^+}\right) \tag{3.150}$$

$$= -\frac{\delta^2}{\pi^2} \ln\left(\frac{\imath v_F t_f}{\alpha}\right) , \tag{3.151}$$

where α/v_F is an ultraviolet cut off.

By Fumi's theorem[38] the terms $\ln \chi_1$ is found to be

$$\ln \chi_1 = \mathrm{Tr}\, n \ln S \tag{3.152}$$

$$= \int_{\epsilon_0}^{\epsilon_F} \mathrm{d}\epsilon\, \imath t_f \Delta E \; . \tag{3.153}$$

This gives us the final result

$$\chi(t) = e^{\imath t_f \Delta E} \left(\frac{\imath v_F t_f}{\alpha} \right)^{-\frac{\delta^2}{\pi}} \quad , \tag{3.154}$$

in agreement with our previous derivation via bosonization, in eq. (3.98) and the Nozières-De Dominicis result [3].

Chapter 4

The Spread of Catastrophe: Spatio-Temporal Propagation of the Fermi-Edge Singularity

Whilst the FES has been studied for 50 years, until recently little attention has been paid to how the orthogonality catastrophe spreads through the system [8, 91]. The introduction of a local impurity cannot instantaneously influence parts of the system an arbitrary distance away, however the textbook treatments focus entirely on quantities, such as the absorption rate, that are essentially local at the site of the impurity or entirely global, such as the overlap integral, which offer no finer spatial resolution.

We examined how the information about the introduction of the impurity spread through the system. We were particularly interested in whether this information spreads in an essentially classical or quantum form. If quantum information about the impurity is being carried outward into the, largely incoherent, system could this be used for coherent quantum manipulation, such as to implementation of a quantum gate?

Parts of this chapter have formed the basis of a paper, recently accepted for publication [98]. Here we give a more thorough treatment of the calculations, as well as a more in depth discussion of the surrounding ideas.

4.1 Model

In order to probe the effect of the impurity some distance away in space, we considered a metallic system with two impurities at different locations. We could then turn on one impurity and see what effect the orthogonality catastrophe in the surrounding Fermi system had on the second.

One of the striking features of the FES is that it is largely independent of the dimension of the metal. This is due to the fact that the impurity is point-like and so physics focused on the impurity site is effectively zero dimensional, regardless of the dimension of the parent medium. This feature cannot be reasonably expected to remain when considering observables localised at different points in space. Signals will generally spread out in a dimension dependent way. The dimension of the system we choose to study will, therefore, likely quantitatively impact our results.

We choose to focus on 1D systems, as this allows the easiest comparison with the existing FES literature, as well as allowing us to use the powerful techniques of bosonization, as used in, for example, [65]. Bosonization allows us to compute a wide range of quantities exactly (and relatively simply compared to methods such as the Riemann-Hilbert approach) but also provides us with a significant amount of insight into the underlying physics.

Limiting our attention to 1D also means that we do not need to worry about the signal spreading out over distance as would happen in higher dimensions. This may result in stronger experimental signal, which may make any effects easier to detect.

Explicitly we will consider a metallic quantum wire and will linearise the dispersion around the Fermi level. We will consider spinless fermions, as we believe that they capture the essential physics of the FES. It will discover below that the results in the spinless case are already complex and cumbersome to work with; we expect the spinful case to simply add to this complexity, without adding much conceptually. We discuss what we expect to happen in the spinful case more in section 4.12.3. This gives us a Hamiltonian of the form

$$H_0 = \sum_\nu \int \mathrm{d}x' \, \left[-\imath\nu \, v_F \, \psi_\nu^\dagger(x') \nabla \psi_\nu(x') \right] \, . \tag{4.1}$$

Where $\psi_\nu(x)$ are the left/right moving fermion operators, with $\nu = 1$ for right movers and $\nu = -1$ for left movers. As we are in a true 1D system, and anticipating our use of bosonization, we can include fermion-fermion interactions, as it will add little extra complication.

$$\begin{aligned} H_{\mathrm{ee}} = \int \mathrm{d}x' \Bigg[& g_2 \psi_+^\dagger(x') \psi_+(x') \psi_-^\dagger(x') \psi_-(x') \\ & + \frac{g_4}{2} \sum_\nu \psi_\nu^\dagger(x') \psi_\nu(x') \psi_\nu^\dagger(x') \psi_\nu(x') \Bigg] \, . \end{aligned} \tag{4.2}$$

For the impurities we will consider a pair of localised fermionic states $d_1^\dagger$ and $d_2^\dagger$. We will assume that that $d_1^\dagger$ is located at 0 and $d_2^\dagger$ is located at x. These states will each interact with the continuum via potentials V_1 and V_2, centred around their respective impurity sites. We will further assume that both potentials have a range much less than the Fermi wavelength and so can be safely approximated by a δ-function potential. We will also assume that the

potential V_1 is turned on when the state $d_1^\dagger$ is *empty* and the potential V_2 is turned on when the state $d_2^\dagger$ is *full*. The reasons for this choice are discussed below, but an alternative choice could easily be accommodated. We assume that each state has an energy E_1, E_2 and that E_1 is below the Fermi level while E_2 is above the Fermi level, that is $E_1 < 0 < E_2$ and that $|E_i| \gg |V_i|$. This means that in the ground state the state $d_1^\dagger$ is filled and $d_2^\dagger$ is empty, so both potentials are turned off.

$$H_{\text{imp}} = \sum_{i\in\{1,2\}} E_i d_i^\dagger d_i + V_1 d_1 d_1^\dagger \rho(0) + V_2 d_2^\dagger d_2 \rho(x) \; . \tag{4.3}$$

The final element we require is a means to turn the impurity states on and off. For this we introduce a term which is able to pump fermions from the wire to localised states and back.

$$H_{\text{pump}} = \sum_{i\in\{1,2\}} \int \frac{\mathrm{d}y}{\sqrt{\alpha}} W_i(t) \lambda_i(y) \psi^\dagger(y) d_i + \text{h.c.} \tag{4.4}$$

The coupling W_i gives an explicit time dependence for this pump term and by choosing different functional forms we can examine a range of situations. For example by choosing $W_i = e^{\imath\omega t}$ we can examine the response at fixed frequency. On the other hand we can choose W_i to be a short pulse and examine the dynamics of the system in the time domain, which we will focus on here.

The parameter α is a short distance cut off parameter, characterising the smallest distance over which the fermions can be treated as a field of point particles. Including this parameter explicitly allows us to choose W_i to have units of energy and λ_i to be dimensionless. This cut off parameter will turn out to play a crucial role in ensuring that the perturbative expansion is well defined and that the resulting density matrix is positive.

The functions λ_i describe the spatial shape of the tunnelling potential into the wire. We will assume that they have the form of a nascent δ-function, i.e. that they are sharply peaked with λ_1 centred around 0 and λ_2 centred around the position x. For the most part we will assume that we can take the limit that the λ_is can be treated as a true δ-function, $\alpha\delta(y)$ or $\alpha\delta(y-x)$, and so, for brevity, omit the integral over space and write the fermionic fields as depending on fixed positions, but we will occasionally need to return to the full integral form in order to show that certain apparently divergent expressions are in fact finite.

We could consider a slight generalisation of this term, in which the functions $W_j(t)$ act differently on left and right moving electrons. In this case we would replace the current term

$$W_i \lambda_i \psi^\dagger(y) d_i + \text{h.c.} \to \sum_\nu W_{i,\nu} \lambda_i \psi_\nu^\dagger(y) d_i + \text{h.c.} \tag{4.5}$$

where $W_{i,\nu}$ now tell us how the pumping term acts on the left and right movers separately. It turns out that with this modification the calculations given below

carry through essentially unaltered. We will not do so, however, in the interests of not cluttering the notation.

Whilst for a true quantum wire $W_{i,\nu}$ will be the same for left and right movers, for other types of 1D system it could be engineered to be stronger for one species than the other. In a quantum Hall edge state, for example, a fixed magnetic field could be applied to bias the system to favour the production of one species of fermion over the other.

4.2 Time evolution of the density matrix

We will aim to calculate the reduced density matrix for the two impurities, tracing out the wire, as a function of time. From this we should be able to calculate any observable of interest for the two localised states. We should, therefore, be able to see how a change in the first state leads to a response in the second. By considering how the density matrix changes with time and the (assumed known) separation of the states we can infer how the influence of the quench spreads through the system.

We focus on the localised states, tracing out the wire degrees of freedom, as this suggests a concrete experimental realisation of how to achieve the desired real space resolved measurement and because this allows us to discard a large amount of largely irrelevant information, leading to a much simpler description.

The density matrix for the full system, including the wire, has a time evolution which can be written as

$$\rho_{\text{full}}(t) = \mathcal{U}(t,0)\rho_{\text{full}}(0)\ , \tag{4.6}$$

$$= U(t,0)\rho_{\text{full}}(0)U^{\dagger}(t,0)\ , \tag{4.7}$$

$$\mathcal{U}(t,0) = T\exp\left[\int_0^t \mathrm{d}\tau\, \mathcal{L}(\tau)\right]\ , \tag{4.8}$$

$$U(t,0) = T\exp\left[-\imath\int_0^t \mathrm{d}\tau\, H(\tau)\right]\ . \tag{4.9}$$

Here eq. (4.7) and eq. (4.9) are written in terms of the Hamiltonian and standard time evolution operator, whilst eq. (4.6) and eq. (4.8) are written in terms of the time evolution superoperator and the Liouvillian, $\mathcal{L}(t) = \imath[H(t),\ \cdot\ ]$. T denotes the standard time ordering operator.

We will work in an interaction picture, treating H_{pump} as a perturbation. Note that we are still treating the interaction in H_{int} exactly, thanks to the exact solvability of the FES problem (not to mention the fermion-fermion interactions). The key observation about this decomposition is that there is no term in the "free" part of the Hamiltonian which can change the occupation of the localised states. These can only be changed by the perturbing pump term. This will allow us to treat the interaction between the localised states and the Fermi sea as a fixed external potential. The turning on-and-off of this potential by H_{pump} can then be seen as a time dependence in this external potential; This

is the same trick used in the Nozières-de Dominicis solution [3]. We will write

$$U_{\text{fixed}}(t',t) = e^{-\imath(H_0+H_{\text{ee}}+H_{\text{inp}})(t'-t)} \,, \tag{4.10}$$

for the canonical mapping between the Schrödinger and interaction pictures.

It is convenient to write the interaction Liouvillian as a sum of terms related to state 1 and state 2.

$$\begin{aligned}\mathcal{L}_{\text{pump}}(t) &= \mathcal{L}_1(t) + \mathcal{L}_2(t) &(4.11)\\ &= -\imath\sqrt{\alpha}[W_1(t)\psi_\nu(0,t)^\dagger d_1(t) + W_1^*(t)d_1^\dagger(t)\psi_\nu(0,t),\ \cdot\,] \\ &\quad - \imath\sqrt{\alpha}[W_2(t)\psi_\nu(x,t)^\dagger d_1(t) + W_2^*(t)d_2^\dagger(t)\psi_\nu(x,t),\ \cdot\,]\,. &(4.12)\end{aligned}$$

We will consider a system initially in its ground state, so that all interactions between the localised state and the continuum are turned off (or alternatively have been fully screened and this has already been accounted for in the definitions of the fermionic fields). This state can be written, by construction, as a product state

$$\rho_{\text{full}} = |1\rangle\langle 1| \otimes |0\rangle\langle 0| \otimes \rho_{T=0}\,. \tag{4.13}$$

That is impurity state 1 is in the occupied state $|1\rangle$, state 2 is empty $|0\rangle$ and the wire is an undisturbed Fermi sea at zero temperature. The extension to finite temperature will be discussed in section 4.12.1.

We can now expand eq. (4.8) perturbatively.

$$\begin{aligned}\mathcal{U}(t,0) = 1 &+ T\int_0^t \mathrm{d}\tau_1\,(\mathcal{L}_1(\tau_1)+\mathcal{L}_2(\tau_1)) \\ &+ \frac{1}{2}T\iint_0^t \mathrm{d}\tau_1\,\mathrm{d}\tau_2\,(\mathcal{L}_1(\tau_1)+\mathcal{L}_2(\tau_1))(\mathcal{L}_1(\tau_2)+\mathcal{L}_2(\tau_2)) + \ldots \end{aligned}\tag{4.14}$$

If we assume that $W_1(t)$ and $W_2(t)$ have disjoint support and that there exists a time t_{mid} such that the support for W_2 consists of times strictly greater than t_{mid} and any time in the support of W_1 is strictly less than t_{mid} then we can write

$$\begin{aligned}\mathcal{U}(0,t) &= \mathcal{U}(t,t_{\text{mid}})\mathcal{U}(t_{\text{mid}},0) &(4.15)\\ &= T\exp\left[\int_{t_{\text{mid}}}^t \mathrm{d}\tau\,\mathcal{L}_2(\tau)\right]\exp\left[\int_0^{t_{\text{mid}}} \mathrm{d}\tau\,\mathcal{L}_1(\tau)\right]\,. &(4.16)\end{aligned}$$

This implies that all $\mathcal{L}_2$ terms be to the left of all $\mathcal{L}_1$ terms in eq. (4.14). From here on we will assume that $\mathcal{L}_1(\tau)$ is non-zero only on the interval $[0,t_1]$ and $\mathcal{L}_2(\tau)$ is non-zero only on the interval $[t_2,t]$, with $t > t_2 > t_1 > 0$. (Considering the density matrix for times earlier than t_2 simply gives the results of the standard FES with a single site and no new physics.)

We can now apply this operator to the initial density matrix ρ_{full} and evaluate term by term. The choice of initial state simplifies the resulting expression considerably, as only terms with creation operators acting on an empty state (or vice versa) do not vanish.

We are ultimately interested in ρ, the reduced density matrix for the localised states, not of the wire. To obtain this we trace out the wire degrees of freedom, writing $\mathrm{tr}_{\mathrm{wire}}[\dots]$ for the partial trace over the wire degrees of freedom. This allows us to obtain explicit expressions for the desired matrix elements and further simplifies the problem, as terms which are off diagonal in the wire particle number basis vanish.

In order to enumerate which terms survive, it is useful to employ a graphical notation. The particular notation needed here is referred to "double-sided Feynman diagrams" [99, 100].

We essentially need to enumerate the different ways to apply the perturbing operators to either the left or right of the density matrix. With that in mind we will draw a pair of lines representing the time evolution of the left and right sides of the density matrix. The upper line will represent the "forward" time evolution applied to the left of the density matrix and the lower line will represent the "backwards" time evolution applied to the right, as shown in Fig. 4.1(a). We can think of the initial state as being at the left hand side of the diagram, with the final state at the right hand end and real time increasing from left to right.

This can be compared to a tensor network diagram, shown in Fig. 4.1(b), where the initial density matrix has 2 "legs". Applying a time evolution operator to each leg results again in a matrix-type tensor, representing the final state. If we trace over the final state, we connect these 2 legs. If we then send the initial state back to $t = -\infty$ we recover the standard Keldysh contour, shown in Fig. 4.1(c).

Figure 4.1

(a) Empty double-sided Feynman diagram

(b) Tensor network diagram

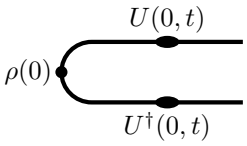

(c) Keldysh contour. Note in this case we trace over the final states

We can represent a perturbing operator by adding an arrow to one of the lines. As illustrated in Fig. 4.2, we will use an arrow pointing "out", away from the line, to represent exciting an electron out of a localised state, into the continuum, and an arrow pointing "in" to represent an operator that takes an electron out of the continuum and puts it into a localised state. We will write the arrows for electrons added at impurity 1 on the left hand end of the line and the arrows for electrons added at impurity 2 on the right hand end, with time advancing from left to right. Since we have restricted our attention to cases where the perturbation at impurity 1 is switched off before the perturbation at impurity 2 is switched on, there is no ambiguity in omitting the explicit information about where the electron is being added or removed, provided the two cases are clearly separated in time. Note that we do not connect these

arrows into loops, as we are merely keeping track of operators applied to the left (respectively right) of the density matrix. As all electrons are indistinguishable we cannot associate the electron added to the continuum at the first impurity site with the electron removed at second impurity site.

Figure 4.2: An example of a double sided Feynman diagram, representing the expectation $\mathrm{tr}_{\mathrm{wire}}\left[d_2(\tau_1)\psi^\dagger(x,\tau_1)\psi(x,\tau_2)d_2^\dagger(\tau_2)\psi^\dagger(0,\tau_3)d_1(\tau_3)\rho_{\mathrm{full}}d_1^\dagger(\tau_4)\psi(0,\tau_4)\right]$ with $\tau_1 \in [t_2, t]$, $\tau_2 \in [t_2, \tau_1]$ and $\tau_3, \tau_4 \in [0, t_1]$. The upward pointing arrow on the left end of the upper line corresponds to the excitation of an electron from state 1 on the forward time evolution $\psi^\dagger(0,\tau_3)d_1(\tau_3)$ and the downward pointing arrow on the left end of the lower line corresponds the same process on the backward time evolution, $d_1^\dagger(\tau_4)\psi(0,\tau_4)$. The pair of arrows on the right hand end of the upper line correspond to exciting and then deexciting an electron into state 2 on the forward time evolution $d_2(\tau_1)\psi^\dagger(x,\tau_1)\psi(x,\tau_2)d_2^\dagger(\tau_2)$. It can be seen that time advances from left to right across the diagram.

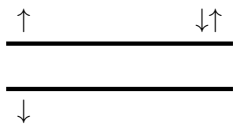

The simplifications due to the choice of initial state translate into restrictions on the allowed diagrams. The fact that we can only put an electron into a localised state if it is empty and vice versa implies that the arrows referring to a given localised state must alternate in and out. For our particular choice of initial state the arrows for state 1 must start pointing out and the arrows for state 2 must start pointing in. In addition, we have the requirement that when we take the trace over the continuum states, the number of electrons in the wire must be the same on both branches. This works out as a requirement that the total number of arrows pointing up must equal the total number pointing down.

With this calculus we can calculate the allowed terms in the perturbative expansion with reasonable efficacy.

If we examine the allowed diagrams there are 5 'fundamental' diagrams, shown in Fig. 4.3, which describe different allowed processes. All other diagrams can be obtained from the fundamental diagrams by adding pairs of arrows, that is we may remove and replace pairs of electrons, at each pulse on each branch.

The first diagram, Fig. 4.3(a), describes the vacuum contribution with no excitation of the localised states. The next two diagrams, Fig. 4.3(b) and 4.3(c), excite an electron (respectively hole) on each of the forward and backward branches. This electron(hole) is added to the wire. These two diagrams describe the excitations of one of the localised states, whilst dissipating the electron into the wire. The fourth diagram, Fig. 4.3(d), (and its time reversed counterpart) can be interpreted as transferring an electron from the first state to the second, thereby exciting both states. (It is worth noting, however, that due to the indistinguishably of electrons it can also be interpreted as, for example, adding

Figure 4.3: The five fundamental diagrams describing the possible processes when a pair of pulses are applied to the system.

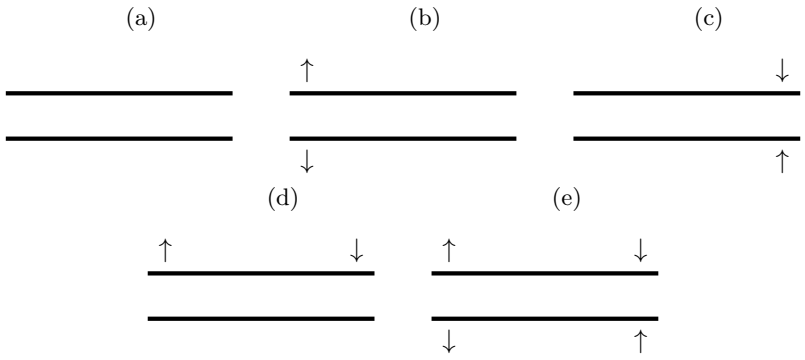

an electron to the wire in the first pulse and a hole in the second pulse, which then later annihilate each other.) The final diagram, Fig. 4.3(e) describes this process happening on both branches of the contour. All other diagrams represent renormalizations of these processes by exciting and deexciting the localised states repeatedly in the different pulses.

Writing out the terms of this expansion up to quadratic order (for brevity), corresponding to the first 4 diagrams in Fig. 4.3 plus diagrams adding a single absorption-emission pair to the first diagram, gives us the expression below.

$$
\begin{aligned}
\rho(t) =& \rho(0) - \alpha \int_0^{t_1} \mathrm{d}\tau_2 \int_0^{\tau_2} \mathrm{d}\tau_1 \, |W_1|^2 \Bigg[\\
&\quad \mathrm{tr}_{\mathrm{wire}} \Big[d_1^\dagger(\tau_2)\psi(0,\tau_2)\psi^\dagger(0,\tau_1)d_1(\tau_1)\rho_{\mathrm{full}}(0) \Big] \\
&+ \mathrm{tr}_{\mathrm{wire}} \Big[\rho_{\mathrm{full}}(0)\psi(0,\tau_1)d_1^\dagger(\tau_1)d_1(\tau_2)\psi^\dagger(0,\tau_2) \Big] \\
&- \mathrm{tr}_{\mathrm{wire}} \Big[\psi^\dagger(0,\tau_1)d_1(\tau_1)\rho_{\mathrm{full}}(0)d_1^\dagger(\tau_2)\psi(0,\tau_2) \Big] \\
&- \mathrm{tr}_{\mathrm{wire}} \Big[\psi^\dagger(0,\tau_2)d_1(\tau_2)\rho_{\mathrm{full}}(0)d_1^\dagger(\tau_1)\psi(0,\tau_1) \Big] \Bigg] \\
&- \alpha \int_{t_2}^{t} \mathrm{d}\tau_2 \int_{t_2}^{\tau_2} \mathrm{d}\tau_1 \, |W_2|^2 \Bigg[\\
&\quad \mathrm{tr}_{\mathrm{wire}} \Big[\psi^\dagger(x,\tau_2)d_2(\tau_2)d_2^\dagger(\tau_1)\psi(x,\tau_1)\rho_{\mathrm{full}}(0) \Big] \\
&+ \mathrm{tr}_{\mathrm{wire}} \Big[\rho_{\mathrm{full}}(0)d_2(\tau_1)\psi^\dagger(x,\tau_1)\psi(x,\tau_2)d_2^\dagger(\tau_2) \Big] \\
&- \mathrm{tr}_{\mathrm{wire}} \Big[d_2^\dagger(\tau_2)\psi(x,\tau_2)\rho_{\mathrm{full}}(0)d_2(\tau_1)\psi(x,\tau_1) \Big]
\end{aligned}
$$

$$
\begin{aligned}
&- \operatorname{tr}_{\text{wire}}\left[d_2^\dagger(\tau_1)\psi(x,\tau_1)\rho_{\text{full}}(0)\psi^\dagger(x,\tau_2)d_2(\tau_2)\right]\Bigg] \\
&- \alpha\int_{t_2}^{t}\mathrm{d}\tau_2\int_0^{t_1}\mathrm{d}\tau_1\Bigg[\\
&\quad W_1W_2\operatorname{tr}_{\text{wire}}\left[d_2^\dagger(\tau_2)\psi(x,\tau_2)\psi^\dagger(0,\tau_1)d_1(\tau_1)\rho_{\text{full}}(0)\right] \\
&\quad + W_1^*W_2^*\operatorname{tr}_{\text{wire}}\left[\rho_{\text{full}}(0)\psi(0,\tau_1)d_1^\dagger(\tau_1)d_2(\tau_2)\psi^\dagger(x,\tau_2)\right]\Bigg] + O(W_{j\nu}^4)
\end{aligned}
\tag{4.17}
$$

One of the key steps in the solution of the original Fermi edge problem by Nozières and De Dominicis [3] was the reduction to a single particle problem, by treating the interaction between the impurity and the Fermi sea as a time dependent potential acting on the metal, which turns on and off depending on the state of the impurity. This is possible due to the fact that nothing in the Hamiltonian, containing the energy of the fermions in the wire and the direct interaction between the wire and the localised states, can change the state of the local impurity.

We have constructed the Hamiltonian $H_0 + H_{\text{ee}} + H_{\text{int}}$ such that this is also true in our system; the state of the localised states can only change due to the action of the perturbing H_{pump}. We can, therefore, apply the same approach here. In our chosen initial state the interaction term is switched off. The state of the localised states only change when one of the d_j operators (or their Hermitian conjugates) is applied. We, therefore, can simply trace through the (forward and backward) time evolution, keeping track of the occupation of the localised states each time it changes and changing the Hamiltonian the fermions in the wire are subject to accordingly.

Each of the diagrams in Fig. 4.3 contributes to a single element of the final reduced density matrix, determined by the occupation numbers of the localised states at the end of each branch of the time evolution. Those diagrams with the same process happening on both branches correspond to diagonal elements of the density matrix, whilst those with different processes on each branch correspond off diagonal elements. Fig. 4.3(a) is a renormalization of the identity and so leave the density matrix in its original state. Figs. 4.3(b) and 4.3(c) correspond to diagonal elements with one of the localised states excited, that is both are unoccupied (if the first state was excited) or both are unoccupied (if the second state was excited). Fig. 4.3(d) has a different number of excitations on the upper and lower branches and so represents an off diagonal element of the density matrix, connecting the initial state (the empty lower branch) with the doubly excited state (represented by the pair of arrows on the upper branch). Fig. 4.3(e) has a similar double excitation on both the upper and lower branches, and so corresponds to the diagonal density matrix element with doubly excited states.

If we order our basis so that the localised states have occupation numbers

$[(0,0),(1,0),(0,1),(1,1)]$ the resulting density matrix has the form

$$\rho(t) = \begin{pmatrix} D_1 & 0 & 0 & 0 \\ 0 & A & F & 0 \\ 0 & F^* & B & 0 \\ 0 & 0 & 0 & D_2 \end{pmatrix} . \tag{4.18}$$

The A term represents the probability of the system remaining in its original state, whist B represents the probability of both states being excited with a net transfer of a fermion from the first localised state to the second. The terms D_1 and D_2 describe the probability of decoherence into the bath. Off diagonal terms F, on the other hand, represent a build up of coherence between the states of the 2 localised states.

It is convenient, when considering the calculation of the various correlation functions, to switch back to a Schrödinger picture, where it is easier to keep track explicitly of which Hamiltonian is to be used for a given segment of the time evolution. We will denote the Hamiltonian for the wire only, with the interaction with the localised states incorporated as an external potential as

$$h_{ij} = H_0 + H_{\text{ee}} + \delta_{1,i}E_1 + \delta_{1,j}E_2 + V_1\delta_{0,i}\psi^\dagger(0)\psi(0) + V_2\delta_{1,j}\psi^\dagger(x)\psi(x) , \tag{4.19}$$

with which we define the family of evolution operators

$$U_{ij}(t',t) = e^{-\imath h_{ij}(t'-t)} . \tag{4.20}$$

Here $i,j \in \{0,1\}$ denote the occupation of the first and second localised states respectively. If $i = 0$ the first localised state is unoccupied and the E_1 term vanishes, whilst the interaction with the wire is switch on. Conversely if $i = 1$ the E_1 energy offset is turned on, while the V_1 interaction term is not. The situation is similar of the second localised state and the j index, however in this case both the fixed E_2 term and the interaction potential are turned off when the site is unoccupied ($j = 0$) and turned on when it is occupied ($j = 1$).

We can now write an explicit expansion for each of the matrix elements. Note that in separating out the different matrix elements we have implicitly reduced the Hilbert space we are considering to only the wire. The expectations, therefore, represent a full trace, rather than a partial trace, and so we can use the cyclic property of the trace. This allows us to do two things.

Firstly we can bring expectation values with operators on the left, right or both sides of the density matrix into a common form, for definiteness with the density operator on the far right of the expression and all other operators to the left of it. In doing this we find that several expectation values that appeared different, and may indeed contribute to different matrix elements, evaluate to the same value. This is not, in fact, coincidental but a requirement for maintaining a unit trace; when summing terms from different matrix elements all terms other than the 1 from the initial state must cancel.

Secondly it allows us to cancel matching forward and backward time evolutions at the ends of each branch, simplifying the expressions obtained. Viewed

another way, by taking a full trace we have done exactly what is described in Fig. 4.1(c). By tracing over the system we have closed the contour and obtained a standard Keldysh contour, which we can distort in the usual manner. To fourth order we find that the matrix elements are

$$B = \int_0^{t_1} \mathrm{d}\tau_4 \int_{t_2}^{t} \mathrm{d}\tau_3 \int_{t_2}^{t} \mathrm{d}\tau_2 \int_0^{t_1} \mathrm{d}\tau_1 \Big[W_1^*(\tau_4) W_2(\tau_3) W_2^*(\tau_2) W_1(\tau_1) \\ \big\langle U_{1,0}(0,\tau_4)\psi(0)U_{0,0}(\tau_4,\tau_3)\psi^\dagger(x)U_{0,1}(\tau_3,\tau_2)\psi(x)U_{0,0}(\tau_2,\tau_1)\psi^\dagger(0)U_{1,0}(\tau_1,0)\big\rangle \Big] + O(W^6)\,, \tag{4.21}$$

$$\begin{aligned} F = &- \int_{t_2}^{t} \mathrm{d}\tau_2 \int_0^{t_1} \mathrm{d}\tau_1 \Big[W_2(\tau_2) W_1(\tau_1) \\ &\big\langle U_{1,0}(0,t)U_{0,1}(t,\tau_2)\psi(x)U_{0,0}(\tau_2,\tau_1)\psi^\dagger(0)U_{1,0}(\tau_1,0)\big\rangle \Big] \\ &+ \int_0^{t_1} \mathrm{d}\tau_4 \int_0^{\tau_4} \mathrm{d}\tau_3 \int_{t_2}^{t} \mathrm{d}\tau_2 \int_0^{t_1} \mathrm{d}\tau_1 \Big[W_1(\tau_4) W_1^*(\tau_3) W_2(\tau_2) W_1(\tau_1) \\ &\big\langle U_{1,0}(0,\tau_4)\psi(0)U_{0,0}(\tau_4,\tau_3)\psi^\dagger(0)U_{1,0}(\tau_3,t)U_{0,1}(t,\tau_2) \\ &\times \psi(x)U_{0,0}(\tau_2,\tau_1)\psi^\dagger(0)U_{1,0}(\tau_1,0)\big\rangle \Big] \\ &+ \int_0^{t_1} \mathrm{d}\tau_4 \int_0^{\tau_4} \mathrm{d}\tau_3 \int_{t_2}^{t} \mathrm{d}\tau_2 \int_0^{t_1} \mathrm{d}\tau_1 \Big[W_2^*(\tau_4) W_2(\tau_3) W_2(\tau_2) W_1(\tau_1) \\ &\big\langle U_{1,0}(0,\tau_4)\psi^\dagger(x)U_{1,1}(\tau_4,\tau_3)\psi(x)U_{1,0}(\tau_3,t)U_{0,1}(t,\tau_2) \\ &\times \psi(x)U_{0,0}(\tau_2,\tau_1)\psi^\dagger(0)U_{1,0}(\tau_1,0)\big\rangle \Big] + O(W^6) \end{aligned} \tag{4.22}$$

$$\begin{aligned} D_1 = &\int_0^{t_1} \mathrm{d}\tau_2 \int_0^{t_1} \mathrm{d}\tau_1 \Big[W_1(\tau_2) W_1^*(\tau_1) \\ &\big\langle U_{1,0}(0,\tau_2)\psi(0)U_{0,0}(\tau_2,\tau_1)\psi^\dagger(0)U_{1,0}(\tau_1,0)\big\rangle \Big] \\ &- \int_0^{t_1} \mathrm{d}\tau_4 \int_0^{t_1} \mathrm{d}\tau_3 \int_0^{\tau_3} \mathrm{d}\tau_2 \int_0^{\tau_2} \mathrm{d}\tau_1 \Big[W_1^*(\tau_4) W_1(\tau_3) W_1^*(\tau_2) W_1(\tau_1) \\ &\big\langle U_{1,0}(0,\tau_4)\psi(0)U_{0,0}(\tau_4,\tau_3)\psi^\dagger(0)U_{1,0}(\tau_3,\tau_2)\psi(0)U_{0,0}(\tau_2,\tau_1)\psi^\dagger(0)U_{1,0}(\tau_1,0)\big\rangle \Big] \\ &- \int_0^{t_1} \mathrm{d}\tau_4 \int_0^{\tau_4} \mathrm{d}\tau_3 \int_0^{\tau_3} \mathrm{d}\tau_2 \int_0^{t_1} \mathrm{d}\tau_1 \Big[W_1^*(\tau_4) W_1(\tau_3) W_1^*(\tau_2) W_1(\tau_1) \\ &\big\langle U_{1,0}(0,\tau_4)\psi(0)U_{0,0}(\tau_4,\tau_3)\psi^\dagger(0)U_{1,0}(\tau_3,\tau_2)\psi(0)U_{0,0}(\tau_2,\tau_1)\psi^\dagger(0)U_{1,0}(\tau_1,0)\big\rangle \Big] \\ &- \int_0^{t_1} \mathrm{d}\tau_4 \int_{t_2}^{t} \mathrm{d}\tau_3 \int_{t_2}^{\tau_3} \mathrm{d}\tau_2 \int_0^{t_1} \mathrm{d}\tau_1 \Big[W_1^*(\tau_4) W_2(\tau_3) W_2^*(\tau_2) W_1(\tau_1) \end{aligned}$$

$$\left\langle U_{1,0}(0,\tau_4)\psi(0)U_{0,0}(\tau_4,\tau_3)\psi^\dagger(x)U_{0,1}(\tau_3,\tau_2)\psi(x)U_{0,0}(\tau_2,\tau_1)\psi^\dagger(0)U_{1,0}(\tau_1,0)\right\rangle\Bigg]$$
$$-\int_0^{t_1}\mathrm{d}\tau_4\int_{t_2}^{t}\mathrm{d}\tau_3\int_{t_2}^{\tau_3}\mathrm{d}\tau_2\int_0^{t_1}\mathrm{d}\tau_1\Bigg[W_1^*(\tau_4)W_2(\tau_2)W_2^*(\tau_3)W_1(\tau_1)$$
$$\left\langle U_{1,0}(0,\tau_4)\psi(0)U_{0,0}(\tau_4,\tau_2)\psi^\dagger(0)U_{0,1}(\tau_2,\tau_3)\psi(0)U_{0,0}(\tau_3,\tau_1)\psi^\dagger(0)U_{1,0}(\tau_1,0)\right\rangle\Bigg]$$
$$+O(W^6) \tag{4.23}$$
$$D_2=\int_{t_2}^{t}\mathrm{d}\tau_2\int_{t_2}^{t}\mathrm{d}\tau_1\Bigg[W_2(\tau_2)W_2^*(\tau_1)$$
$$\left\langle U_{1,0}(0,\tau_2)\psi^\dagger(x)U_{1,1}(\tau_2,\tau_1)\psi(x)U_{1,0}(\tau_1,0)\right\rangle\Bigg]$$
$$-\int_{t_2}^{t}\mathrm{d}\tau_4\int_{t_2}^{t}\mathrm{d}\tau_3\int_0^{t_1}\mathrm{d}\tau_2\int_0^{\tau_2}\mathrm{d}\tau_1\Bigg[W_2(\tau_4)W_2^*(\tau_3)W_1(\tau_2)W_1^*(\tau_1)$$
$$\left\langle U_{1,0}(0,\tau_4)\psi^\dagger(x)U_{1,1}(\tau_4,\tau_3)\psi(x)U_{1,0}\psi(0)U_{0,0}(\tau_2,\tau_1)\psi^\dagger(0)U_{1,0}(\tau_1,0)\right\rangle\Bigg]$$
$$-\int_0^{t_1}\mathrm{d}\tau_4\int_0^{\tau_4}\mathrm{d}\tau_3\int_{t_2}^{t}\mathrm{d}\tau_2\int_{t_2}^{t}\mathrm{d}\tau_1\Bigg[W_1(\tau_4)W_1^*(\tau_3)W_2(\tau_2)W_2^*(\tau_1)$$
$$\left\langle U_{1,0}(0,\tau_4)\psi(0)U_{1,1}(\tau_4,\tau_3)\psi^\dagger(0)U_{1,0}\psi^\dagger(x)U_{0,0}(\tau_2,\tau_1)\psi(x)U_{1,0}(\tau_1,0)\right\rangle\Bigg]$$
$$-\int_{t_2}^{t}\mathrm{d}\tau_4\int_{t_2}^{t}\mathrm{d}\tau_3\int_{t_2}^{\tau_3}\mathrm{d}\tau_2\int_{t_2}^{\tau_2}\mathrm{d}\tau_1\Bigg[W_2(\tau_4)W_2^*(\tau_3)W_2(\tau_2)W_2^*(\tau_1)$$
$$\left\langle U_{1,0}(0,\tau_4)\psi^\dagger(x)U_{1,1}(\tau_4,\tau_3)\psi(x)U_{1,0}(\tau_3,\tau_2)\psi^\dagger(x)U_{1,1}(\tau_2,\tau_1)\psi^\dagger(x)U_{1,0}(\tau_1,0)\right\rangle\Bigg]$$
$$-\int_{t_2}^{t}\mathrm{d}\tau_4\int_{t_2}^{\tau_4}\mathrm{d}\tau_3\int_{t_2}^{\tau_2}\mathrm{d}\tau_2\int_{t_2}^{t}\mathrm{d}\tau_1\Bigg[W_2(\tau_4)W_2^*(\tau_3)W_2(\tau_2)W_2^*(\tau_1)$$
$$\left\langle U_{1,0}(0,\tau_2)\psi^\dagger(x)U_{1,1}(\tau_2,\tau_3)\psi(x)U_{1,0}(\tau_3,\tau_4)\psi^\dagger(x)U_{1,1}(\tau_4,\tau_1)\psi^\dagger(x)U_{1,0}(\tau_1,0)\right\rangle\Bigg]$$
$$+O(W^6) \tag{4.24}$$
$$A=1-\int_0^{t_1}\mathrm{d}\tau_2\int_0^{\tau_2}\mathrm{d}\tau_1\Bigg[W_1(\tau_2)W_1^*(\tau_1)$$
$$\left\langle U_{1,0}(0,\tau_2)\psi(0)U_{0,0}(\tau_2,\tau_1)\psi^\dagger(0)U_{1,0}(\tau_1,0)\right\rangle\Bigg]$$
$$-\int_0^{t_1}\mathrm{d}\tau_2\int_0^{\tau_2}\mathrm{d}\tau_1\Bigg[W_1(\tau_1)W_1^*(\tau_2)$$
$$\left\langle U_{1,0}(0,\tau_1)\psi(0)U_{0,0}(\tau_1,\tau_2)\psi^\dagger(0)U_{1,0}(\tau_2,0)\right\rangle\Bigg]$$
$$-\int_{t_2}^{t}\mathrm{d}\tau_2\int_{t_2}^{\tau_2}\mathrm{d}\tau_1\Bigg[W_1(\tau_2)W_1^*(\tau_1)$$

$$\left\langle U_{1,0}(0,\tau_2)\psi^\dagger(x)U_{1,1}(\tau_2,\tau_1)\psi(x)U_{1,0}(\tau_1,0)\right\rangle\Bigg]$$
$$-\int_{t_2}^{t}\mathrm{d}\tau_2\int_{t_2}^{\tau_2}\mathrm{d}\tau_1\Big[W_1(\tau_1)W_1^*(\tau_2)$$
$$\left\langle U_{1,0}(0,\tau_1)\psi^\dagger(x)U_{1,1}(\tau_1,\tau_2)\psi(x)U_{1,0}(\tau_2,0)\right\rangle\Bigg]$$
$$+\int_0^{t_1}\mathrm{d}\tau_4\int_0^{\tau_4}\mathrm{d}\tau_3\int_0^{\tau_3}\mathrm{d}\tau_2\int_0^{\tau_2}\mathrm{d}\tau_1\Big[W_1^*(\tau_4)W_1(\tau_3)W_1^*(\tau_2)W_1(\tau_1)$$
$$\left\langle U_{1,0}(0,\tau_4)\psi(0)U_{0,0}(\tau_4,\tau_3)\psi^\dagger(0)U_{1,0}(\tau_3,\tau_2)\psi(0)U_{0,0}(\tau_2,\tau_1)\psi^\dagger(0)U_{1,0}(\tau_1,0)\right\rangle\Bigg]$$
$$+\int_0^{t_1}\mathrm{d}\tau_4\int_0^{\tau_4}\mathrm{d}\tau_3\int_0^{t_1}\mathrm{d}\tau_2\int_0^{\tau_2}\mathrm{d}\tau_1\Big[W_1^*(\tau_3)W_1(\tau_4)W_1^*(\tau_2)W_1(\tau_1)$$
$$\left\langle U_{1,0}(0,\tau_3)\psi(0)U_{0,0}(\tau_3,\tau_4)\psi^\dagger(0)U_{1,0}(\tau_4,\tau_2)\psi(0)U_{0,0}(\tau_2,\tau_1)\psi^\dagger(0)U_{1,0}(\tau_1,0)\right\rangle\Bigg]$$
$$+\int_0^{t_1}\mathrm{d}\tau_4\int_0^{\tau_4}\mathrm{d}\tau_3\int_0^{\tau_3}\mathrm{d}\tau_2\int_0^{\tau_2}\mathrm{d}\tau_1\Big[W_1^*(\tau_1)W_1(\tau_2)W_1^*(\tau_3)W_1(\tau_4)$$
$$\left\langle U_{1,0}(0,\tau_1)\psi(0)U_{0,0}(\tau_1,\tau_2)\psi^\dagger(0)U_{1,0}(\tau_2,\tau_3)\psi(0)U_{0,0}(\tau_3,\tau_4)\psi^\dagger(0)U_{1,0}(\tau_4,0)\right\rangle\Bigg]$$
$$+\int_{t_2}^{t}\mathrm{d}\tau_4\int_{t_2}^{\tau_4}\mathrm{d}\tau_3\int_{t_2}^{\tau_3}\mathrm{d}\tau_2\int_{t_2}^{\tau_2}\mathrm{d}\tau_1\Big[W_2(\tau_4)W_2^*(\tau_3)W_2(\tau_2)W_2^*(\tau_1)$$
$$\left\langle U_{1,0}(0,\tau_4)\psi^\dagger(x)U_{1,1}(\tau_4,\tau_3)\psi(x)U_{1,0}(\tau_3,\tau_2)\psi^\dagger(x)U_{1,1}(\tau_2,\tau_1)\psi(x)U_{1,0}(\tau_1,0)\right\rangle\Bigg]$$
$$+\int_{t_2}^{t}\mathrm{d}\tau_4\int_{t_2}^{\tau_4}\mathrm{d}\tau_3\int_{t_2}^{t}\mathrm{d}\tau_2\int_{t_2}^{\tau_2}\mathrm{d}\tau_1\Big[W_2(\tau_3)W_2^*(\tau_4)W_2(\tau_2)W_2^*(\tau_1)$$
$$\left\langle U_{1,0}(0,\tau_3)\psi^\dagger(x)U_{1,1}(\tau_3,\tau_4)\psi(x)U_{1,0}(\tau_4,\tau_2)\psi^\dagger(x)U_{1,1}(\tau_2,\tau_1)\psi(x)U_{1,0}(\tau_1,0)\right\rangle\Bigg]$$
$$+\int_{t_2}^{t}\mathrm{d}\tau_4\int_{t_2}^{\tau_4}\mathrm{d}\tau_3\int_{t_2}^{\tau_3}\mathrm{d}\tau_2\int_{t_2}^{\tau_2}\mathrm{d}\tau_1\Big[W_2(\tau_1)W_2^*(\tau_2)W_2(\tau_3)W_2^*(\tau_4)$$
$$\left\langle U_{1,0}(0,\tau_1)\psi^\dagger(x)U_{1,1}(\tau_1,\tau_2)\psi(x)U_{1,0}(\tau_2,\tau_3)\psi^\dagger(x)U_{1,1}(\tau_3,\tau_4)\psi(x)U_{1,0}(\tau_4,0)\right\rangle\Bigg]$$
$$+\int_{t_2}^{t}\mathrm{d}\tau_4\int_{t_2}^{\tau_4}\mathrm{d}\tau_3\int_0^{t_1}\mathrm{d}\tau_2\int_0^{\tau_2}\mathrm{d}\tau_1\Big[W_2(\tau_4)W_2^*(\tau_3)W_1^*(\tau_2)W_1(\tau_1)$$
$$\left\langle U_{1,0}(0,\tau_4)\psi^\dagger(x)U_{1,1}(\tau_4,\tau_3)\psi(x)U_{1,0}(\tau_3,\tau_2)\psi(0)U_{0,0}(\tau_2,\tau_1)\psi^\dagger(0)U_{1,0}(\tau_1,0)\right\rangle\Bigg]$$
$$+\int_{t_2}^{t}\mathrm{d}\tau_4\int_{t_2}^{\tau_4}\mathrm{d}\tau_3\int_0^{t_1}\mathrm{d}\tau_2\int_0^{\tau_2}\mathrm{d}\tau_1\Big[W_2(\tau_3)W_2^*(\tau_4)W_1^*(\tau_2)W_1(\tau_1)$$
$$\left\langle U_{1,0}(0,\tau_3)\psi^\dagger(x)U_{1,1}(\tau_3,\tau_4)\psi(x)U_{1,0}(\tau_4,\tau_2)\psi(0)U_{0,0}(\tau_2,\tau_1)\psi^\dagger(0)U_{1,0}(\tau_1,0)\right\rangle\Bigg]$$

$$+\int_0^{t_1}\mathrm{d}\tau_4\int_0^{\tau_4}\mathrm{d}\tau_3\int_{t_2}^{t}\mathrm{d}\tau_2\int_{t_2}^{\tau_2}\mathrm{d}\tau_1\Big[W_1^*(\tau_3)W_1(\tau_4)W_2(\tau_2)W_2^*(\tau_1)$$
$$\left\langle U_{1,0}(0,\tau_3)\psi(0)U_{0,0}(\tau_3,\tau_4)\psi^\dagger(0)U_{1,0}(\tau_4,\tau_2)\psi^\dagger(x)U_{1,1}(\tau_2,\tau_1)\psi(x)U_{1,0}(\tau_1,0)\right\rangle\Big]$$
$$+\int_0^{t_1}\mathrm{d}\tau_4\int_0^{\tau_4}\mathrm{d}\tau_3\int_{t_2}^{t}\mathrm{d}\tau_2\int_{t_2}^{\tau_2}\mathrm{d}\tau_1\Big[W_1^*(\tau_3)W_2^*(\tau_4)W_2(\tau_1)W_1(\tau_2)$$
$$\left\langle U_{1,0}(0,\tau_3)\psi(0)U_{0,0}(\tau_3,\tau_4)\psi^\dagger(0)U_{1,0}(\tau_4,\tau_1)\psi^\dagger(x)U_{1,1}(\tau_1,\tau_2)\psi(x)U_{1,0}(\tau_2,0)\right\rangle\Big]$$
$$+O(W^6) \tag{4.25}$$

It can be explicitly verified that these expressions do satisfy the trace condition $A+B+D_1+D_2=1$ on an order by order basis. For example at 4th order A has ten contributing diagrams, and corresponding terms, of which three match two of the 4th order terms written down for D_1, whilst the remaining six match the four terms written down for D_2. The remaining diagrams for D_1 cancel with the single term for B. The diagrams do not cancel on a one to one basis as some diagrams allow for more flexibility in the time ordering than others. For example the 2nd order contribution to D_1 has a single diagram, with no constraint on the time ordering of the operators as they are on different branches of the contour. This cancels with a pair of diagrams in A, one for the time ordered and one for the anti-time ordered case.

The leading order term in F can be seen to have the form of the overlap between the state in which a fermion has been transferred from state 1 to state 2 and a state where no process has taken place, that is the Loschmidt amplitude of the process. This is analogous to the result in the standard Fermi edge that the Green's function for the impurity state is given by the Loschmidt amplitude for the evolution of the metal with and without the impurity present.

Multidimensional coherent spectroscopy experiments may be able to directly examine the response of the system described by eq. (4.21) to (4.25) [101–104]. These experiments use a series of carefully timed pulses to excite the system and then measure an emitted spectrum that depends not only on the frequency of the pumping pulses but also on the Fourier transforms of the differences between the times that the system was excited. For example the first term of eq. (4.22) would give a contribution to the second order response depending on the Fourier transforms of $\tau_2-\tau_1$ and $t-\tau_2$. The frequency of the driving pulses enters through W_1 and W_2, which would take the form

$$W_i(t)=e^{-\imath\omega_{\mathrm{pulse},i}t}f_i(t)\ , \tag{4.26}$$

where $\omega_{\mathrm{pulse},i}$ is the frequency of the pulse beam and $f_i(t)$ is the pulse shape. This dependence on (the Fourier conjugate of) multiple time parameters allows the influence of higher order response functions to be differentiated from the first order contribution, and so may allow effects that depend on time internal to the system, such as the time of flight for a signal between the localised states, to be measured directly.

4.3 Structure of the density matrix and eigenvalues

In order to study the entanglement structure of the system it will be helpful to calculate the eigenvalues and eigenvectors of this matrix. D_1 and D_2 are obviously eigenvalues. The remaining two eigenvalues and corresponding eigenstates can be found straightforwardly.

$$p_\pm = \frac{1}{2}\left(A + B \pm \sqrt{\chi}\right) . \tag{4.27}$$

$$v_\pm = \frac{1}{\mathcal{N}} \begin{pmatrix} 0 \\ 2F \\ A - B \mp \sqrt{\chi} \\ 0 \end{pmatrix} , \tag{4.28}$$

$$\mathcal{N}^2 = 2\left(\chi \mp (A-B)\sqrt{\chi}\right) , \tag{4.29}$$

$$\chi = (A-B)^2 + 4|F|^2 . \tag{4.30}$$

The requirements that the density matrix have unit trace and be positive semi-definite impose constraints on the matrix elements. These can be deduced from the eigenvalues

$$A = 1 - D_1 - D_2 - B , \tag{4.31}$$

$$D_1, D_2 \geq 0 , \tag{4.32}$$

$$A + B \geq 0 , \tag{4.33}$$

$$AB \geq |F|^2 . \tag{4.34}$$

Eq. (4.31) is the requirement for unit trace, whilst the remaining inequalities give the necessary and sufficient conditions for positivity of the density matrix. Eq. (4.33) is required for at least one of $p_\pm$ to be positive and, given eq. (4.33), the requirement for them both to be positive is $A + B \geq \sqrt{\chi}$, which reduces to eq. (4.34). Eq.(4.34) tells us that if we wish to observe any physics beyond simple dissipation, i.e. F is to be non-zero, we must also have that $B > 0$. The only fundamental diagram to contribute to B (and so the lowest order diagram to contribute to B at all), is, however, 4^{th} order in the W_j terms. We must, therefore, take the expansion in eq. (4.17) to at least 4th order to have any hope of achieving physically meaningful, non-trivial results.

4.4 Narrow Pulses

We will now specialise to the limit where each pulse narrows down to a δ-function. We will see below that the various correlation functions have the form of a product of power laws. The integrals of these power laws in eq. (4.21) to eq. (4.25) generally cannot be performed analytically but their asymptotic form is another (slightly modified) power law. By choosing the functions $W_i(t)$ to be a delta

pulse, however, we can perform the time integrals explicitly. We can view this as a process of taking a limit in which the range of the integration shrinks to zero, whilst increasing the weight in the remaining range so that the result does not vanish. Since both the initial integral and the final result have power law asymptotics, we might hope that many qualitative feature of the resulting long time physics should be unchanged. By considering a delta pulse we capture the quench physics central to the FES, whilst dramatically simplifying the problem.

We will, without loss of generality, assume that the first pulse occurs at time 0 and the second occurs at time $t > 0$. We will then calculate the density matrix for the system at the final time $t_f > t$.

In this limit we can resum the perturbation series eq. (4.14) to all orders and solve the evolution exactly.

We will begin by expanding out the expression for the interaction picture evolution operator. In the interests of conciseness we will make a slight abuse of notation and write

$$\begin{aligned}&\left(\alpha W_2 \delta(t_1 - t)\psi^\dagger(x_2, t_1)d_2 + \text{h.c.}\right)\left(\alpha W_2 \delta(t_2 - t)\psi^\dagger(x_2, t_2)d_2 + \text{h.c.}\right)\dots \\ &\cdots \times \left(\alpha W_2 \delta(t_n - t)\psi^\dagger(x_2, t_n)d_2 + \text{h.c.}\right) = \left(\alpha W_2 \delta(t_i - t)\psi^\dagger(x_2, t_i)d_2 + \text{h.c.}\right)^n .\end{aligned} \tag{4.35}$$

Taking advantage of the group property of the evolution operator we then have that

$$U(t_f, 0) = U(t_f, t/2)U(t/2, 0) \tag{4.36}$$

$$\begin{aligned}&= \sum_{n,m=0}^{\infty}\left[\frac{(-\imath)^{n+m}}{n!m!}\, T\int_{t/2}^{t_f} \mathrm{d}t_1 \dots \mathrm{d}t_n \, \left(\alpha W_2 \delta(t_i - t)\psi^\dagger(x_2, t_i)d_2 + \text{h.c.}\right)^n \right. \\ &\qquad \left. \times T\int_0^{t/2} \mathrm{d}t_1 \dots \mathrm{d}t_m \, \left(\alpha W_1 \delta(t_i)\psi^\dagger(x_1, t_i)d_1 + \text{h.c.}\right)^m\right]\end{aligned} \tag{4.37}$$

$$= T\sum_{n,m=1}^{\infty} \frac{(-\imath)^{n+m}}{n!m!}\left(\alpha W_2 \psi^\dagger(x_2, t)d_2 + \text{h.c.}\right)^n \left(\alpha W_1 \psi^\dagger(x_1, 0)d_1 + \text{h.c.}\right)^m . \tag{4.38}$$

We will consider the cubic and higher terms in this expansion. Our aim to to find a reduction formula to collapse the higher order terms in the series. If we expand out the spatial distribution of where the electron is injected into the wire, as in eq. (4.4), we find that

$$\begin{aligned}&\left(\alpha W_j \psi^\dagger(x_j, t)d_j + \text{h.c.}\right)^3 \\ &= \int \mathrm{d}x_1\, \mathrm{d}x_2\, \mathrm{d}x_3 \left[\alpha^{-3/2}\lambda_j(x_1)\lambda_j(x_2)\lambda_j(x_3)\right. \\ &\qquad \left. \times \left(W_j^2 W_j^* \psi^\dagger(x_1, t)\psi(x_2, t)\psi^\dagger(x_3, t)d_j d_j^\dagger d_j + \text{h.c}\right)\right]\end{aligned} \tag{4.39}$$

$$= \int \mathrm{d}x_1\, \mathrm{d}x_2\, \mathrm{d}x_3\, \alpha^{-3/2} \lambda_j(x_1)\lambda_j(x_2)\lambda_j(x_3)$$
$$\times \left(W_j^2 W_j^* \left(\delta(x_1 - x_2) - \psi(x_2,t)\psi^\dagger(x_1,t) \right) \psi^\dagger(x_3,t) d_j d_j^\dagger d_j + \text{h.c} \right) \quad (4.40)$$
$$= \left(|W_j|^2 \int \frac{\mathrm{d}x_2}{\alpha} \lambda_j^2(x_2) \right) \int \mathrm{d}x_3\, \alpha^{-1/2} \lambda_j(x_1) \left(W_j \psi^\dagger(x_3,t) d_j + \text{h.c} \right) \quad (4.41)$$
$$= w_j^2 \left(\alpha W_j \psi^\dagger(x_j,t) d_j + \text{h.c.} \right) \ , \quad (4.42)$$

where w_j is defined by

$$w_j^2 = \left(|W_j|^2 \int \frac{\mathrm{d}x_2}{\alpha} \lambda_j^2(x_2) \right) \ . \quad (4.43)$$

We have, therefore, expressed the third order term in terms of the first order term and the constants w_j. Note that it is necessary to consider at least third order terms; at lower orders the term resulting from anticommuting the fermion operators past each other in eq. (4.40) does not vanish.

With this we can collect even and odd ordered terms together and resum the series in eq. (4.38) to obtain

$$U(t,0) = \left(1 - \imath\alpha\gamma_2 W_2 \psi^\dagger(x_2,t) d_2 - \alpha^2 \beta_2 |W_2|^2 d_2^\dagger \psi(x_2,t) \psi^\dagger(x_2,t) d_2 + \text{h.c.} \right)$$
$$\times \left(1 - \imath\alpha\gamma_1 W_1 \psi^\dagger(x_1,0) d_1 - \alpha^2 |W_1|^2 \beta_1 d_1^\dagger \psi(x_1,0) \psi^\dagger(x_1,0) d_1 + \text{h.c.} \right) \ , \quad (4.44)$$

where

$$\gamma_j = \frac{\sin w_j}{w_j} \ , \quad (4.45)$$
$$\beta_j = \frac{1 - \cos w_j}{w_j^2} \ . \quad (4.46)$$

These coefficients γ_j and β_j obey a non-trivial relationship, which is essential for ensuring trace preservation of the density matrix.

$$\gamma_i^2 + w_i^2 \beta_i^2 = \left(\frac{\sin w_i}{w_i} \right)^2 + w_i^2 \left(\frac{1 - \cos w_i}{w_i^2} \right)^2 \quad (4.47)$$
$$= \frac{1}{w_i^2} \left(\sin^2 w_i + \cos^2 w_i - 2\cos w_i + 1 \right) \quad (4.48)$$
$$= \frac{2}{w_i^2} \left(1 - \cos w_i \right) \ . \quad (4.49)$$
$$= 2\beta_i \ . \quad (4.50)$$

We can now apply this U to the full density matrix and move back to the Schrödinger picture by multiplying by U_{fixed} (or $U_{\text{fixed}}^\dagger$ as appropriate), giving us

$\rho_{\text{full}}(t_f)$

$$
\begin{aligned}
&= U_{\text{fixed}}(t_f,0) \\
&\times \left(1 - \imath\alpha\gamma_2 W_2 \psi^\dagger(x_2,t)d_2 - \alpha^2\beta_2|W_2|^2 d_2^\dagger\psi(x_2,t)\psi^\dagger(x_2,t)d_2 + \text{h.c.}\right) \\
&\times \left(1 - \imath\alpha\gamma_1 W_1 \psi^\dagger(x_1,0)d_1 - \alpha^2|W_1|^2\beta_1 d_1^\dagger\psi(x_1,0)\psi^\dagger(x_1,0)d_1 + \text{h.c.}\right) \\
&\times \rho(0)\left(1 + \imath\alpha\gamma_1 W_1 \psi^\dagger(x_1,0)d_1 - \alpha^2|W_1|^2\beta_1 d_1^\dagger\psi(x_1,0)\psi^\dagger(x_1,0)d_1 + \text{h.c.}\right) \\
&\times \left(1 + \imath\alpha\gamma_2 W_2 \psi^\dagger(x_2,t)d_2 - \alpha^2\beta_2|W_2|^2 d_2^\dagger\psi(x_2,t)\psi^\dagger(x_2,t)d_2 + \text{h.c.}\right) \\
&\times U_{\text{fixed}}^\dagger(t_f,0)\ . \qquad (4.51)
\end{aligned}
$$

Finally we can trace out the wire degrees of freedom and move to a formalism treating the interaction between the localised states and the fermions in the wire as a time dependent external potential, as we did in the case of a finite width pulse. This allows us to obtain an exact expression for the reduced density matrix.

$$
\begin{aligned}
B &= \alpha^4\gamma_1^2\gamma_2^2|W_1|^2|W_2|^2 C_3\ , && (4.52)\\
F &= \alpha^2\gamma_2\gamma_1 W_2 W_1 F_1 - \alpha^4\gamma_2\gamma_1\beta_1 W_2 W_1|W_1|^2 F_2 \\
&\quad - \alpha^4\gamma_2\gamma_1\beta_2 W_2 W_1|W_2|^2 F_3 + \alpha^6\gamma_2\gamma_1\beta_2\beta_1 W_2 W_1|W_2|^2|W_1|^2 F_4\ , && (4.53)\\
D_1 &= \alpha^2\gamma_1^2|W_1|^2 C_1^{(1)} + \alpha^4\gamma_1^2\left(w_2^2\beta_2^2 - 2\beta_2\right)|W_2|^2|W_1|^2 C_3\ , && (4.54)\\
D_2 &= \alpha^2\gamma_2^2|W_2|^2 C_1^{(2)} - 2\alpha^4\gamma_2^2\beta_1|W_1|^2|W_2|^2\text{Re}\left[C_2\right] + \alpha^6\gamma_2^2\beta_1^2|W_1|^4|W_2|^2 C_4\ , && (4.55)\\
A &= 1 + \alpha^2(w_1^2\beta_1^2 - 2\beta_1)|W_1|^2 C_1^{(1)} + \alpha^2(w_2^2\beta_2^2 - 2\beta_2)|W_2|^2 C_1^{(2)} \\
&\quad + 2\alpha^4\beta_1(2\beta_2 - w_2\beta_2^2)|W_1|^2|W_2|^2\text{Re}\left[C_2\right] \\
&\quad + \alpha^6\beta_1^2(w_2^2\beta_2^2 - 2\beta_2)|W_1|^4|W_2|^2 C_4\ , && (4.56)
\end{aligned}
$$

in terms of the correlation functions

$$
\begin{aligned}
C_1^{(1)} &= \left\langle \psi(0)\psi^\dagger(0)\right\rangle\ , && (4.57)\\
C_1^{(2)} &= \left\langle U_{1,0}(0,t)\psi^\dagger(x)\psi(x)U_{1,0}(t,0)\right\rangle\ , && (4.58)\\
C_2 &= \left\langle U_{1,0}(0,t)\psi^\dagger(x)\psi(x)U_{1,0}(t,0)\psi(0)\psi^\dagger(0)\right\rangle\ , && (4.59)\\
C_3 &= \left\langle \psi(0)U_{0,0}(0,t)\psi^\dagger(x)\psi(x)U_{0,0}(t,0)\psi^\dagger(0)\right\rangle\ , && (4.60)\\
C_4 &= \left\langle \psi(0)\psi^\dagger(0)U_{1,0}(0,t)\psi^\dagger(x)\psi(x)U_{1,0}(t,0)\psi^\dagger(0)\psi(0)\right\rangle\ , && (4.61)\\
F_1 &= \left\langle U_{1,0}(0,t_f)U_{0,1}(t_f,t)\psi(x)U_{0,0}(t,0)\psi^\dagger(0)\right\rangle\ , && (4.62)\\
F_2 &= \left\langle \psi(0)\psi^\dagger(0)U_{1,0}(0,t_f)U_{0,1}(t_f,t)\psi(x)U_{0,0}(t,0)\psi^\dagger(0)\right\rangle\ , && (4.63)\\
F_3 &= \left\langle U_{1,0}(0,t)\psi^\dagger(x)\psi(x)U_{1,0}(t,t_f)U_{0,1}(t_f,t)\psi(x)U_{0,0}(t,0)\psi^\dagger(0)\right\rangle\ , && (4.64)\\
F_4 &= \left\langle \psi(0)\psi^\dagger(0)U_{1,0}(0,t)\psi^\dagger(x)\psi(x)U_{1,0}(t,t_f)U_{0,1}(t_f,t)\psi(x)U_{0,0}(t,0)\psi^\dagger(0)\right\rangle\ . && (4.65)
\end{aligned}
$$

We have, therefore, an explicit expression for the reduced density matrix in terms of a reasonable small set of correlators. It can been checked explicitly that the trace preservation equation is satisfied due to eq. (4.50). All we must do now is evaluate the various correlation functions.

4.5 Bosonization

To compute the various correlation functions appearing in our calculation of the density matrix we will employ a bosonization approach, as outlined in section 3.1. When expressed in terms of the bosonized operators we can write (omitting the Klein factors)

$$\psi_r(x,t) = \sum_{r=\pm 1} \frac{1}{\sqrt{2\pi\alpha}} e^{r\imath k_F x} e^{-\frac{\imath}{2}\sum_{\nu=\pm 1}(r+\frac{\nu}{K})\tilde{\varphi}_\nu(x-\nu u t)} \ . \tag{4.66}$$

When written in terms of the bosonized operators H_0 and H_{ee} take the standard Luttinger liquid form of eq. (3.62)

$$H_0 + H_{\text{ee}} = \frac{u}{2K}\sum_\nu \int \frac{\mathrm{d}y}{2\pi} \left(\nabla\tilde{\varphi}_\nu(y)\right)^2 \ , \tag{4.67}$$

whilst the interaction Hamiltonian takes the form

$$H_{\text{int}} = \frac{V_{1f}}{2\pi} d_1 d_1^\dagger \sum_\nu \nabla\tilde{\varphi}_\nu(0) + \frac{V_{2f}}{2\pi} d_2^\dagger d_2 \sum_\nu \nabla\tilde{\varphi}_\nu(x) \ , \tag{4.68}$$

where we have for the moment neglected the possibility of backscattering off the localised states. The backscattering terms have the form

$$\frac{V_{ib}}{\pi\alpha}\cos\left(\tilde{\varphi}_+(0) + \tilde{\varphi}_-(0)\right) \ , \tag{4.69}$$

which is a transcendental function of the bosonic fields and prevents us from analytically solving the system. This is in general relevant, in the renormalisation group sense, and in the standard FES leads to contribution of $-\frac{1}{8}$ to the OC power law decay, independent of the potential strength. This contribution, however, is seen in the long time limit and it takes time for the many-body correlations that lead to this renormalised contribution to develop. The time scale for the development of these correlations is given by [77]

$$t_{i,\text{back}} = V_{ib}^{-1}\left[V_{ib}\alpha u\right]^{\frac{K}{1-K}} \ , \tag{4.70}$$

where V_{ib} if the backscattering contribution of the potential V_i, that is the part of the potential which scatters states with a momentum difference $\sim 2k_F$. The time scales $t_{i,\text{back}}$ depend on the strength of the backscattering impurity, but also strongly depend on the interactions in the Luttinger liquid. In particular $t_{i,\text{back}}$ diverges as $K \to 1$ from below, that is the non-interacting limit of a Luttinger liquid with attractive interactions. We can, therefore, tune the system

so the backscattering interactions can be safely neglected on the time scales of interest by requiring that the interactions in the Luttinger liquid be sufficiently weak and attractive. Alternatively, we can consider a system where the backscattering term identically vanishes. This can be achieved by considering chiral quantum Hall or helical edge states, where backscattering is prevented by spin conservation. We will discuss the impact of backscattering off the impurity in Section 4.12.2.

When we move to the external potential picture of the interaction potential this becomes

$$H_{\text{int}} = \frac{V_{1f}(t)}{2\pi} \sum_{\nu} \nabla\tilde{\varphi}_{\nu}(0) + \frac{V_{2f}(t)}{2\pi} \sum_{\nu} \nabla\tilde{\varphi}_{\nu}(x) \, . \tag{4.71}$$

We can, as in chapter 3.1.1 and reference [65], map the combined Hamiltonian back to the Luttinger liquid Hamiltonian by a unitary 'shift' operator.

$$R_j = e^{\imath \frac{1}{K} \frac{\delta_j}{\pi} \sum_{\nu=\pm 1} \nu \tilde{\varphi}_{\nu}(x_j)} \, , \tag{4.72}$$

$$R_j^{\dagger} \tilde{\varphi}_{\nu}(x) R_j = \tilde{\varphi}_{\nu}(x) - \frac{\delta_j}{2} \operatorname{sgn}(x - x_j) \, , \tag{4.73}$$

$$R_j^{\dagger} \left(\nabla\tilde{\varphi}_{\nu}(x)\right) R_j = \tilde{\varphi}_{\nu}(x) - \delta_j \delta(x - x_j) \, , \tag{4.74}$$

$$R_1^{\dagger} h_{0,i} R_1 = h_{1,i} - E_1 + \frac{u\delta_1^2}{2\alpha K} \, , \tag{4.75}$$

$$R_2^{\dagger} h_{i,1} R_2 = h_{i,0} + E_2 + \frac{u\delta_2^2}{2\alpha K} \, , \tag{4.76}$$

where $x_1 = 0$, $x_2 = x$, $\delta_i = \frac{KV_{if}}{u}$ is the scattering phase shift from the impurity in the Born approximation and h_{ij} were defined in eq. (4.19). The last two term on the right hand side of each of eq. (4.75) and eq. (4.76) are constant shifts in the Hamiltonian, and so only contributes a phase. We define

$$\Delta E_1 = -E_1 + \frac{u\delta_1^2}{2\alpha K} \, , \tag{4.77}$$

$$\Delta E_2 = E_2 + \frac{u\delta_2^2}{2\alpha K} \, , \tag{4.78}$$

giving the constant energy shift due to having each of the localised states excited.

With this we can calculate the expectation values in eq. (4.57) to (4.65). We can write the correlation functions we are interested in as a product of fermionic operators and shift operators time evolving under the Hamiltonian without the impurity potential present.

For example we can write

$$F_1 = \left\langle U_{1,0}(0, t_f) U_{0,1}(t_f, t) \psi(x) U_{0,0}(t, 0) \psi^{\dagger}(0) \right\rangle \tag{4.79}$$

$$= e^{-\imath \Delta E_1 t_f} e^{-\imath \Delta E_2 (t_f - t)} \times \left\langle U_{1,0}(0, t_f) R_1^{\dagger} R_2^{\dagger} U_{1,0}(t_f, t) R_2 R_1 \psi(x) R_1^{\dagger} U_{1,0}(t, 0) R_1 \psi^{\dagger}(0) \right\rangle \tag{4.80}$$

$$= e^{-\imath\Delta E_1 t_f} e^{-\imath\Delta E_2 (t_f - t)} \left\langle R_1^\dagger(t_f) R_2^\dagger(t_f) R_2(t) R_1(t) \psi(x,t) R_1^\dagger(t) R_1(0) \psi^\dagger(0,0) \right\rangle \tag{4.81}$$

where $R_j(t) = U_{1,0}(0,t) R_j U_{1,0}(t,0)$ so that the time evolution in the last line is entirely due to the Hamiltonian $h_{1,0}$, that is the standard Luttinger liquid Hamiltonian. When the correlator is expressed in this form we can see the reason for our choice to express the bosonized fields in terms of the normal mode operators $\tilde{\varphi}_\nu$. Since the time evolution of these operators under $h_{1,0}$ is simply given by

$$U_{1,0}(0,t) \tilde{\varphi}_\nu(x) U_{1,0}(t,0) = \tilde{\varphi}_\nu(x - \nu u t) \, , \tag{4.82}$$

that is the left moving mode simply travels to the left and vice versa, we can directly see the various signals propagating through the system when expressed in these terms.

Since both $R_j(t)$ and $\psi(x,t)$ have the form of an exponential in the bosonized formalism, these expectations can be evaluated using the general machinery of Bosonization discussed in section 3.1. By repeated application of the formulae

$$e^P e^Q = e^{\frac{1}{2}[P,Q]} e^{P+Q} \, , \tag{4.83}$$

$$\left\langle e^P \right\rangle = e^{\frac{1}{2}\langle P^2 \rangle} \, , \tag{4.84}$$

valid when P and Q are linear combinations of bosonic operators, we can find an explicit expression for this correlator. More generally we can consider a product of n exponentials

$$\prod_{i=1}^{n} e^{\imath \sum_\nu A_{i,\nu} \tilde{\varphi}_\nu(x_i)} \tag{4.85}$$

where the x_i are all distinct and

$$\sum_{i=1}^{n} A_{i,\nu} = 0 \tag{4.86}$$

for $\nu = \pm 1$. It can be shown [24] that the expectation in eq. (4.85) vanishes if this constraint is not satisfied. Its role is to ensure that all divergent terms in the bosonic expectation values cancel as they should. We can now write

$$\begin{aligned} &\left\langle \prod_{i=1}^{n} e^{\imath \sum_\nu A_{i,\nu} \tilde{\varphi}_\nu(x_i)} \right\rangle \\ &= \left\langle e^{-\frac{1}{2}\sum_\nu A_{1\nu} A_{2,\nu} [\tilde{\varphi}_\nu(x_1), \tilde{\varphi}_\nu(x_2)]} e^{\imath \sum_\nu A_{1_\nu} \tilde{\varphi}_\nu(x_1) + A_{2_\nu} \tilde{\varphi}_\nu(x_2)} \prod_{i=3}^{n} e^{\imath \sum_\nu A_{i,\nu} \tilde{\varphi}_\nu(x_i)} \right\rangle \\ &= \exp\left(-\frac{1}{2} \sum_\nu \sum_{i<j} A_{i,\nu} A_{j,\nu} [\tilde{\varphi}_\nu(x_i), \tilde{\varphi}_\nu(x_j)] \right) \end{aligned} \tag{4.87}$$

$$\times \left\langle \exp\left(\imath \sum_{\nu,i} A_{i,\nu} \tilde{\varphi}_\nu(x_i) \right) \right\rangle \tag{4.88}$$

$$= \exp\left(-\frac{1}{2} \sum_\nu \sum_{i<j} A_{i,\nu} A_{j,\nu} [\tilde{\varphi}_\nu(x_i), \tilde{\varphi}_\nu(x_j)] \right) \times \exp\left(-\frac{1}{2} \sum_\nu \left\langle \left(\sum_i A_{i,\nu} \tilde{\varphi}_\nu(x_i) \right)^2 \right\rangle \right) , \tag{4.89}$$

where we have used the fact that the expectation $\langle \tilde{\varphi}_+(x) \tilde{\varphi}_-(y) \rangle$ vanishes. We now consider the exponent term

$$\left(\sum_i A_{i,\nu} \tilde{\varphi}_\nu(x_i) \right)^2 = \sum_i A_{i,\nu}^2 \tilde{\varphi}_\nu^2(x_i) + \sum_{i \neq j} A_{i,\nu} A_{j,\nu} \tilde{\varphi}_\nu(x_i) \tilde{\varphi}_\nu(x_j) \tag{4.90}$$

$$= \sum_i A_{i,\nu}^2 \tilde{\varphi}_\nu^2(x_i) + \sum_{i \neq j} A_{i,\nu} A_{j,\nu} \Big[\tilde{\varphi}_\nu(x_i) \tilde{\varphi}_\nu(x_j) + \frac{1}{2} \tilde{\varphi}_\nu^2(x_i) - \frac{1}{2} \tilde{\varphi}_\nu^2(x_i) + \frac{1}{2} \tilde{\varphi}_\nu^2(x_j) - \frac{1}{2} \tilde{\varphi}_\nu^2(x_j) \Big] \tag{4.91}$$

$$= \sum_i A_{i,\nu}^2 \tilde{\varphi}_\nu^2(x_i) + \frac{1}{2} \sum_{i \neq j} A_{i,\nu} A_{j,\nu} \left(\tilde{\varphi}_\nu^2(x_i) + \tilde{\varphi}_\nu^2(x_j) \right) - \frac{1}{2} \sum_{i \neq j} A_{i,\nu} A_{j,\nu} \left[\tilde{\varphi}_\nu^2(x_i) - 2 \tilde{\varphi}_\nu(x_i) \tilde{\varphi}_\nu(x_j) + \tilde{\varphi}_\nu^2(x_j) \right] \tag{4.92}$$

$$= \sum_i A_{i,\nu}^2 \tilde{\varphi}_\nu^2(x_i) + \sum_{i \neq j} A_{i,\nu} A_{j,\nu} \tilde{\varphi}_\nu^2(x_i) - \sum_{i<j} A_{i,\nu} A_{j,\nu} \left[\tilde{\varphi}_\nu^2(x_i) - 2 \tilde{\varphi}_\nu(x_i) \tilde{\varphi}_\nu(x_j) + \tilde{\varphi}_\nu^2(x_j) \right] + \sum_{i>j} A_{i,\nu} A_{j,\nu} [\tilde{\varphi}_\nu(x_i), \tilde{\varphi}_\nu(x_j)] \tag{4.93}$$

$$= \sum_i A_{i,\nu} \left(\sum_j A_{j,\nu} \right) \tilde{\varphi}_\nu^2(x_i) - \sum_{i<j} A_{i,\nu} A_{j,\nu} \left(\tilde{\varphi}_\nu(x_i) - \tilde{\varphi}_\nu(x_j) \right)^2 - \sum_{i<j} A_{i,\nu} A_{j,\nu} [\tilde{\varphi}_\nu(x_i), \tilde{\varphi}_\nu(x_j)] . \tag{4.94}$$

The first term in eq. (4.94) vanishes by eq. (4.86). The final term cancels with the commutator in eq. (4.89). This leaves only the middle term, which has a well

defined expectation value given by eq. (3.71). Plugging this back into eq. (4.89) we find that

$$\left\langle \prod_{i=1}^{n} e^{\imath \sum_\nu A_{i,\nu}\tilde{\varphi}_\nu(x_i)} \right\rangle = \exp\left[\frac{1}{2} \sum_{\nu=\pm 1} \sum_{1\leq i<j\leq n} A_{i,\nu}A_{j,\nu} \left\langle (\tilde{\varphi}_\nu(x_i) - \tilde{\varphi}_\nu(x_j))^2 \right\rangle \right] . \tag{4.95}$$

With this result we can systematically evaluate many of the correlation functions we have encountered. A key advantage of using eq. (4.95) over direct application of the formulae eqs. (4.83) and (4.84) is that evaluation of eq. (4.95) can be straightforwardly automated by computational algebra engines, allowing the large number of distinct correlation functions we have encountered to be efficiently evaluated. All of our results obtained in this way have been validated by comparing with independently written numerical codes.

In principle these techniques can be used to evaluate all of the correlation functions that appear eqs. (4.21) to (4.25). We will not perform a thorough analysis of these, however, and will instead focus on the correlation functions in section 4.4, as the result is more physically transparent.

When calculating the correlation functions listed at the end of section 4.4, care must be taken when considering operators at equal times and positions. For example, if we consider $C_1^{(2)}$, naively plugging in eq. (4.66) we find that

$$\left\langle U_{1,0}(0,t)\psi^\dagger(x)\psi(x)U_{1,0}(t,0)\right\rangle \stackrel{?}{=} \frac{1}{2\pi\alpha} \tag{4.96}$$

when clearly the correct result is the fermion density $C_1^{(2)} = \frac{N}{L} + \frac{1}{\pi}\sum_\nu \langle \nabla\tilde{\varphi}_\nu(x - \nu u t)\rangle$. (In this case the second term vanishes, but it is important in more complex correlators and far less obvious than the first term.)

In these cases, formally, a point splitting procedure must be applied to obtain the correct result. In practice the simplest method of evaluating these types of correlators is to rewrite the correlation function by bringing together pairs of fermionic operators, evaluated at the same position and time, to form fermion density operators, the form of which is a standard result. As the density operator can be expressed in terms of the gradient of the bosonic operators (eq. (3.70)), we can sidestep explicit point splitting in practice. (This problem can be ignored in the case of a finite width pulse as the set of points where this problem occurs has measure zero and can be taken care of by treating the principal value of the integrals.) We will go through this procedure in detail in the next section.

Instead of appealing to a point splitting procedure, we could have expanded the pump terms in terms of the functions $\lambda_i(x)$. This would have separated the coincident points in the correlation function, allowing us to evaluate them directly. In this approach taking the limit that we take the width of the pulse to zero is essentially equivalent to point splitting, but is somewhat less transparent; as the width of the pulses is reduced, spatial coordinates will be brought together as in point splitting, however it is less immediately obvious that the resulting divergence corresponds to the ground state density, or that further density fluctuations should be included.

As the point splitting procedure converts pairs of fermionic operators, which are exponential in the bosonic fields, into fermion density operators, which are linear in the (gradients of) bosonic operators, it can result in correlation functions which contain a mixture of terms which are linear and terms which are exponential in the bosonic fields. We will therefore have to deal with terms of this form. For example the correlator F_3 leads to correlation functions of the form

$$\Big\langle \nabla\tilde{\varphi}_\nu(x,t) R_2^\dagger(t_f) R_1^\dagger(t_f) R_1(t) R_2(t) \\ e^{-\frac{\imath}{2}\sum_{\nu'}\left(r+\frac{\nu'}{K}\right)\tilde{\varphi}_{\nu'}(x-\nu' u t)} R_1^\dagger(t) R_1(0) e^{\frac{\imath}{2}\sum_{\nu'}\left(r+\frac{\nu'}{K}\right)\tilde{\varphi}_{\nu'}(0)} \Big\rangle \tag{4.97}$$

which has a term linear in $i\nabla\tilde{\varphi}_\nu$ in addition to the exponential terms. To evaluate correlation functions of this form we can explicitly (boson) normal order the operators. This reduces the correlator to a part which vanishes due to normal ordering and a number of commutators [72]. Since the commutators of bosonic operators are c-numbers, we can then easily separate the linear and exponential terms into parts that can be evaluated independently. For example, consider the operator

$$P e^{\imath Q} \tag{4.98}$$

where P and Q are linear combinations of bosonic operators. (The correlation function in expression eq. (4.97) can be brought to this form.) Writing P_+ and P_- for the creation and annihilation parts of P respectively, and similarly for Q, we can write

$$P e^{\imath Q} = (P_+ + P_-) e^{\imath Q_+} e^{\imath Q_-} e^{\frac{1}{2}[Q_+, Q_-]} \tag{4.99}$$

$$= e^{\imath Q_+} \left(P_+ + P_- + \left[P_-, e^{\imath Q_+}\right]\right) e^{\imath Q_-} e^{\frac{1}{2}[Q_+, Q_-]} \,. \tag{4.100}$$

Since $[P_-, Q_+] \in \mathbb{C}$ we can use the relation[1]

$$[P_-, f(Q_+)] = [P_-, Q_+] f'(Q_+) \,, \tag{4.104}$$

where f is an analytic function of Q_-. Applying this to the exponential above we find

$$P e^{\imath Q} = e^{\imath Q_+} \left(P_+ + P_- + \imath[P_-, Q_+]\right) e^{\imath Q_-} e^{\frac{1}{2}[Q_+, Q_-]} \,. \tag{4.105}$$

[1] We can prove this relation by Taylor expanding f

$$[P_-, f(Q_+)] = \sum_n \frac{f^{(n)}(0)}{n!} [P_-, Q_+^n] \tag{4.101}$$

$$= \sum_n \frac{f^{(n)}(0)}{n!} n [P_-, Q_+] Q_+^{n-1} \tag{4.102}$$

$$= [P_-, Q_+] f'(Q_+) \,, \tag{4.103}$$

where on the second line we have used that $[P_-, Q_+] \in \mathbb{C}$ to commute it past the Q_+s obtained by expanding the commutator.

This expression is boson normal ordered, so its expectation can be found trivially. Noting that

$$[P_-, Q_+] = \langle PQ \rangle \ , \tag{4.106}$$

$$e^{\frac{1}{2}[Q_+, Q_-]} = \left\langle e^{\imath Q} \right\rangle \tag{4.107}$$

$$= e^{-\frac{1}{2}\langle Q^2 \rangle} \ , \tag{4.108}$$

we can rewrite eq. (4.105) as

$$e^{\imath Q_+} \left(P_+ + P_- + \imath \langle PQ \rangle \right) e^{\imath Q_-} \left\langle e^{Q} \right\rangle \ , \tag{4.109}$$

in which the exponential and linear correlation functions have been separated, as desired. Similar methods can be applied to more complex correlation functions and we will do so explicitly in the next section.

4.6 Correlation Functions

In this section we will explicitly evaluate the correlation functions introduced in the last two sections.

The leading order terms in in D_1 and D_2 have the forms

$$\left\langle \psi(x,t)\psi^\dagger(x,t) \right\rangle \ , \tag{4.110}$$

$$\left\langle \psi^\dagger(x,t)\psi(x,t) \right\rangle \ , \tag{4.111}$$

respectively these are simply the hole and particle densities in the wire. We therefore have

$$C_1^{(1)} = \Lambda - \frac{N}{L} \ , \tag{4.112}$$

$$C_1^{(2)} = \frac{N}{L} \ , \tag{4.113}$$

where $\Lambda \sim \frac{1}{\alpha}$ is the bandwidth.

The C_2 correlator is the standard correlation function between the fermion and hole densities. Using the canonical anticommutation relations we have that

$$C_2 = \Lambda C_1^{(2)} - \left\langle \psi^\dagger(x,t)\psi(x,t)\psi^\dagger(0,0)\psi(0,0) \right\rangle \tag{4.114}$$

$$= \Lambda \frac{N}{L} - \sum_{r_1,r_2,r_3,r_4=\pm 1} e^{\imath k_F (r_1 - r_2)x} \left\langle \psi^\dagger_{r_1}(x,t)\psi_{r_2}(x,t)\psi^\dagger_{r_3}(0,0)\psi_{r_4}(0,0) \right\rangle \tag{4.115}$$

$$= \left(\Lambda - \frac{N}{L} \right) \frac{N}{L} - \frac{1}{2\pi} \sum_\nu \langle \nabla\tilde{\varphi}_\nu(x - \nu u t) \nabla\tilde{\varphi}_\nu(0) \rangle$$

$$- \frac{1}{(2\pi\alpha)^2} \sum_{r=\pm 1} e^{2r\imath k_F x} \left\langle e^{-\imath \sum_{\nu=\pm 1} r\tilde{\varphi}_\nu(x - \nu u t)} e^{\imath \sum_{\nu=\pm 1} r\tilde{\varphi}_\nu(0)} \right\rangle \tag{4.116}$$

$$= \left(\Lambda - \frac{N}{L}\right)\frac{N}{L} - \frac{K}{2\pi}\frac{x^2+(\imath\eta+ut)^2}{(x^2-(\imath\eta+ut)^2)^2} + \frac{1}{2\pi}\alpha^{2K-2}\cos(2k_F x)(\eta+\imath(ut-x))^{-K}(\eta+\imath(ut+x))^{-K} \ , \quad (4.117)$$

where η is the usual short time cut off that is required to ensure the convergence of the real time correlation functions in field theory, distinguishing the different Green's functions. In principle this is distinct from the cut off, α, that arises in the bosonization procedure. In practice both cut offs are typically set by the bandwidth and can often be taken to be equal.

Evaluating the function C_3 is more subtle. First we must separate the different possible combinations of left and right moving components.

$$C_3 = \left\langle \psi(0)U_{0,0}(0,t)\psi^\dagger(x)\psi(x)U_{0,0}(t,0)\psi^\dagger(0)\right\rangle \quad (4.118)$$

$$= \sum_{r=\pm 1}\left(C_3^{(1)r} + C_3^{(2)r} + C_3^{(3)r}\right) \quad (4.119)$$

$$C_3^{(1)r} = \left\langle \psi_r(0)U_{0,0}(0,t)\psi_r^\dagger(x)\psi_r(x)U_{0,0}(t,0)\psi_r^\dagger(0)\right\rangle \quad (4.120)$$

$$C_3^{(2)r} = \left\langle \psi_r(0)U_{0,0}(0,t)\psi_{-r}^\dagger(x)\psi_{-r}(x)U_{0,0}(t,0)\psi_r^\dagger(0)\right\rangle \quad (4.121)$$

$$C_3^{(3)r} = \left\langle \psi_r(0)U_{0,0}(0,t)\psi_{-r}^\dagger(x)\psi_r(x)U_{0,0}(t,0)\psi_{-r}^\dagger(0)\right\rangle \ . \quad (4.122)$$

All other combinations vanish, as they do not satisfy eq. (4.86), i.e. the coefficients for the bosonic fields in the exponents do not sum to zero. The last term above, $C_3^{(3)r}$, does not contain any fermionic operators with the same position, time and chirality and so can be evaluated directly via eq. (4.95) yielding

$$C_3^{(3)r} = \frac{1}{4\pi^2}\alpha^{2K-2}e^{-2\imath k_F r x}(\eta-\imath x)^{\frac{2\delta_1 r}{\pi}}(\eta+\imath x)^{-\frac{2\delta_1 r}{\pi}} \times \prod_{\nu=\pm 1}(\eta-\imath(x-\nu ut))^{-\frac{K-r}{2}-r\frac{\delta_1}{\pi}}(\eta+\imath(x-\nu ut))^{-\frac{K+r}{2}+r\frac{\delta_1}{\pi}} \ . \quad (4.123)$$

It is worth noting that time reversing this expression is equivalent to making the substitution $r \to -r$, so the sum of this expression over r is a real quantity.

To evaluate the other two terms we cannot immediately apply eq. (4.95) due to the presence of fermionic operators at the same space-time point and point splitting considerations. To overcome these issues we must first collect fermionic operators together into density operators. To do this we must first commute one of the fermionic operators at time 0 past the pair of operators at time t to bring it to the other operator at time 0. In effect we must move it from one branch of the Keldysh contour to the other. To do this we first consider the operator

$$U_{0,0}(0,t)\psi_r^\dagger(x)\psi_r(x)U_{0,0}(t,0)$$

$$= R_1^\dagger U_{1,0}(0,t) R_1 \left(\frac{N}{2L} - \frac{1}{4\pi} \sum_{\nu=\pm 1} r \left(r + \frac{\nu}{K} \right) \nabla \tilde{\varphi}_\nu(x) \right) R_1^\dagger U_{1,0}(t,0) R_1 \tag{4.124}$$

$$= \frac{N}{2L} - \frac{r}{4\pi} \sum_{\nu=\pm 1} \left(r + \frac{\nu}{K} \right) \left(\nabla \tilde{\varphi}_\nu(x - \nu u t) + \imath \nu \frac{\delta_1}{\pi K} \left[\nabla \tilde{\varphi}_\nu(x), \tilde{\varphi}_\nu(0) \right] \right.$$
$$\left. - \imath \nu \frac{\delta_1}{\pi K} \left[\nabla \tilde{\varphi}_\nu(x - \nu u t), \tilde{\varphi}_\nu(-\nu u t) \right] \right) \tag{4.125}$$

where in the last line we have employed eq. (4.74) and eq. (4.82) in succession. Notice that we have written the commutators in the shifts in an unevaluated form. We could evaluate these as in eq. (4.74) to arrive at δ-functions, however if this is done naively we will end up with naked δ-functions in our final density matrix. Formally the δ-functions should be treated by expanding the δ-functions in the pump terms and doing the proper integral over the $\lambda(x)$. This would amount to replacing the δ functions with λs, however since the $\lambda(x)$ are assumed to have a width on the order of the cut off distance, it is reasonable to assume that other cut off dependent processes may come into play. We will therefore express the commutator in the following way

$$\left[\nabla \tilde{\varphi}_\nu(x - \nu u t), \tilde{\varphi}_\mu(y - \nu u \tau) \right] = \left\langle \left[\nabla \tilde{\varphi}_\nu(x - \nu u t), \tilde{\varphi}_\nu(y - \nu u \tau) \right] \right\rangle \tag{4.126}$$
$$= \left\langle \nabla \tilde{\varphi}_\nu(x - \nu u t) \tilde{\varphi}_\nu(y - \nu u \tau) \right\rangle - \left\langle \tilde{\varphi}_\nu(y - \nu u \tau) \nabla \tilde{\varphi}_\nu(x - \nu u t) \right\rangle \tag{4.127}$$
$$= K \delta_{\nu\mu} \left(\frac{1}{x - \nu u t - y + \nu u \tau + \imath \nu \eta} - \frac{1}{x - \nu u t - y + \nu u \tau - \imath \nu \eta} \right) \tag{4.128}$$
$$= \frac{2 \imath K \nu \delta_{\nu\mu} \eta}{(x - \nu u t - y + \nu u \tau)^2 + \eta^2} \tag{4.129}$$
$$= 2\pi \imath K \nu \delta_{\nu\mu} \xi_\nu(x - y, t - \tau) \, . \tag{4.130}$$

We recognise the function $\xi_\nu(x,t) = \frac{1}{\pi} \frac{\eta}{(x - \nu u t)^2 + \eta^2}$ as a nascent Dirac δ, which will give back the expected δ-function in the limit that $\eta \to 0$, which formally it must do. If, however, we introduce a cut off, represented by keeping η and α at some finite value, we will instead get a sharply peaked function with a width on the order of the cut off. In effect this procedure has told us which nascent δ-function is the correct way to represent the cut off physics.

We must now commute one of the outer fermionic operators past the central density operator so that it can be combined with the matching fermionic operator on the other side to form a second density operator.

We will also need that

$$\left[- \frac{1}{4\pi} \sum_{\mu=\pm 1} \left(1 + \frac{r\mu}{K} \right) \nabla \tilde{\varphi}_\mu(x - \mu u t), e^{\frac{\imath}{2} \sum_{\nu=\pm 1} (r' + \frac{\nu}{K}) \tilde{\varphi}_\nu(0)} \right]$$
$$= - \frac{\imath}{8\pi} \sum_{\mu,\nu=\pm 1} \left(1 + \frac{r\mu}{K} \right) \left(r' + \frac{\nu}{K} \right) \nabla \left[\tilde{\varphi}_\mu(x - \mu u t), \tilde{\varphi}_\nu(0) \right] e^{\frac{\imath}{2} \sum_{\nu=\pm 1} (r' + \frac{\nu}{K}) \tilde{\varphi}_\nu(0)} \tag{4.131}$$

$$= \frac{1}{4\pi} \sum_{\nu=\pm 1} \left(1 + \frac{r\nu}{K}\right) (K\nu r' + 1) \frac{\eta}{(x - \nu u t)^2 + \eta^2} e^{\frac{\imath}{2} \sum_{\nu'=\pm 1} \left(r' + \frac{\nu'}{K}\right) \tilde{\varphi}_{\nu'}(0)} \tag{4.132}$$

$$= \frac{1}{4} \sum_{\nu=\pm 1} \left(1 + \frac{r\nu}{K}\right) (K\nu r' + 1) \, \xi_\nu(x,t) e^{\frac{\imath}{2} \sum_{\nu'=\pm 1} \left(r' + \frac{\nu'}{K}\right) \tilde{\varphi}_{\nu'}(0)} \tag{4.133}$$

$$\xrightarrow{\eta \to 0} \frac{1}{4} e^{\frac{\imath}{2} \sum_{\nu'=\pm 1} \left(r' + \frac{\nu'}{K}\right) \tilde{\varphi}_{\nu'}(0)} \sum_{\nu=\pm 1} \left(1 + rr' + \nu \left(\frac{r}{K} + Kr'\right)\right) \delta(x - \nu u t) \, , \tag{4.134}$$

with which we obtain

$$\begin{aligned} \psi_r(0) \psi^\dagger_{r'}(x,t) \psi_{r'}(x,t) = \psi^\dagger_{r'}(x,t) \psi_{r'}(x,t) \psi_r(0) \\ + \sum_{\nu=\pm 1} \frac{1 + rr' + \nu \left(\frac{r}{K} - Kr'\right)}{4} \xi_\nu(x,t) \psi_r(0) \, . \end{aligned} \tag{4.135}$$

Finally then, we find that

$$\begin{aligned} C_3 = \sum_{r=\pm 1} \Bigg[& \left\langle \psi_r(0) U_{0,0}(0,t) \psi^\dagger_r(x) \psi_r(x) U_{0,0}(t,0) \psi^\dagger_r(0) \right\rangle \\ & + \left\langle \psi_r(0) U_{0,0}(0,t) \psi^\dagger_{-r}(x) \psi_{-r}(x) U_{0,0}(t,0) \psi^\dagger_r(0) \right\rangle \\ & + \left\langle \psi_r(0) U_{0,0}(0,t) \psi^\dagger_{-r}(x) \psi_r(x) U_{0,0}(t,0) \psi^\dagger_{-r}(0) \right\rangle \Bigg] \end{aligned} \tag{4.136}$$

$$\begin{aligned} = & \left(\Lambda - \frac{N}{L}\right) \frac{N}{L} + \frac{K}{2\pi} \frac{x^2 + (\imath\eta + ut)^2}{(x^2 - (\imath\eta + ut)^2)^2} \\ & + \frac{1}{2\pi^2} \alpha^{2K-2} \mathrm{Re} \Bigg[e^{-2\imath k_F r x} \left(\eta - \imath x\right)^{\frac{2\delta_1 r}{\pi}} \left(\eta + \imath x\right)^{-\frac{2\delta_1 r}{\pi}} \\ & \quad \times \prod_{\nu=\pm 1} \left(\eta - \imath(x - \nu u t)\right)^{-\frac{K-r}{2} - r\frac{\delta_1}{\pi}} \left(\eta + \imath(x - \nu u t)\right)^{-\frac{K+r}{2} + r\frac{\delta_1}{\pi}} \Bigg] \\ & + \frac{1}{2} \sum_{r=\pm 1} \left[\left(\frac{\Lambda}{2} - \frac{N_r}{L}\right) \sum_{\nu=\pm 1} \left(\left(\frac{\delta_1}{\pi} + (1 - Kr)\right) \xi_\nu(x,t) - \frac{\delta_1}{\pi} \xi_\nu(x,0) \right) \right] . \end{aligned} \tag{4.137}$$

The correlation function C_4 has the form of a product of fermion and hole densities, so we can perform the point splitting procedure immediately.

$$C_4 = \langle \psi(0,0) \psi^\dagger(0,0) \psi^\dagger(x,t) \psi(x,t) \psi(0,0) \psi^\dagger(0,0) \rangle \tag{4.138}$$

$$= \sum_{r_1, r_2, r_3 = \pm 1} \left\langle \left(\frac{1}{2}\Lambda - \frac{N_{r_1}}{L} + \frac{1}{4\pi} \sum_{\nu=\pm 1} \left(1 + \frac{r_1 \nu}{K}\right) \nabla \tilde{\varphi}_\nu(0) \right.\right.$$

$$+\psi_{r_1}(0,0)\psi^\dagger_{-r_1}(0,0)\Big)$$
$$\times\left(\frac{N_{r_2}}{L}-\frac{1}{4\pi}\sum_{\nu=\pm1}\left(1+\frac{r_2\nu}{K}\right)\nabla\tilde{\varphi}_\nu(x-\nu ut)+\psi^\dagger_{r_2}(x,t)\psi_{-r_2}(x,t)\right)$$
$$\times\left(\frac{1}{2}\Lambda-\frac{N_{r_3}}{L}+\frac{1}{4\pi}\sum_{\nu=\pm1}\left(1+\frac{r_3\nu}{K}\right)\nabla\tilde{\varphi}_\nu(0)+\psi_{r_3}(0,0)\psi^\dagger_{-r_3}(0,0)\right)\Bigg\rangle \tag{4.139}$$

$$=\frac{N}{L}\left(\Lambda-\frac{N}{L}\right)^2-\frac{1}{2\pi^2}\left(\Lambda-\frac{N}{L}\right)\sum_{\nu=\pm1}\mathrm{Re}\left[\langle\nabla\tilde{\varphi}_\nu(x-\nu ut)\nabla\tilde{\varphi}_\nu(0)\rangle\right]$$
$$+\frac{1}{4\pi^2}\frac{N}{L}\sum_{\nu=\pm1}\langle\nabla\tilde{\varphi}_\nu(0)\nabla\tilde{\varphi}_\nu(0)\rangle$$
$$+2\sum_{r=\pm1}\mathrm{Re}\Bigg[\Bigg\langle\left(\Lambda-\frac{N}{L}+\frac{1}{2\pi}\sum_{\nu=\pm1}\nabla\tilde{\varphi}_\nu(0)\right)$$
$$\times\psi^\dagger_r(x,t)\psi_{-r}(x,t)\psi_r(0,0)\psi^\dagger_{-r}(0,0)\Bigg\rangle\Bigg]$$
$$+\sum_{r=\pm1}\Bigg\langle\psi_r(0,0)\psi^\dagger_{-r}(0,0)\left(\frac{N}{L}-\frac{1}{2\pi}\sum_{\nu=\pm1}\nabla\tilde{\varphi}_\nu(x-\nu ut)\right) \tag{4.140}$$
$$\times\psi_{-r}(0,0)\psi^\dagger_r(0,0)\Bigg\rangle\,. \tag{4.141}$$

The first two terms in eq. (4.141) are straightforward to deal with.

The third term is formally divergent like $O\left(\frac{1}{\eta^2}\right)$, however this does not present a serious problem. The correlation function C_4 does not appear until 6th order in αW in the matrix elements, so this divergence can be interpreted as saying that the diagrams that contributed to C_4 can be resummed to give a contribution which is 4th order in α and η. Alternatively we can observe that the variance in the density of left/right movers is given by

$$\sigma^2_{\rho_r}=-\frac{1}{4\pi}\sum_{\nu=\pm1}\left(1+\frac{r\nu}{K}\right)\langle\nabla\tilde{\varphi}_\nu(0)\nabla\tilde{\varphi}_\nu(0)\rangle\ . \tag{4.142}$$

Since we cannot resolve distances smaller that the cut off distance, the density of left (respectively right) movers has an upper bound on the order of $\frac{N_r}{\alpha}$. This implies that $\sigma^2_{\rho_r}$ has an upper bound $\frac{N_r^2}{\alpha^2}$. This is not, therefore necessarily an unphysical value for this correlator.

The fourth term in eq. (4.141) contains a mixture of operators that are linear and exponential in the bosonic operators. Therefore, whilst the $\Lambda-\frac{N}{L}$ term can be evaluated using eq. (4.95), we must resort to eq. (4.218) to evaluate the term

with the linear bosonic contribution.

$$\sum_{r=\pm 1}\left\langle\left(\Lambda-\frac{N}{L}+\frac{1}{2\pi}\sum_{\nu=\pm 1}\nabla\tilde{\varphi}_\nu(0)\right)\psi_r^\dagger(x,t)\psi_{-r}(x,t)\psi_r(0,0)\psi_{-r}^\dagger(0,0)\right\rangle$$

$$=\sum_{r=\pm 1}\frac{1}{4\pi^2}\alpha^{2K-2}e^{-2\imath k_F r x}\left(\Lambda-\frac{N}{L}+\frac{Kr}{2\pi}\left[\sum_{\nu=\pm 1}\frac{1}{x-\nu ut-\nu\imath\eta}\right]\right)$$
$$\times\prod_{\nu=\pm 1}\left(\eta-\nu\imath(x-\nu tu)\right)^{-K} \tag{4.143}$$

$$=\frac{1}{2\pi^2}\alpha^{2K-2}\left(\left[\Lambda-\frac{N}{L}\right]\cos(2k_Fx)-\imath\sin(2k_Fx)\frac{K}{\pi}\frac{x}{x^2-(ut-\imath\eta)^2}\right)$$
$$\times\left(x^2-(ut-\imath\eta)^2\right)^{-K}\ . \tag{4.144}$$

The final term in eq. (4.141) requires us to perform some further point splitting in order to obtain an expression we can evaluate

$$\left\langle\psi_r(0,0)\psi_{-r}^\dagger(0,0)\left(\frac{N}{L}-\frac{1}{2\pi}\sum_{\nu=\pm 1}\nabla\tilde{\varphi}_\nu(x-\nu ut)\right)\psi_{-r}(0,0)\psi_r^\dagger(0,0)\right\rangle$$

$$=\left\langle\left(\frac{N}{L}-\frac{1}{2\pi}\sum_{\nu=\pm 1}\nabla\tilde{\varphi}_\nu(x-\nu ut)-\frac{K}{2}\sum_{\nu=\pm 1}r\nu\xi_\nu(x,t)\right)\right.$$
$$\left.\times\,\psi_r(0,0)\psi_{-r}^\dagger(0,0)\psi_{-r}(0,0)\psi_r^\dagger(0,0)\right\rangle \tag{4.145}$$

$$=\left\langle\left(\frac{N}{L}-\frac{1}{2\pi}\sum_{\nu=\pm 1}\nabla\tilde{\varphi}_\nu(x-\nu ut)-\frac{K}{2}\sum_{\nu=\pm 1}r\nu\xi_\nu(x,t)\right)\right.$$
$$\left.\times\,\psi_r(0,0)\left(\frac{N_{-r}}{L}-\frac{1}{4\pi}\sum_{\nu=\pm 1}\left(1-\frac{r\nu}{K}\right)\nabla\tilde{\varphi}_\nu(0)\right)\psi_r^\dagger(0,0)\right\rangle \tag{4.146}$$

$$=\left\langle\left(\frac{N}{L}-\frac{1}{2\pi}\sum_{\nu=\pm 1}\nabla\tilde{\varphi}_\nu(x-\nu ut)-\frac{K}{2}\sum_{\nu=\pm 1}r\nu\xi_\nu(x,t)\right)\right.$$
$$\times\left(\frac{1}{2}\Lambda-\frac{N_r}{L}+\frac{1}{4\pi}\sum_{\nu=\pm 1}\left(1+\frac{\nu r}{K}\right)\nabla\tilde{\varphi}_\nu(0)\right)$$
$$\left.\times\left(\frac{N_{-r}}{L}-\frac{1}{4\pi}\sum_{\nu=\pm 1}\left(1-\frac{r\nu}{K}\right)\nabla\tilde{\varphi}_\nu(0)-\frac{1}{4}\sum_{\nu=\pm 1}\left(r+\frac{\nu}{K}\right)\nu\xi_\nu(0,0)\right)\right\rangle \tag{4.147}$$

$$=\left(\frac{1}{2}\Lambda-\frac{N_r}{L}\right)\left(\frac{N_{-r}}{L}-\frac{1}{2}\frac{1}{\eta K}\right)\left(\frac{N}{L}-\frac{K}{2}\sum_{\nu=\pm 1}r\nu\xi_\nu(x,t)\right)$$
$$+\frac{1}{8\pi^2}\sum_{\nu=\pm 1}\left[\left(\left(\frac{N_{-r}}{L}-\frac{1}{2}\frac{1}{K\eta}\right)\left(1+\frac{r\nu}{K}\right)^2-\left(\frac{1}{2}\Lambda-\frac{N_r}{L}\right)\left(1-\frac{1}{K^2}\right)\right)\right.$$

$$\times \langle \nabla\tilde{\varphi}_\nu(x-\nu ut)\nabla\tilde{\varphi}_\nu(0)\rangle \Big]$$
$$- \left(\frac{N}{L} - \frac{K}{2}\sum_{\nu'=\pm 1} r\nu' \xi_{\nu'}(x,t)\right)\left(1-\frac{1}{K^2}\right)\sum_{\nu=\pm 1}\langle \nabla\tilde{\varphi}_\nu(0)\nabla\tilde{\varphi}_\nu(0)\rangle \ . \tag{4.148}$$

Putting this together we find that

$$\begin{aligned} C_4 = {} & \frac{N}{L}\left(\Lambda - \frac{N}{L}\right)^2 + \frac{N}{L}\frac{2}{\eta^2}\left[\left(K-\frac{1}{K}\right) - \frac{K}{4\pi^2}\right] \\ & - \frac{K}{\pi^2}\left(\Lambda - \frac{N}{L}\right)\sum_{\nu=\pm 1}\frac{1}{(x-\nu ut)^2+\eta^2} \\ & + \frac{1}{\pi^2}\alpha^{(K-\frac{1}{K})(K+1-\frac{1}{K})}\mathrm{Re}\Bigg[\Bigg(\left[\Lambda - \frac{N}{L}\right]\cos(2k_F x) \\ & \quad - \imath \sin(2k_F x)\frac{K}{\pi}\frac{x}{x^2-(ut-\imath\eta)^2}\Bigg)\left(x^2-(ut-\imath\eta)^2\right)^{-K}\Bigg] \\ & + \sum_{r=\pm 1}\left(\frac{1}{2}\Lambda - \frac{N_r}{L}\right)\left(\frac{N_{-r}}{L} - \frac{1}{2}\frac{1}{\eta K}\right)\left(\frac{N}{L} - \frac{K}{2}\sum_{\nu=\pm 1} r\nu\xi_\nu(x,t)\right) \\ & + \frac{1}{8\pi^2}\sum_{\nu=\pm 1}\frac{\left(\frac{N}{L}-\frac{1}{K\eta}\right)\left(K+\frac{1}{K}\right) - \left(\Lambda - \frac{N}{L}\right)\left(K-\frac{1}{K}\right) + 2\nu\frac{J}{L}}{(x-\nu ut+\nu\imath\eta)^2}\ , \end{aligned} \tag{4.149}$$

where $J = N_r - N_{-r}$ is the ground state current.

The F_1 correlator was briefly discussed in section 4.5. It will be convenient to split it into two terms, corresponding to respectively left and right moving fermions being transferred.

$$F_1 = \sum_{r=\pm 1} F_1^r \tag{4.150}$$
$$F_1^r = \left\langle U_{1,0}(0,t_f)U_{0,1}(t_f,t)\psi_r(x)U_{0,0}(t,0)\psi_r^\dagger(0)\right\rangle \ . \tag{4.151}$$

The terms with different chiralities on the ferimonic operators vanish as the number of fermions of each chirality must match at each end of the Keldysh contour. Using eq. (4.95) we can evaluate this correlation function and find that

$$F_1^r = \left\langle U_{1,0}(0,t_f)U_{0,1}(t_f,t)\psi_r(x)U_{0,0}(t,0)\psi_r^\dagger(0)\right\rangle \tag{4.152}$$
$$= e^{-\imath\Delta E_1 t_f}e^{-\imath\Delta E_2(t_f-t)}\left\langle R_2^\dagger(t_f)R_1^\dagger(t_f)R_1(t)R_2(t)\psi_r(x,t)R_1^\dagger(t)R_1(0)\psi_r^\dagger(0,0)\right\rangle \tag{4.153}$$
$$= \frac{1}{2\pi}\alpha^{\frac{2\delta_1^2}{\pi^2 K}+\frac{\delta_1}{\pi K}+\frac{2\delta_2^2}{\pi^2 K}+\frac{\delta_2}{\pi K}+\frac{K^2-1}{2K}-1}e^{-\imath\Delta E_1 t_f}e^{-\imath\Delta E_2(t_f-t)}e^{ik_F r x}$$

$$\times (\eta + \imath u t_f)^{-2\frac{\delta_1^2}{\pi^2 K} + \frac{\delta_1}{\pi K}} (\eta + \imath u(t_f - t))^{-2\frac{\delta_2^2}{\pi^2 K} - \frac{\delta_2}{\pi K}}$$
$$\times \prod_{\nu=\pm 1} \Bigg[(\eta - \imath\nu x)^{\frac{\delta_1\delta_2}{\pi^2 K} - \nu r \frac{\delta_1}{\pi}} (\eta - \imath(\nu x - u t_f))^{-\frac{\delta_1\delta_2}{\pi^2 K} + \frac{\delta_2}{\pi}\frac{(K\nu r+1)}{2K}}$$
$$\times (\eta - \imath(\nu x - u t))^{\frac{\delta_1\delta_2}{\pi^2 K} - \frac{\delta_1}{\pi}\frac{(Kr+\nu)}{2K} + \frac{\delta_2}{\pi}\frac{(Kr+\nu)}{2K} - \frac{(K+\nu r)^2}{4K}}$$
$$\times (\eta - \imath(\nu x - u(t_f - t)))^{-\frac{\delta_1\delta_2}{\pi^2 K} + \frac{\delta_1}{\pi}\frac{(K\nu r-1)}{2K}} \Bigg] . \tag{4.154}$$

This expression contains all of the essential phenomonology of the spatial spread of the orthogonality catastrophe and will be a central point of our later discussion, so we will put off a thorough examination of this term for now.

The F_2 to F_4 correlators require some more work. Firstly we must get them into a form that removes point splitting issues. Then, it will turn out we must separate linear and exponential terms in the expectation value.

Let us first consider the correlation function F_3. Neglecting phase shifts due to an overall shift in the energy for the moment, this consists of terms of the form

$$\left\langle \psi^\dagger_{r_1}(x,t)\psi_{r_2}(x,t)\mathcal{R}_1\psi_{r_3}(x,t)\mathcal{R}_2\psi^\dagger_{r_4}(0,0)\right\rangle , \tag{4.155}$$

where $\mathcal{R}_1 = R_2^\dagger(t_f)R_1^\dagger(t_f)R_1(t)R_2(t)$ and $\mathcal{R}_2 = R_1^\dagger(t)R_1(0)$. In order to match the left and right moving fermion numbers along the contour, we must have $r_1 + r_4 = r_2 + r_3$. This results in 3 distinct cases; $r_1 = r_2 = r_3 = r_4$, $r_1 = r_2 = -r_3 = -r_4$ and $r_1 = -r_2 = -r_3 = r_4$.

In what follows we will use the fact that

$$\mathcal{R}_1\psi_r(x,t) = e^{\imath\mathcal{A}_r}\psi_r(x,t)\mathcal{R}_1 \tag{4.156}$$
$$\mathcal{R}_2\psi^\dagger_r(0,0) = e^{\imath\mathcal{B}_r}\psi^\dagger_r(0,0)\mathcal{R}_2 \tag{4.157}$$
$$\mathcal{R}_1\psi^\dagger_r(0,0) = e^{\imath\mathcal{C}_r}\psi^\dagger_r(0,0)\mathcal{R}_1 , \tag{4.158}$$

where $\mathcal{A}_r, \mathcal{B}_r, \mathcal{C}_r \in \mathbb{R}$. We can explicitly find the form of these terms using the identity

$$e^P e^Q = e^{[P,Q]}e^Q e^P , \tag{4.159}$$

valid when $[P,Q] \in \mathbb{C}$. We define

$$\Gamma_r(x_1 - x_2, t_1 - t_2)$$
$$= -\imath\left[\frac{1}{\pi K}\sum_{\nu=\pm1}\nu\tilde{\varphi}_\nu(x_1 - \nu u t), \frac{1}{2}\sum_{\mu=\pm1}\left(r + \frac{\mu}{K}\right)\tilde{\varphi}_\mu(x_2 - \mu u t_2)\right] \tag{4.160}$$
$$= -\frac{\imath}{2\pi K}\sum_{\mu,\nu=\pm1}\nu\left(r + \frac{\mu}{K}\right)[\tilde{\varphi}_\nu(x_1 - \nu u t_1), \tilde{\varphi}_\mu(x_2 - \mu u t_2)] \tag{4.161}$$
$$= \frac{1}{2}\sum_{\nu=\pm1}\left(r + \frac{\nu}{K}\right)\mathrm{sgn}\left(x_1 - x_2 - \nu u(t_1 - t_2)\right). \tag{4.162}$$

Here we have used the fact that

$$[\tilde{\varphi}_\nu(x), \tilde{\varphi}_\mu(y)] = \imath\pi K\nu\delta_{\nu,\mu}\,\mathrm{sgn}(x-y)\ . \tag{4.163}$$

We can now write

$$\begin{aligned}
\mathcal{R}_2\psi_r(x,t) &= R_2^\dagger(t_f)R_1^\dagger(t_f)R_1(t)R_2(t)\psi_r(x,t) && (4.164)\\
&= e^{-\imath\delta_2\Gamma_r(0,0)}R_2^\dagger(t_f)R_1^\dagger(t_f)R_1(t)\psi_r(x,t)R_2(t) && (4.165)\\
&= e^{-\imath\delta_2\Gamma_r(0,t_f-t)-\imath\delta_1\Gamma_r(-x,t_f-t)+\imath\Gamma_r(-x,0)-\imath\delta_2\Gamma_r(0,0)}\psi_r(x,t)\mathcal{R}_2\ . && (4.166)
\end{aligned}$$

Comparing this with eq. (4.156) and performing a similar calculation for $\mathcal{C}_r$ and $\mathcal{B}_r$ we find that

$$\mathcal{A}_r = \frac{\delta_2}{K} - \delta_1 r\,\mathrm{sgn}(x) + \frac{\delta_1}{2}\sum_{\nu=\pm1}\left(r-\frac{\nu}{K}\right)\mathrm{sgn}(x-u(t_f-t)) \tag{4.167}$$

$$\mathcal{B}_r = -\frac{\delta_1}{K} \tag{4.168}$$

$$\mathcal{C}_r = \frac{\delta_2}{2}\sum_{\nu=\pm1}\left(r+\frac{\nu}{K}\right)\left(\mathrm{sgn}(x-\nu u t_f)-\mathrm{sgn}(x-\nu u t)\right)\ . \tag{4.169}$$

We will need in particular the r odd parts of these expressions, which offer some significant simplifications.

$$\begin{aligned}
\Delta\mathcal{A}_r &= \mathcal{A}_r - \mathcal{A}_{-r} && (4.170)\\
&= -r\delta_2\left[2\,\mathrm{sgn}(x) - \sum_{\nu=\pm1}\mathrm{sgn}(x-\nu u(t_f-t))\right]\ , && (4.171)\\
\Delta\mathcal{B}_r &= \mathcal{B}_r - \mathcal{B}_{-r} && (4.172)\\
&= 0\ , && (4.173)\\
\Delta\mathcal{C}_r &= \mathcal{C}_r - \mathcal{C}_{-r} && (4.174)\\
&= r\delta_2\sum_{\nu=\pm1}\left(\mathrm{sgn}(x-\nu u t_f)-\mathrm{sgn}(x-\nu u t)\right)\ . && (4.175)
\end{aligned}$$

Returning to the various terms in F_3, for the case that $r_1 = r_2 = -r_3 = -r_4 = -r$ we have that

$$\begin{aligned}
&\left\langle\psi_{-r}^\dagger(x,t)\psi_{-r}(x,t)\mathcal{R}_1\psi_r(x,t)\mathcal{R}_2\psi_r^\dagger(0,0)\right\rangle\\
&\quad= \left\langle\left(N_{-r} - \frac{1}{4\pi}\sum_\nu\left(1-\frac{r\nu}{K}\right)\nabla\tilde{\varphi}_\nu(x-\nu u t)\right)\mathcal{R}_1\psi_r(x,t)\mathcal{R}_2\psi_r^\dagger(0,0)\right\rangle\ .
\end{aligned} \tag{4.176}$$

That is there is no real point splitting ambiguity in this case and it can be evaluated by simply replacing $\psi_{-r}^\dagger(x,t)\psi_{-r}(x,t)$ with the coresponding hole density.

Similarly for the case that $r_1 = r_2 = r_3 = r_4 = r$ we have that

$$\begin{aligned}
&\left\langle \psi_r^\dagger(x,t)\psi_r(x,t)\mathcal{R}_1\psi_r(x,t)\mathcal{R}_2\psi_r^\dagger(0,0)\right\rangle \\
&\quad = \left\langle \left(N_r - \frac{1}{4\pi}\sum_\nu \left(1+\frac{r\nu}{K}\right)\nabla\tilde{\varphi}_\nu(x-\nu ut)\right)\mathcal{R}_1\psi_r(x,t)\mathcal{R}_2\psi_r^\dagger(0,0)\right\rangle .
\end{aligned} \tag{4.177}$$

Finally for the case that $r_1 = -r_2 = r_3 = -r_4 = r$ we have that

$$\begin{aligned}
&\left\langle \psi_r^\dagger(x,t)\psi_{-r}(x,t)\mathcal{R}_1\psi_r(x,t)\mathcal{R}_2\psi_{-r}^\dagger(0,0)\right\rangle \\
&= e^{\imath\mathcal{A}_r}\left\langle \psi_r^\dagger(x,t)\psi_{-r}(x,t)\psi_r(x,t)\mathcal{R}_1\mathcal{R}_2\psi_{-r}^\dagger(0,0)\right\rangle && (4.178)\\
&= -e^{\imath(\mathcal{A}_r-\mathcal{A}_{-r})}\left\langle \psi_r^\dagger(x,t)\psi_r(x,t)\mathcal{R}_1\psi_{-r}(x,t)\mathcal{R}_2\psi_{-r}^\dagger(0,0)\right\rangle && (4.179)\\
&= -e^{\imath\Delta\mathcal{A}_r}\left\langle \left(N_r - \frac{1}{4\pi}\sum_\nu \left(1+\frac{r\nu}{K}\right)\nabla\tilde{\varphi}_\nu(x-\nu ut)\right)\right. \\
&\qquad\qquad \left.\times\,\mathcal{R}_1\psi_{-r}(x,t)\mathcal{R}_2\psi_{-r}^\dagger(0,0)\right\rangle . && (4.180)
\end{aligned}$$

If we define the function

$$\begin{aligned}
f_{r_1,r_2} = e^{-\imath\Delta E_1 t_f}e^{-\imath\Delta E_2(t_f-t)}&\left\langle \left(N_{r_1} - \frac{1}{4\pi}\sum_\nu \left(1+\frac{r_1\nu}{K}\right)\nabla\tilde{\varphi}_\nu(x-\nu ut)\right)\right. \\
&\left.\times\,\mathcal{R}_1\psi_{r_2}(x,t)\mathcal{R}_2\psi_{r_2}^\dagger(0,0)\right\rangle
\end{aligned} \tag{4.181}$$

reinstating the constant energy shifts, then we can write

$$F_3 = \sum_{r=\pm 1}\left(f_{r,r} + f_{r,-r} - e^{\imath\Delta\mathcal{A}_r}f_{r,-r}\right) . \tag{4.182}$$

We can do analogous calculations for F_2, which has the form

$$\left\langle \psi_{r_1}(0,0)\psi_{r_2}^\dagger(0,0)\mathcal{R}_1\psi_{r_3}(x,t)\mathcal{R}_2\psi_{r_4}^\dagger(0,0)\right\rangle . \tag{4.183}$$

We note that the bosonized operators ψ_r and $\psi_{r'}^\dagger$ obey the relation

$$\psi_{r_1}(x,t)\psi_{r_2}^\dagger(0,0) = e^{\imath\mathcal{D}_{r_1,r_2}}\psi_{r_2}^\dagger(0,0)\psi_{r_1}(x,t) , \tag{4.184}$$

with

$$\begin{aligned}
\mathcal{D}_{r_1,r_2} &= \frac{\pi}{4}\sum_{\nu=\pm 1}\left(r_1+r_2+\nu\left(\frac{1}{K}+Kr_1r_2\right)\right)\operatorname{sgn}(x-\nu ut) && (4.185)\\
&= \begin{cases} \pi r_1\delta_{r_1,r_2}\operatorname{sgn}(x) & |x| > |ut| \\ -\pi\frac{\frac{1}{K}+Kr_1r_2}{2}\operatorname{sgn}(ut) & |x| < |ut| \end{cases} , && (4.186)
\end{aligned}$$

$$\Delta\mathcal{D}_{r1,r_2} = \mathcal{D}_{r_1,r_2} - \mathcal{D}_{r_1,-r_2} \tag{4.187}$$

$$= \frac{\pi}{2}\sum_{\nu=\pm 1}(r_2 + \nu K r_1 r_2)\,\mathrm{sgn}(x-\nu u t) \tag{4.188}$$

$$= \begin{cases} \pi r_1 r_2\,\mathrm{sgn}(x) & |x| > |ut| \\ -\pi K r_1 r_2\,\mathrm{sgn}(ut) & |x| < |ut| \end{cases} . \tag{4.189}$$

Note that for equal times we recover the standard anticommutation relation.

As was the case for F_3 there are three possible distinct forms of term in F_2 and they can be computed in an analogous manner. With the definition

$$\tilde{f}_{r_1,r_2} = e^{-\imath\Delta E_1 t_f} e^{-\imath\Delta E_2(t_f-t)} \Bigg\langle \left(\frac{1}{2}\Lambda - N_{r_1} + \frac{1}{4\pi}\sum_\nu \left(1+\frac{r_1\nu}{K}\right)\nabla\tilde{\varphi}_\nu(0)\right) \times \mathcal{R}_1\psi_{r_2}(x,t)\mathcal{R}_2\psi^\dagger_{r_2}(0,0)\Bigg\rangle \tag{4.190}$$

$$\tag{4.191}$$

we have

$$\left\langle \psi_{-r}(0,0)\psi^\dagger_{-r}(0,0)\mathcal{R}_1\psi_r(x,t)\mathcal{R}_2\psi^\dagger_r(0,0)\right\rangle = e^{\imath\Delta E_1 t_f} e^{\imath\Delta E_2(t_f-t)}\tilde{f}_{-r,r}\ , \tag{4.192}$$

$$\left\langle \psi_{r}(0,0)\psi^\dagger_{r}(0,0)\mathcal{R}_1\psi_r(x,t)\mathcal{R}_2\psi^\dagger_r(0,0)\right\rangle = e^{\imath\Delta E_1 t_f} e^{\imath\Delta E_2(t_f-t)}\tilde{f}_{r,r}\ , \tag{4.193}$$

$$\left\langle \psi_{r}(0,0)\psi^\dagger_{-r}(0,0)\mathcal{R}_1\psi_{-r}(x,t)\mathcal{R}_2\psi^\dagger_r(0,0)\right\rangle = -e^{\imath\Delta E_1 t_f} e^{\imath\Delta E_2(t_f-t)} \times e^{\imath(\Delta\mathcal{B}_r+\Delta\mathcal{C}_r+\Delta\mathcal{D}_{-r,r})}\tilde{f}_{r,-r}\ . \tag{4.194}$$

The F_4 term can be treated in a similar manner, however there are far more possible combinations of chirality indices (ten up to the symmetry of reversing all chiralities, as opposed to three).

The terms in F_4 have the form

$$F_4^{r_1,r_2,r_3,r_4,r_5,r_6} = e^{-\imath\Delta E_1 t_f} e^{-\imath\Delta E_2(t_f-t)} \times \left\langle \psi_{r_1}(0,0)\psi^\dagger_{r_2}(0,0)\psi^\dagger_{r_3}(x,t)\psi_{r_4}(x,t)\mathcal{R}_1\psi_{r_5}(x,t)\mathcal{R}_2\psi^\dagger_{r_6}(0,0)\right\rangle . \tag{4.195}$$

Similarly to the cases above we will express F_4 in terms of

$$g_{r_1,r_2,r_3} = e^{-\imath\Delta E_1 t_f} e^{-\imath\Delta E_2(t_f-t)} \Bigg\langle \left(\frac{1}{2}\Lambda - N_{r_1} + \frac{1}{4\pi}\sum_\nu \left(1+\frac{r_1\nu}{K}\right)\nabla\tilde{\varphi}_\nu(0)\right) \times \left(N_{r_2} - \frac{1}{4\pi}\sum_\nu\left(1+\frac{r_2\nu}{K}\right)\nabla\tilde{\varphi}_\nu(x-\nu u t)\right)\mathcal{R}_1\psi_{r_3}(x,t)\mathcal{R}_2\psi^\dagger_{r_3}(0,0)\Bigg\rangle. \tag{4.196}$$

The various terms in F_4 can then be found via the same means as above, coupled with using eq. (4.133) to move the fermion operators past density operators, to give

$$F_4^{r,r,r,r,r,r} = g_{r,r,r} \ , \tag{4.197}$$

$$F_4^{r,r,-r,-r,r,r} = g_{r,-r,r} \ , \tag{4.198}$$

$$F_4^{r,r,r,r,-r,-r} = g_{r,r,-r} \ , \tag{4.199}$$

$$F_4^{r,r,-r,-r,-r,-r} = g_{r,-r,-r} \ , \tag{4.200}$$

$$F_4^{r,r,r,-r,r,-r} = -e^{\imath\Delta\mathcal{A}_r} g_{r,r,-r} \ , \tag{4.201}$$

$$F_4^{r,r,-r,r,-r,r} = -e^{\imath\Delta\mathcal{A}_{-r}} g_{r,-r,r} \ , \tag{4.202}$$

$$\begin{aligned} F_4^{r,-r,r,r,-r,r} &= -e^{\imath(\Delta\mathcal{B}_r+\Delta\mathcal{C}_r+\Delta\mathcal{D}_{-r,r})} \\ &\quad \times \left(g_{r,r,-r} + \frac{1}{4} \sum_{\nu=\pm 1} \left(2 + \left(K + \frac{1}{K} \right) \nu r \right) \xi_\nu(x,t) \tilde{f}_{r,-r} \right) \ , \end{aligned} \tag{4.203}$$

$$\begin{aligned} F_4^{r,-r,-r,-r,-r,r} &= -e^{\imath(\Delta\mathcal{B}_r+\Delta\mathcal{C}_r+\Delta\mathcal{D}_{-r,r})} \\ &\quad \times \left(g_{r,-r,-r} + \frac{1}{4} \sum_{\nu=\pm 1} \left(2 + \left(K + \frac{1}{K} \right) \nu r \right) \xi_\nu(x,t) \tilde{f}_{r,-r} \right) , \end{aligned} \tag{4.204}$$

$$\begin{aligned} F_4^{r,-r,-r,r,-r,r} &= e^{\imath(\Delta\mathcal{A}_r+\Delta\mathcal{B}_r+\Delta\mathcal{C}_r+\Delta\mathcal{D}_{r,r})} \\ &\quad \times \left(g_{r,r,-r} + \frac{1}{4} \sum_{\nu=\pm 1} \left(K - \frac{1}{K} \right) \nu r \xi_\nu(x,t) \tilde{f}_{r,-r} \right) \ . \end{aligned} \tag{4.205}$$

In addition to the above there is one term which does not require the use of a point spliting procedure, that is the $r_1 = -r_2 = r_3 = -r_4 = -r_5 = -r_6 = r$ term. This term can be evaluated directly using eq. (4.95) to give

$$\begin{aligned} F_4^{r,-r,r,-r,-r,-r} &= \frac{F_1^{-r}}{4\pi^2} \alpha^{(K-\frac{1}{K})^2} \eta^{3K-\frac{1}{K}} e^{-2ik_F rx} \\ &\quad \times \prod_{\nu=\pm 1} \Big[(\eta + \imath(x-\nu ut))^{-\frac{3K-\nu r}{2}+\nu r\frac{\delta_2}{\pi}} (\eta - \imath(x-\nu ut))^{-\frac{K-\nu r}{2}-\nu r\frac{\delta_1}{\pi}} \\ &\qquad \times (\eta + \nu\imath(x-ut_f))^{-\nu r\frac{\delta_2}{\pi}} (\eta + \nu\imath(x-\nu u(t_f-t))^{-\nu r\frac{\delta_1}{\pi}} \Big] \ . \end{aligned} \tag{4.206}$$

All that remains is to evaluate the functions f_{r_1,r_2}, $\tilde{f}_{r_1,r_2}$ and g_{r_1,r_2,r_3}. These correlation functions contain a mixture of terms linear in the bosonic operators and terms exponential in them. As mentioned in section 4.5 these types of correlation functions can be evaluated by explicit normal ordering.

The expectations f_{r_1,r_2} and f_{r_1,r_2} have the form

$$\left\langle A \prod_i e^{C_i} \right\rangle . \tag{4.207}$$

whilst the expectation g_{r_1,r_2,r_3} has the form

$$\left\langle AB \prod_i e^{C_i} \right\rangle , \tag{4.208}$$

where A, B and C_i are linear combinations of bosonic operators and their derivatives. The exponential terms can be combined into a single exponential term $e^C = e^\gamma \prod_i e^{C_i}$, where $\gamma \in \mathbb{C}$, so it is sufficient to consider the case where there is only a single C_i.

Splitting each of these terms into creation and annihilation parts $A = A_+ + A_-$, $B = B_+ + B_-$ and $e^C = e^{C_+} e^{C_-} e^{-\frac{1}{2}[Q_+,Q_-]}$, we can write

$$\begin{aligned}
\left\langle Ae^C \right\rangle &= \left\langle (A_+ + A_-)\, e^{C_+} e^{C_-} e^{-\frac{1}{2}[C_+,C_-]} \right\rangle && (4.209)\\
&= \left\langle e^{C_+} \left(A_+ + A_- + \langle AC \rangle\right) e^{C_-} \right\rangle \left\langle e^C \right\rangle && (4.210)\\
&= \langle AC \rangle \left\langle e^C \right\rangle , && (4.211)
\end{aligned}$$

and similarly

$$\begin{aligned}
\left\langle ABe^C \right\rangle &= \left\langle (A_+ + A_-)\,(B_+ + B_-)\, e^{C_+} e^{C_-} e^{-\frac{1}{2}[C_+,C_-]} \right\rangle && (4.212)\\
&= \left\langle e^{C_+} \left(A_+ + A_- + \langle AC \rangle\right)\left(B_+ + B_- + \langle BC \rangle\right) e^{C_-} \right\rangle \left\langle e^C \right\rangle && (4.213)\\
&= \Big\langle e^{C_+} \big((A_+ + \langle AC \rangle)(B_- + \langle BC \rangle) + A_-(B_- + \langle BC \rangle)\\
&\qquad + (A_+ + \langle AC \rangle)B_+ + B_+A_- + \langle AB \rangle\big) e^{C_-} \Big\rangle \langle e^C \rangle && (4.214)\\
&= \left(\langle AC \rangle \langle BC \rangle + \langle AB \rangle\right) \left\langle e^C \right\rangle . && (4.215)
\end{aligned}$$

Note that if $e^C = e^\gamma \prod_i e^{C_i}$ then

$$\begin{aligned}
\left\langle A \prod_i e^{C_i} \right\rangle &= e^{-\gamma} \left\langle Ae^C \right\rangle && (4.216)\\
&= e^{-\gamma} \langle AC \rangle \left\langle e^C \right\rangle && (4.217)\\
&= \langle AC \rangle \left\langle \prod_i e^{C_i} \right\rangle . && (4.218)
\end{aligned}$$

Since $C = \sum_i C_i$ and $\left\langle \prod_i e^{C_i} \right\rangle$ can be calculated directly using eq. (4.95) we can evaluate terms of this form without having to explicitly evaluate γ. We also note that in all the cases we consider $\left\langle \prod_i e^{C_i} \right\rangle = F_1^r$.

With this we can explicitly obtain expression for the functions f_{r_1,r_2}, $\tilde{f}_{r_1,r_2}$ and g_{r_1,r_2,r_3}. We find that

$$f_{r_1,r_2} = \frac{F_1^{r_2}}{8\pi K} \left[8\pi K \frac{N}{L} - \frac{\delta_2}{\pi} \frac{4K}{\imath\eta} - r_2 \frac{2K(r_1+r_2)}{\imath\eta} + \frac{\delta_2}{\pi} \frac{4K}{u(t_f - t) + \imath\eta} \right.$$

$$+\sum_{\nu=\pm1}\Bigg(-\nu\frac{\delta_1}{\pi}\frac{2\left(K-\nu r_1\right)}{x-\nu u(t_f-t)-\nu\imath\eta}-\nu\frac{\delta_1}{\pi}\frac{2\left(K+\nu r_1\right)}{x-\nu ut+\nu\imath\eta}$$
$$+r_2\frac{\left(K-r_1\nu\right)\left(K-r_2\nu\right)}{x-\nu ut+\nu\imath\eta}\Bigg)\Bigg], \tag{4.219}$$

$$\tilde{f}_{r_1,r_2}=\frac{F_1^{r_2}}{8\pi K}\Bigg[8\pi K\left(\frac{1}{2}\Lambda-N_{r_1}\right)+\frac{\delta_1}{\pi}\frac{4K}{\imath\eta}-r_2\frac{K(r_1+r_2)}{\imath\eta}-\frac{\delta_1}{\pi}\frac{4K}{ut_f+\imath\eta}$$
$$+\sum_{\nu=\pm1}\Bigg(-\frac{2\nu\frac{\delta_2}{\pi}\left(K+\nu r_1\right)+\nu r_2(K+\nu r_1)(K+\nu r_2)}{x-\nu ut-\imath\eta}$$
$$+\nu\frac{\delta_2}{\pi}\frac{2\left(K+\nu r_1\right)}{x-\nu ut_f-\imath\eta}\Bigg)\Bigg], \tag{4.220}$$

$$g_{r_1,r_2,r_3}=\frac{F_1^{r_3}}{64\pi^2K}\Bigg[-\sum_{\nu=\pm1}\frac{4K\left(K+\nu r_1\right)\left(K+\nu r_2\right)}{\left(x-\nu ut-\nu\imath\eta\right)^2}$$
$$-\Bigg(8\pi K\left(\frac{1}{2}\Lambda-\frac{N_{r_1}}{L}\right)+\frac{\delta_1}{\pi}\frac{4K}{\imath\eta+t_fu}+\frac{\delta_1}{\pi}\frac{4K}{\imath\eta}+r_3\frac{K(r_1+r_3)}{\imath\eta}$$
$$+\sum_{\nu_1=\pm1}\Bigg(\nu_1\frac{\delta_2}{\pi}\frac{2\left(K+\nu_1r_1\right)}{x-\nu_1ut_f-\nu_1\imath\eta}-\nu_1\frac{\delta_2}{\pi}\frac{2\left(K+\nu_1r_1\right)}{x-\nu_1ut-\nu_1\imath\eta}$$
$$-\nu_1r_3\frac{\left(K+\nu_1r_1\right)\left(K+\nu_1r_3\right)}{x-\nu_1ut-\nu_1\imath\eta}\Bigg)\Bigg)$$
$$\times\Bigg(8\pi K\frac{N_{r_2}}{L}+\frac{\delta_2}{\pi}\frac{4K}{u(t_f-t)+\imath\eta}-\frac{\delta_2}{\pi}\frac{4K}{\imath\eta}-r_3\frac{K(r_2+r_3)}{\imath\eta}$$
$$+\sum_{\nu_2=\pm1}\Bigg(-\nu_2\frac{\delta_1}{\pi}\frac{2\left(K-\nu_2r_2\right)}{x-\nu_2u(t_f-t)-\nu_2\imath\eta}-\nu_2\frac{\delta_1}{\pi}\frac{2\left(K+\nu_2r_2\right)}{x-\nu_2ut+\nu_2\imath\eta}$$
$$+r_3\frac{\left(K+r_2\right)\left(K+r_3\right)}{x-\nu_2ut+\nu_2\imath\eta}\Bigg)\Bigg)\Bigg]. \tag{4.221}$$

With this we have fully evaluated all of the correlation functions needed and so have an exact expression for the reduced density matrix of the localised states.

4.7 Matrix elements

The density matrix in eq. (4.18), together with the expressions for the various terms calculated in the previous section, describe the physics of the system.

The various matrix elements are given by

$$A=1+\alpha^2(w_1^2\beta_1^2-2\beta_1)|W_1|^2\left(\Lambda-\frac{N}{L}\right)+\alpha^2(w_2^2\beta_2^2-2\beta_2)|W_2|^2\frac{N}{L}$$

$$
\begin{aligned}
&+ 2\alpha^4\beta_1(2\beta_2 - w_2\beta_2^2)|W_1|^2|W_2|^2\mathrm{Re}\Bigg[\left(\Lambda - \frac{N}{L}\right)\frac{N}{L} - \frac{K}{2\pi}\frac{x^2+(\imath\eta+ut)^2}{(x^2-(\imath\eta+ut)^2)^2}\\
&+ \frac{1}{2\pi}\alpha^{2K-2}\cos(2k_Fx)(\eta+\imath(ut-x))^{-K}(\eta+\imath(ut+x))^{-K}\Bigg]\\
&+ \alpha^6\beta_1^2(w_2^2\beta_2^2 - 2\beta_2)|W_1|^4|W_2|^2\Bigg[\frac{N}{L}\left(\Lambda-\frac{N}{L}\right)^2\\
&+ \frac{N}{L}\frac{2}{\eta^2}\left[\left(K-\frac{1}{K}\right) - \frac{K}{4\pi^2}\right] - \frac{K}{\pi^2}\left(\Lambda-\frac{N}{L}\right)\sum_{\nu=\pm1}\frac{1}{(x-\nu ut)^2+\eta^2}\\
&+ \frac{1}{\pi^2}\alpha^{(K-\frac{1}{K})(K+1-\frac{1}{K})}\mathrm{Re}\Bigg[\left(\left[\Lambda-\frac{N}{L}\right]\cos(2k_Fx) - \imath\sin(2k_Fx)\frac{K}{\pi}\frac{x}{x^2-(ut-\imath\eta)^2}\right)\\
&\qquad\qquad \left(x^2-(ut-\imath\eta)^2\right)^{-K}\Bigg]\\
&+ \sum_{r=\pm1}\left(\frac{1}{2}\Lambda - \frac{N_r}{L}\right)\left(\frac{N_{-r}}{L} - \frac{1}{2}\frac{1}{\eta K}\right)\left(\frac{N}{L} - \frac{K}{2}\sum_{\nu=\pm1}r\nu\xi_\nu(x,t)\right)\\
&+ \frac{1}{8\pi^2}\sum_{\nu=\pm1}\frac{\left(\frac{N}{L}-\frac{1}{K\eta}\right)\left(K+\frac{1}{K}\right) - \left(\Lambda-\frac{N}{L}\right)\left(K-\frac{1}{K}\right) + 2\nu\frac{J}{L}}{(x-\nu ut+\nu\imath\eta)^2}\Bigg],
\end{aligned}
\tag{4.222}
$$

$$
\begin{aligned}
B = \alpha^4\gamma_1^2\gamma_2^2|W_1|^2|W_2|^2\Bigg[&\left(\Lambda-\frac{N}{L}\right)\frac{N}{L} + \frac{K}{2\pi}\frac{x^2+(\imath\eta+ut)^2}{(x^2-(\imath\eta+ut)^2)^2}\\
&+ \frac{1}{2\pi^2}\alpha^{2K-2}\mathrm{Re}\Bigg[e^{-2\imath k_Frx}\left(\eta-\imath x\right)^{\frac{2\delta_1 r}{\pi}}\left(\eta+\imath x\right)^{-\frac{2\delta_1 r}{\pi}}\\
&\quad\times\prod_{\nu=\pm1}\left(\eta-\imath(x-\nu ut)\right)^{-\frac{K-r}{2}-r\frac{\delta_1}{\pi}}\left(\eta+\imath(x-\nu ut)\right)^{-\frac{K+r}{2}+r\frac{\delta_1}{\pi}}\Bigg]\\
&+ \frac{1}{2}\sum_{r=\pm1}\Bigg[\left(\frac{\Lambda}{2}-\frac{N_r}{L}\right)\sum_{\nu=\pm1}\left(\left(\frac{\delta_1}{\pi}+(1-Kr)\right)\xi_\nu(x,t) - \frac{\delta_1}{\pi}\xi_\nu(x,0)\right)\Bigg]\Bigg],
\end{aligned}
\tag{4.223}
$$

$$
\begin{aligned}
D_1 = \alpha^2\gamma_1^2|W_1|^2\left(\Lambda-\frac{N}{L}\right) + \alpha^4\gamma_1^2\left(w_2^2\beta_2^2-2\beta_2\right)|W_2|^2|W_1|^2\Bigg[&\\
&\left(\Lambda-\frac{N}{L}\right)\frac{N}{L} + \frac{K}{2\pi}\frac{x^2+(\imath\eta+ut)^2}{(x^2-(\imath\eta+ut)^2)^2}\\
&+ \frac{1}{2\pi^2}\alpha^{K-2}\mathrm{Re}\Bigg[e^{-2\imath k_Frx}\left(\eta-\imath x\right)^{\frac{2\delta_1 r}{\pi}}\left(\eta+\imath x\right)^{-\frac{2\delta_1 r}{\pi}}\\
&\quad\times\prod_{\nu=\pm1}\left(\eta-\imath(x-\nu ut)\right)^{-\frac{K-r}{2}-r\frac{\delta_1}{\pi}}\left(\eta+\imath(x-\nu ut)\right)^{-\frac{K+r}{2}+r\frac{\delta_1}{\pi}}\Bigg]
\end{aligned}
$$

$$+\frac{1}{2}\sum_{r=\pm 1}\left[\left(\frac{\Lambda}{2}-\frac{N_r}{L}\right)\sum_{\nu=\pm 1}\left(\left(\frac{\delta_1}{\pi}+(1-Kr)\right)\xi_\nu(x,t)-\frac{\delta_1}{\pi}\xi_\nu(x,0)\right)\right]\Bigg], \tag{4.224}$$

$$\begin{aligned}
D_2 &= \alpha^2\gamma_2^2|W_2|^2\frac{N}{L}\\
&\quad -2\alpha^4\gamma_2^2\beta_1|W_1|^2|W_2|^2\mathrm{Re}\Bigg[\left(\Lambda-\frac{N}{L}\right)\frac{N}{L}-\frac{K}{2\pi}\frac{x^2+(\imath\eta+ut)^2}{(x^2-(\imath\eta+ut)^2)^2}\\
&\quad +\frac{1}{2\pi}\alpha^{2K-2}\cos(2k_Fx)(\eta+\imath(ut-x))^{-K}(\eta+\imath(ut+x))^{-K}\Bigg]\\
&\quad +\alpha^6\gamma_2^2\beta_1^2|W_1|^4|W_2|^2\Bigg[\frac{N}{L}\left(\Lambda-\frac{N}{L}\right)^2\\
&\quad +\frac{N}{L}\frac{2}{\eta^2}\left[\left(K-\frac{1}{K}\right)-\frac{K}{4\pi^2}\right]-\frac{K}{\pi^2}\left(\Lambda-\frac{N}{L}\right)\sum_{\nu=\pm 1}\frac{1}{(x-\nu ut)^2+\eta^2}\\
&\quad +\frac{1}{\pi^2}\alpha^{(K-\frac{1}{K})(K-\frac{1}{K}+1)}\\
&\qquad \times\mathrm{Re}\Bigg[\left(\left[\Lambda-\frac{N}{L}\right]\cos(2k_Fx)-\imath\sin(2k_Fx)\frac{K}{\pi}\frac{x}{x^2-(ut-\imath\eta)^2}\right)\\
&\qquad\qquad \times\left(x^2-(ut-\imath\eta)^2\right)^{-K}\Bigg]\\
&\quad +\sum_{r=\pm 1}\left(\frac{1}{2}\Lambda-\frac{N_r}{L}\right)\left(\frac{N_{-r}}{L}-\frac{1}{2}\frac{1}{\eta K}\right)\left(\frac{N}{L}-\frac{K}{2}\sum_{\nu=\pm 1}r\nu\xi_\nu(x,t)\right)\\
&\quad +\frac{1}{8\pi^2}\sum_{\nu=\pm 1}\frac{\left(\frac{N}{L}-\frac{1}{K\eta}\right)\left(K+\frac{1}{K}\right)-\left(\Lambda-\frac{N}{L}\right)\left(K-\frac{1}{K}\right)+2\nu\frac{J}{L}}{(x-\nu ut+\nu\imath\eta)^2}\Bigg],
\end{aligned} \tag{4.225}$$

$$\begin{aligned}
F &= \alpha^2\gamma_2\gamma_1W_2W_1\sum_r\Bigg\{F_1^r-\alpha^2\beta_1|W_1|^2\left(\tilde{f}_{rr}-\left(1-e^{-\imath(\Delta\mathcal{C}_r+\mathcal{D}_{r,r})}\right)\tilde{f}_{-r,r}\right)\\
&\quad -\alpha^2\beta_2|W_2|^2\left(f_{rr}+\left(1-e^{-\imath\Delta\mathcal{A}_r}\right)f_{-r,r}\right)\\
&\quad +\alpha^4\beta_2\beta_1|W_2|^2|W_1|^2\\
&\qquad \times\Bigg(g_{r,r,r}+\left[1-e^{-\imath\Delta\mathcal{A}_r}\right]g_{r,-r,r}+\left[1-e^{-\imath(\Delta\mathcal{C}_r+\Delta\mathcal{D}_{r,r})}\right]g_{-r,r,r}\\
&\quad +\left[1-e^{-\imath\Delta\mathcal{A}_r}-e^{-\imath(\Delta\mathcal{C}_r+\Delta\mathcal{D}_{-r,r})}+e^{-\imath(\Delta\mathcal{A}_r+\Delta\mathcal{C}_r+\Delta\mathcal{D}_{r,r})}\right]g_{-r,-r,r}\\
&\quad +F_4^{-r,r,-r,r,r,r}+\frac{1}{2}e^{-\imath\Delta\mathcal{C}_r}\tilde{f}_{-r,r}\sum_{\nu=\pm 1}\Bigg[\left(\frac{\nu r}{2}e^{-\imath(\Delta\mathcal{A}_r+\Delta\mathcal{D}_{r,r})}\left[K-\frac{1}{K}\right]\right)
\end{aligned}$$

$$- e^{-\imath\Delta\mathcal{D}_{-r,r}}\left(2+\nu r\left[K+\frac{1}{K}\right]\right)\xi_\nu(x,t)\Bigg]\Bigg)\Bigg\} \tag{4.226}$$

$$= \alpha^2\gamma_2\gamma_1 W_2 W_1 \sum_r F_1^r F_{\text{renorm}}^r\,, \tag{4.227}$$

with

$$\begin{aligned}
F_{\text{renorm}}^r &= 1+\frac{1}{8\pi K}\alpha^2\beta_1|W_1|^2\Bigg(\\
&\quad 8\pi K\left(\frac{1}{2}\Lambda-\frac{N_r}{L}\right)-\frac{4K}{\imath\eta}\left(1-\frac{\delta_1}{\pi}\right)-\frac{\delta_1}{\pi}\frac{4K}{ut_f+\imath\eta}\\
&+\sum_{\nu=\pm1}\left(\nu\frac{\delta_2}{\pi}\frac{2\left(K+\nu r\right)}{x-\nu ut_f-\imath\eta}-\frac{2\nu\frac{\delta_2}{\pi}\left(K+\nu r\right)+\nu r(K+\nu r)^2}{x-\nu ut-\imath\eta}\right)\\
&+\left(1-e^{-\imath(\Delta\mathcal{C}_r+\Delta\mathcal{D}_{r,r})}\right)\Bigg[8\pi K\left(\frac{1}{2}\Lambda-\frac{N_{-r}}{L}\right)+\frac{\delta_1}{\pi}\frac{4K}{\imath\eta}-\frac{\delta_1}{\pi}\frac{4K}{ut_f+\imath\eta}\\
&+\sum_{\nu=\pm1}\left(\nu\frac{\delta_2}{\pi}\frac{2\left(K-\nu r\right)}{x-\nu ut_f-\imath\eta}-\frac{2\nu\frac{\delta_2}{\pi}\left(K-\nu r\right)+\nu r(K^2-1)}{x-\nu ut-\imath\eta}\right)\Bigg]\Bigg)\\
&-\frac{1}{8\pi K}\alpha^2\beta_2|W_2|^2\Bigg(8\pi K\frac{N_r}{L}-\left(1+\frac{\delta_2}{\pi}\right)\frac{4K}{\imath\eta}+\frac{\delta_2}{\pi}\frac{4K}{u(t_f-t)+\imath\eta}\\
&+\sum_{\nu=\pm1}\left(-\nu\frac{\delta_1}{\pi}\frac{2\left(K-\nu r\right)}{x-\nu u(t_f-t)-\nu\imath\eta}-\nu\frac{\delta_1}{\pi}\frac{2\left(K+\nu r\right)}{x-\nu ut+\nu\imath\eta}+r\frac{\left(K-r\nu\right)^2}{x-\nu ut+\nu\imath\eta}\right)\\
&+\left(1-e^{-\imath\Delta\mathcal{A}_r}\right)\Bigg[8\pi K\frac{N_{-r}}{L}-\frac{\delta_2}{\pi}\frac{4K}{\imath\eta}+\frac{\delta_2}{\pi}\frac{4K}{u(t_f-t)+\imath\eta}\\
&+\sum_{\nu=\pm1}\left(r\frac{\left(K^2-1\right)}{x-\nu ut+\nu\imath\eta}-\nu\frac{\delta_1}{\pi}\frac{2\left(K+\nu r\right)}{x-\nu u(t_f-t)-\nu\imath\eta}-\nu\frac{\delta_1}{\pi}\frac{2\left(K-\nu r\right)}{x-\nu ut+\nu\imath\eta}\right)\Bigg]\Bigg)\\
&+\frac{1}{64\pi^2K}\alpha^4\beta_2\beta_1|W_2|^2|W_1|^2\Bigg(\Bigg[\sum_{\nu=\pm1}\frac{4K\left(K+\nu r\right)^2}{\left(x-\nu ut-\nu\imath\eta\right)^2}\\
&-\Bigg(\frac{\delta_1}{\pi}\frac{4K}{\imath\eta+t_fu}+\frac{2K}{\imath\eta}\left(1-2\frac{\delta_1}{\pi}\right)+\sum_{\nu_1=\pm1}\Bigg(-\nu_1\frac{\delta_2}{\pi}\frac{2\left(K+\nu_1 r\right)}{x-\nu_1ut_f-\nu_1\imath\eta}\\
&\qquad+\nu_1\frac{\delta_2}{\pi}\frac{2\left(K+\nu_1 r\right)}{x-\nu_1ut-\nu_1\imath\eta}+\nu_1 r\frac{\left(K+\nu_1 r\right)^2}{x-\nu_1ut-\nu_1\imath\eta}\Bigg)\Bigg)\\
&\times\Bigg(\frac{\delta_2}{\pi}\frac{4K}{u(t_f-t)+\imath\eta}-\frac{2K}{\imath\eta}\left(1+2\frac{\delta_2}{\pi}\right)+\sum_{\nu_2=\pm1}\Bigg(r\frac{\left(K+r\right)^2}{x-\nu_2ut+\nu_2\imath\eta}\\
&\qquad-\nu_2\frac{\delta_1}{\pi}\frac{2\left(K-\nu_2 r\right)}{x-\nu_2u(t_f-t)-\nu_2\imath\eta}-\nu_2\frac{\delta_1}{\pi}\frac{2\left(K+\nu_2 r\right)}{x-\nu_2ut+\nu_2\imath\eta}\Bigg)\Bigg)\Bigg]
\end{aligned}$$

$$
\begin{aligned}
&+\left(1-e^{-\imath\Delta\mathcal{A}_r}\right)\left[\sum_{\nu=\pm1}\frac{4K\left(K^2-1\right)}{\left(x-\nu ut-\nu\imath\eta\right)^2}\right.\\
&-\left(\frac{\delta_1}{\pi}\frac{4K}{\imath\eta+t_f u}+\frac{2K}{\imath\eta}\left(1-\frac{\delta_1}{\pi}\right)+\sum_{\nu_1=\pm1}\left(-\nu_1\frac{\delta_2}{\pi}\frac{2\left(K+\nu_1 r\right)}{x-\nu_1 ut_f-\nu_1\imath\eta}\right.\right.\\
&\qquad\left.\left.+\nu_1\frac{\delta_2}{\pi}\frac{2\left(K+\nu_1 r\right)}{x-\nu_1 ut-\nu_1\imath\eta}+\nu_1 r\frac{\left(K+\nu_1 r\right)^2}{x-\nu_1 ut-\nu_1\imath\eta}\right)\right)\\
&\times\left(\frac{\delta_2}{\pi}\frac{4K}{u(t_f-t)+\imath\eta}-\frac{\delta_2}{\pi}\frac{4K}{\imath\eta}+\sum_{\nu_2=\pm1}\left(-\nu_2\frac{\delta_1}{\pi}\frac{2\left(K+\nu_2 r\right)}{x-\nu_2 u(t_f-t)-\nu_2\imath\eta}\right.\right.\\
&\qquad\left.\left.\left.-\nu_2\frac{\delta_1}{\pi}\frac{2\left(K-\nu_2 r\right)}{x-\nu_2 ut+\nu_2\imath\eta}+r\frac{\left(K^2-1\right)}{x-\nu_2 ut+\nu_2\imath\eta}\right)\right)\right]\\
&+\left(1-e^{-\imath(\Delta\mathcal{C}_r+\Delta\mathcal{D}_{r,r})}\right)\left[\sum_{\nu=\pm1}\frac{4K\left(K^2-1\right)}{\left(x-\nu ut-\nu\imath\eta\right)^2}\right.\\
&-\left(\frac{\delta_1}{\pi}\frac{4K}{\imath\eta+t_f u}-\frac{\delta_1}{\pi}\frac{4K}{\imath\eta}+\sum_{\nu_1=\pm1}\left(-\nu_1\frac{\delta_2}{\pi}\frac{2\left(K-\nu_1 r\right)}{x-\nu_1 ut_f-\nu_1\imath\eta}\right.\right.\\
&\qquad\left.\left.+\nu_1\frac{\delta_2}{\pi}\frac{2\left(K-\nu_1 r\right)}{x-\nu_1 ut-\nu_1\imath\eta}+\nu_1 r\frac{\left(K^2-1\right)}{x-\nu_1 ut-\nu_1\imath\eta}\right)\right)\\
&\times\left(\frac{\delta_2}{\pi}\frac{4K}{u(t_f-t)+\imath\eta}-\frac{2K}{\imath\eta}\left(1-2\frac{\delta_2}{\pi}\right)\right.\\
&\quad+\sum_{\nu_2=\pm1}\left(-\nu_2\frac{\delta_1}{\pi}\frac{2\left(K-\nu_2 r\right)}{x-\nu_2 u(t_f-t)-\nu_2\imath\eta}-\nu_2\frac{\delta_1}{\pi}\frac{2\left(K+\nu_2 r\right)}{x-\nu_2 ut+\nu_2\imath\eta}\right.\\
&\qquad\left.\left.\left.+r\frac{\left(K+r\right)^2}{x-\nu_2 ut+\nu_2\imath\eta}\right)\right)\right]\\
&+\left(1-e^{-\imath\Delta\mathcal{A}_r}-e^{-\imath(\Delta\mathcal{C}_r+\Delta\mathcal{D}_{-r,r})}+e^{-\imath(\Delta\mathcal{A}_r+\Delta\mathcal{C}_r+\Delta\mathcal{D}_{r,r})}\right)\\
&\qquad\times\left[\sum_{\nu=\pm1}\frac{4K\left(K-\nu r\right)^2}{\left(x-\nu ut-\nu\imath\eta\right)^2}-\left(\frac{\delta_1}{\pi}\frac{4K}{\imath\eta+t_f u}-\frac{\delta_1}{\pi}\frac{4K}{\imath\eta}\right.\right.\\
&\qquad\quad+\sum_{\nu_1=\pm1}\left(-\nu_1\frac{\delta_2}{\pi}\frac{2\left(K-\nu_1 r\right)}{x-\nu_1 ut_f-\nu_1\imath\eta}+\nu_1\frac{\delta_2}{\pi}\frac{2\left(K-\nu_1 r\right)}{x-\nu_1 ut-\nu_1\imath\eta}\right.\\
&\qquad\qquad\left.\left.\left.+\nu_1 r\frac{\left(K^2-1\right)}{x-\nu_1 ut-\nu_1\imath\eta}\right)\right)\right.\\
&\times\left(\frac{\delta_2}{\pi}\frac{4K}{u(t_f-t)+\imath\eta}-\frac{\delta_2}{\pi}\frac{4K}{\imath\eta}+\sum_{\nu_2=\pm1}\left(-\nu_2\frac{\delta_1}{\pi}\frac{2\left(K+\nu_2 r\right)}{x-\nu_2 u(t_f-t)-\nu_2\imath\eta}\right.\right.
\end{aligned}
$$

$$
\begin{aligned}
&\quad - \nu_2 \frac{\delta_1}{\pi} \frac{2\left(K - \nu_2 r\right)}{x - \nu_2 u t + \nu_2 \imath\eta} + r \frac{\left(K^2 - 1\right)}{x - \nu_2 u t + \nu_2 \imath\eta} \Bigg) \Bigg) \Bigg] \\
&+ \frac{1}{4\pi^2} \alpha^{\left(K - \frac{1}{K}\right)^2} \eta^{3K - \frac{1}{K}} e^{2 i k_F r x} \\
&\quad \times \prod_{\nu = \pm 1} \Bigg[\left(\eta + \imath(x - \nu u t)\right)^{-\frac{3K + \nu r}{2} - \nu r \frac{\delta_2}{\pi}} \left(\eta - \imath(x - \nu u t)\right)^{-\frac{K + \nu r}{2} + \nu r \frac{\delta_1}{\pi}} \\
&\qquad \times \left(\eta + \nu \imath(x - u t_f)\right)^{\nu r \frac{\delta_2}{\pi}} \left(\eta + \nu \imath(x - \nu u (t_f - t)\right)^{\nu r \frac{\delta_1}{\pi}} \Bigg] \\
&\quad + 4\pi e^{-\imath \Delta \mathcal{C}_r} \Bigg[8\pi K \left(\frac{1}{2} \Lambda - N_{-r} \right) + \frac{\delta_1}{\pi} \frac{4K}{\imath\eta} - \frac{\delta_1}{\pi} \frac{4K}{u t_f + \imath\eta} \\
&\qquad + \sum_{\nu = \pm 1} \left(+ \nu \frac{\delta_2}{\pi} \frac{2\left(K - \nu r\right)}{x - \nu u t_f - \imath\eta} - \frac{2\nu \frac{\delta_2}{\pi} \left(K - \nu r\right) + \nu r (K^2 - 1)}{x - \nu u t - \imath\eta} \right) \Bigg] \\
&\qquad \times \sum_{\nu' = \pm 1} \Bigg[\left(\frac{\nu' r}{2} e^{-\imath\left(\Delta \mathcal{A}_r + \Delta \mathcal{D}_{r,r}\right)} \left(K - \frac{1}{K} \right) \right) \\
&\qquad - e^{-\imath \Delta \mathcal{D}_{-r,r}} \left(2 + \nu' r \left(K + \frac{1}{K} \right) \right) \Bigg) \xi_{\nu'}(x,t) \Bigg] \,, \qquad (4.228)
\end{aligned}
$$

and

$$
\begin{aligned}
F_1^r = &\frac{1}{2\pi} \alpha^{\frac{2\delta_1^2}{\pi^2 K} + \frac{\delta_1}{\pi K} + \frac{2\delta_2^2}{\pi^2 K} + \frac{\delta_2}{\pi K} + \frac{K^2 - 1}{2K} - 1} e^{-\imath \Delta E_1 t_f} e^{-\imath \Delta E_2 (t_f - t)} e^{i k_F r x} \\
&\times \left(\eta + \imath u t_f\right)^{-2 \frac{\delta_1^2}{\pi^2 K} + \frac{\delta_1}{\pi K}} \left(\eta + \imath u (t_f - t)\right)^{-2 \frac{\delta_2^2}{\pi^2 K} - \frac{\delta_2}{\pi K}} \\
&\times \prod_{\nu = \pm 1} \Bigg[\left(\eta - \imath \nu x\right)^{\frac{\delta_1 \delta_2}{\pi^2 K} - \nu r \frac{\delta_1}{\pi}} \left(\eta - \imath\left(\nu x - u t_f\right)\right)^{-\frac{\delta_1 \delta_2}{\pi^2 K} + \frac{\delta_2}{\pi} \frac{(K \nu r + 1)}{2K}} \\
&\times \left(\eta - \imath\left(\nu x - u t\right)\right)^{\frac{\delta_1 \delta_2}{\pi^2 K} - \frac{\delta_1}{\pi} \frac{(K r + \nu)}{2K} + \frac{\delta_2}{\pi} \frac{(K r + \nu)}{2K} - \frac{(K + \nu r)^2}{4K}} \\
&\times \left(\eta - \imath\left(\nu x - u (t_f - t)\right)\right)^{-\frac{\delta_1 \delta_2}{\pi^2 K} + \frac{\delta_1}{\pi} \frac{(K \nu r - 1)}{2K}} \Bigg] \,. \qquad (4.152 \text{ revisited})
\end{aligned}
$$

We have reprinted the expression for F_1^r in eq. (4.152) for convenience, both because it appears in the previous expression for F in eq. (4.227) and because it will be referred to extensively below. With this exact expression for the reduced density matrix we have completely characterised the response of the localised states to the sequence of pulses.

All the matrix elements consist of complicated combinations of power laws in either distance, one of the times or "light-cone" coordinate combinations $x \pm ut$, for some time t. The first two of these represent the expected decay of any correlations with distance and time. The light-cone coordinate terms suggest signals about the various quenches propagating through the system.

We notice that A and D_2 are completely independent of the scattering phase shifts δ_1 and δ_2, whilst B and D_1 show only a weak dependence. This suggests that these terms are wholly or largely unaffected by the FES physics and are instead dominated by the physics of the Luttinger liquid ground state. In the case of the D_is this is not very surprising. These terms represent one of the localised states being excited and the fermion/hole generated being lost into the wire. The asymmetry between the two terms is due to the renormalisation of the D_1 term by processes in which the second localised state is repeatedly excited and deexcited. As these processed take place in the presence of the impurity potential and FES from the excitation of the first localised state, they introduce a weak dependence on the FES physics. In the case of D_2 there are no later events to be influenced by the FES from exciting the second state, and so there is no dependence on FES physics.

The A term is independent of FES physics for similar reasons to the D_2 term. All the processes that contribute to it involve localised states being excited and immediately deexcited, so there is no time for the orthogonality catastrophe to occur.

Given the requirement for trace conservation and the fact that none of the other diagonal elements as strongly dependent on the FES, it is not possible for B to show a strong dependence either. It does have a weak dependence on δ_1, mirroring the weak dependence of D_1.

The off diagonal coherence F shows a much stronger dependence on both δ_1 and δ_2, suggesting that the FES physics plays a more prominent role here. We can see in eq. (4.227) that F consists of two terms, corresponding to the release at the first localised state and the absorption at the second localised state of a left or right moving fermion respectively. Each of these terms has the form of the leading order term F_1^r, renormalised by a complicated combination of power laws, F^r_{renorm}, physically caused by repeatedly exciting and deexciting the localised states during the two pulses. Each of the power laws in F^r_{renorm} is peaked at positions where there are already peaks in F_1^r, so these renormalisations are simply quantitative corrections to the shape of the peak; the term F_1^r exhibits examples of all of the qualitative feature and all of the essential physics. We will therefore focus our analysis on this term for simplicity.

Firstly we will examine the operator form of F_1^r in eq. (4.152). We see that it has the form of a Loschmidt echo; it can be read as introducing a fermion into the wire at the origin, time evolving forward to time t in the presence of the impurity potential from the first state, removing a fermion at position x, time evolving forward to time t_f now with both impurity potentials turned on and then comparing with the evolution of the initial state if no particles were added and no impurity potentials were present. This image is reinforced if we consider the diagram in Fig. 4.3(d) that gives rise to it. This is strongly reminiscent of the calculation of the absorption matrix element in the standard FES and, indeed, if we set $t_f = t$ and $x = 0$ (or alternatively we consider the limit that $ut \gg x$) we find that

$$F_1^r \sim t^{-2\frac{\delta_1}{\pi K}\left(\frac{\delta_1}{\pi}-1\right)-\frac{1}{2}\left(K+\frac{1}{K}\right)}\,, \tag{4.229}$$

which is exactly the Nozières-De Dominicis result, up to corrections due to the interactions in the Luttinger liquid and orthogonality catastrophe in the channel the fermion was not emitted into [3, 65, 105].

Next we note that there are terms of the form

$$(\eta - \nu\imath(x - \nu u t))^{-\mathcal{P}} , \tag{4.230}$$

which result in a peak at $x = \pm ut$. This peak (slighty modified by contributions from F^r_{renorm}) is illustrated in Fig. 4.4. This strongly suggests the presence of a signal propagating at a speed of u the renormalised Fermi velocity, with an increase in density matrix coherences if the time between the pulses matches time of flight of the signal. The dependence of the power law exponent $\mathcal{P}$ on the impurity scattering phase shifts, clearly shown in Fig. 4.4, is indicative of the important roll being played by FES physics.

Similarly there are terms of the form

$$(\eta - \nu\imath(x - \nu u t_f))^{-\mathcal{Q}} , \tag{4.231}$$

giving a peak if the time between the first pulse and the final measurement matches the signal time of flight. We note that all of the power law exponents in F_1^r depend on ν and r only through the combination νr, so that it is only whether the direction of propagation of the term matches or goes against the chirality of the added fermion that matters. Terms propagating "the wrong way" are permitted due to the presence of backscattering interactions in the Luttinger liquid. In this case the right moving fermion includes a contribution from the left moving normal mode, which can semi-classically be interpreted in terms of a fermion being backscattered, propagating against its original chirality and then being backscattered again. In the absence of bulk backscattering interactions $K = 1$ and many terms drop out of F_1^r, so that terms where $\nu r = -1$ make only a "pure orthogonality catastrophe" contribution of the form $\frac{\delta_1\delta_2}{\pi^2}$ or $\frac{\delta_i^2}{\pi^2}$, with no contribution from the propagating fermion.

Figure 4.4: The full off diagonal matrix element, F, including all higher order corrections, as a function of the time between the pulses, in units of the time of flight $\frac{x}{u}$, with $t_f = t$, for a range of values of the scattering phase shift δ_1. Data is plotted using the values $K = 1.0$, $W_1 = W_2 = 1.3$, $\alpha = \eta = 0.01x$ and $k_F = \frac{2\pi N}{L} = 10/x$. The signal propagating at u can be clearly seen, as can the effect of the FES physics, encapsulated in the signal's dependence on δ_1.

(a)

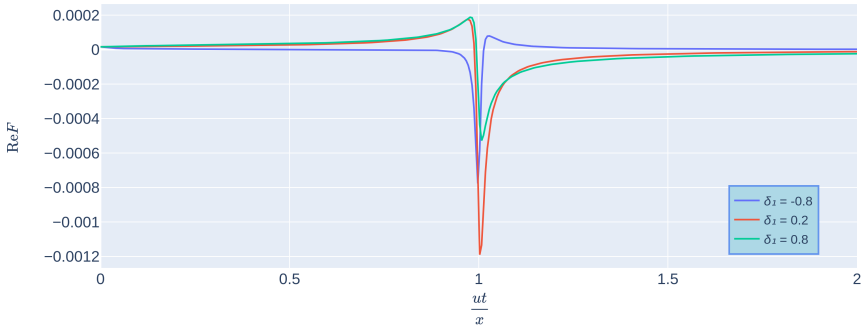

(b)

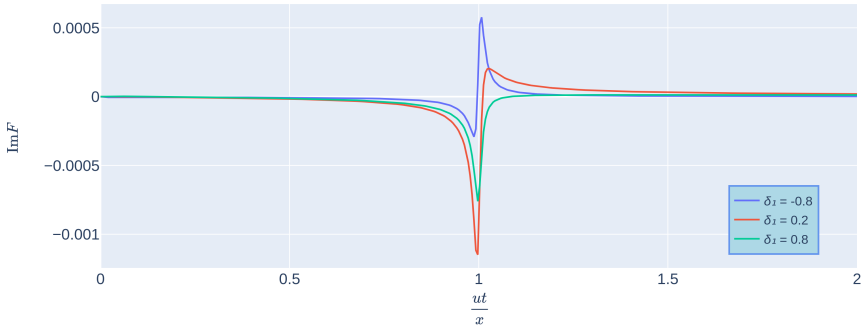

(c)

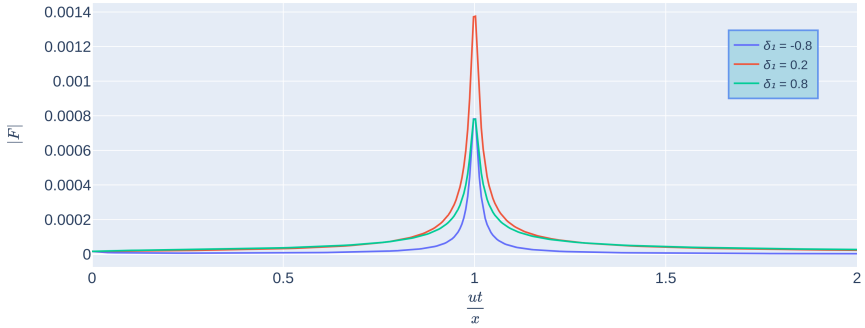

4.8 Entanglement and the Spread of Information

It is natural to consider how information about the transitions of the localised states travels through the system. One natural quantity to consider is the degree of entanglement between the localised states. This can be straightforwardly calculated from the density matrix eq. (4.18). Unfortunately it turns out that in our model the mutual entanglement [106] vanishes for all times.

The vanishing entanglement is due to too much information about the localised states being lost to the wire, expressed by the entries D_1 and D_2 in the density matrix, washing out any measurable entanglement between the localised states. Since the same processes are responsible for the dissipation into the bath as the transfer of information between the localised states D_1 and D_2 end up being a comparable size to F, which contains the quantum correlations between the localised states. In other similar, but more complex, models, however, these processes need not have comparable strength and so this problem should not necessarily arise. For example if the state of the impurity represented a spin, rather than charge, degree of freedom we would expect the impurity state to be more resistant to decoherence and would have a more complex interaction between the impurity and the wire. In this case we would still expect FES physics very similar to in our simpler model here, but it may be possible to retain a measurable level of entanglement between the impurities.

In order to study the spread of quantum information in a way which will hopefully generalise to more complex models, we will again, therefore, focus on the off diagonal term F, which must bound any reasonable measure of quantum correlations between the two localised states, as any such measure should vanish for a classical ensemble. We will, furthermore, focus this analysis on the term F_1^r for the reasons discussed above.

As discussed above F_1^r has peaks at times corresponding to the time of flight between the localised states. We also find, however, that there is a difficulty in using this as a means to transmit quantum information. If we take the limit that $t_f \gg t, \frac{x}{u}$, we find that

$$F_1^r \sim t_f^{-\frac{(\delta_1+\delta_2)^2}{\pi^2}} \quad . \tag{4.232}$$

This result is quite remarkable. It means at long times the off diagonal terms will always decay to zero, washing out any transmitted quantum information. This can only be prevented if the scattering phase shifts are finely tuned to $\delta_1 = -\delta_2$.

The same long time decay is observed if we consider the full F, rather than just F_1^r, as can be seen in Fig. 4.5. At times $\frac{u(t_f-t)}{x} > 10$, for both $\delta_1 = \pm 0.8$, the graph $|F|$ decreases linearly on the log-log scale, indicating a power law decay. In the case of $\delta_1 = 0.2 = -\delta_2$, however $|F|$ does not decay but remains at a constant value.

We notice that the decay exponent in eq. (4.232) has the form of the orthogonality catastrophe decay exponent for a scatterer with phase shift $\delta_1 + \delta_2$ (with

no propagating fermion). This suggests that what we are seeing at long times is a manifestation of the orthogonality catastrophe taking place in the bath due to the pair of scatterers. As the localised states have become entangled with the state of the wire, and the wire tends to a state orthogonal to its initial state, the quantum coherence of the localised states is lost.

This is an important result for quantum information applications based on many-fermion systems, for example quantum dot based quantum computing. The decay of the off diagonal element seems to be due to universal OC physics and we do not expect to be unique to our specific model. The loss of coherence to the OC in the bath, therefore, represents an obstacle to the practical use of many-fermion systems to transmit quantum information arising from fundamental many-body physics. To avoid these problems the system must either be engineered so that the phase shifts exactly cancel, which may be non-trivial if possible at all (especially if there are several combinations of states being "on" and "off" which must be considered), or the switching of the impurity states must be slow enough to avoid quenching the wire, and so avoid the OC. This, naturally limits the speed at which the information processing system can operate.

Figure 4.5: The full off diagonal matrix element, F, including all higher order corrections, as a function of the time between the second pulse and the measurement, in units of the time of flight $\frac{x}{u}$, for a several of values of the scattering phase shift δ_1. Data is plotted using the values $t = \frac{x}{u}$, $\delta_2 = -0.2$, $K = 1.0$, $W_1 = W_2 = 1.3$, $\alpha = \eta = 0.01x$ and $k_F = \frac{2\pi N}{L} = 10/x$. At long times, for both $\delta_1 = 0.8 > -\delta_2$ and $\delta_1 = -0.8 < -\delta_2$, $|F|$ can be clearly seen to decay with power laws. In the case of $\delta_1 = 0.2 = -\delta_2$, however, $|F|$ does not decay but tends to a constant. All three curves display an "echo peak" at $\frac{u(t_f-t)}{x} = 1$.

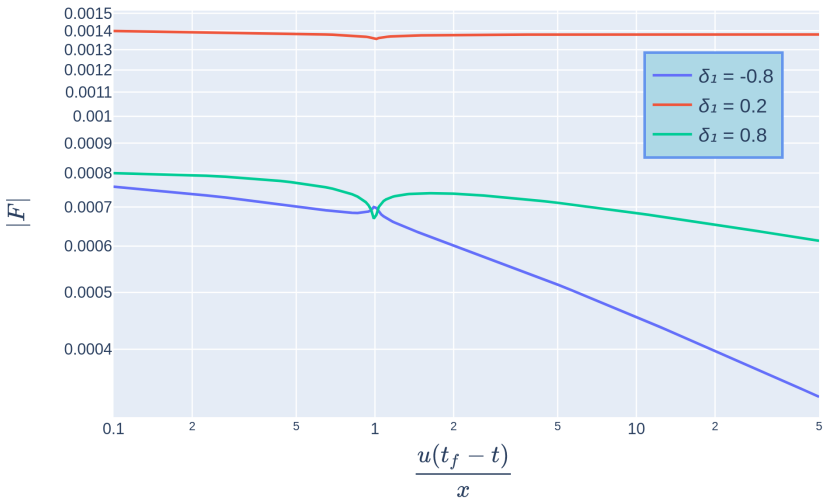

4.9 Echos of Catastrophe

All three terms in Fig. 4.5 display a feature at $\frac{u(t_f-t)}{x} = 1$. This arises from a somewhat surprising term appearing in F_1^r. The last term in eq. (4.154) has the form

$$(\eta - \imath(\nu x - u(t_f - t)))^{-\mathcal{S}} \ . \tag{4.233}$$

What is surprising about this term is that it becomes singular at a time $t_f - t = \left|\frac{x}{u}\right|$. That is at the point when a signal propagating out from the second localised state at the time of the second pulse reaches the position of the first localised state. This seems like a reasonable place to see a feature, except that, as there is no pulse at this time, *the occupation numbers of the localised states cannot change*. This implies that this peak is a pure interference effect and not associated with any transition in the occupation number basis.

It is fairly straightforward to trace the origin of this term in the calculation of eq. (4.154); it arises from the combination of the shift term from the first pulse time evolved to t_f, $R_1^\dagger(t_f)$ and the terms describing the removal of the fermion

and the shift in the Hamiltonian at the second pulse $\psi_r(x,t)$ and $R_2(t)$. The two FES at times 0 and t both create a large number of charge density wave excitations (with a wide range of energies) which gradually dephase, leading to the orthogonality catastrophe. What we have found here is that at $t_f - t = \left|\frac{x}{u}\right|$ these many excitations are able to come back into phase and interfere constructively, to give a singular peak.

Physically the term can be seen to arise from interaction between the first impurity and the signal from the second pulse. The charge density at the site of the first impurity is coupled to the impurity potential. As the signal passes the impurity the charge density is altered, resulting in a shift in energy. This shift in energy results in a phase shift and leads to the echo peak.

This echo peak appears to be a novel and surprising feature of the spatial spread of the FES, however as it is not associated with any change in the occupation number of the localised states, it may be difficult to detect experimentally in setups similar to the one described here. Based on the discussion above, however, we would expect it to be a fairly generic feature of systems with multiple FES events happening at different spatial locations, so it may be possible to devise a setup where it could be detected directly.

4.10 Causality?

It is interesting to note that, whilst the results above require that $t_f > t > 0$, there is no requirement that $t, t_f > \frac{x}{u}$. In other words there is no sharp signal front for the propagating information about the FES event after the first pulse. This can be seen, in large part, as a consequence of the highly correlated nature of the ground state of a many-fermion system, before any external intervention was applied.

Consider the expression for F_1^r given in eq. (4.154). In the limit that $x \gg ut, ut_f$, that is far outside the light cone of the propagating signal we find that

$$F_1^r \sim \sum_{r=\pm 1} \prod_{\nu=\pm 1} (\eta - \nu x)^{-\frac{(K+\nu r)^2}{4K}} \tag{4.234}$$

which has the form of the standard Luttinger liquid correlation function. In other words, far outside the light cone of the signal the chances of adding and removing an electron from the wire are exactly what they would have been in a Luttinger liquid with no FES effect, which is exactly what would be expected.

The decay of the time dependence of F_1 with distance is, however, algebraic rather than exponential. Despite the signal travelling out at a speed of u, it should be possible to detect it some distance ahead of the peak at $x = ut$. The calculation of the reduced density matrix is unambiguous and the effect does seem to be physical.

This occurs do to the extended nature of the electronic wavefunctions in the ground state of the system leading to long ranged spatial correlations and the fact that the Hamiltonian is fundamentally non-relativistic and allows, in principle, arbitrarily fast transmission of information.

4.11 Time non-local interactions

We can view the process of one localised site emitting a fermion into the wire and a second site absorbing it as a form of interaction between them. This mediation of an interaction between local impurities by the continuum is reminiscent of the RKKY interaction, however there are a number of crucial differences. Most obviously there is the addition and absorption of a full electron in the system, rather than simply exchanging density fluctuations, however this is a choice specific to our particular model, made to keep the form of the correlators as simple as possible, and should not have a bearing on the underlying OC physics. More importantly, since we are interested in the dynamics of the system, there is a time delay between the emission and absorption of the fermion.

The standard treatment of RKKY is concerned with determining properties of the spectrum, and in particular the ground state, of the Hamiltonian and so quietly averages over any real time dynamics, considering only the $\omega = 0$ limit. Indeed any attempt to describe a quantum process with an effective Hamiltonian must reduce the dynamics to something time local, and so this type of averaging is necessary if we want to have a description in the form of an effective Schrödinger equation. In order to formalise this picture of an electron mediated interaction between the sites, whilst maintaining the full information about the dynamics, we will therefore consider an effective *action* for the system. By considering the full path of the system an effective action is able to incorporate the time delay due to the fermion flight time, manifesting itself as a time non-local interaction, coupling the state of the impurities at different times.

We will neglect electron-electron interactions for this section, as dealing with both interactions and adding and removing fermions explicitly within the path integral formalism is non-trivial and we know from the bosonized treatment that while interactions in the wire renormalise various coefficients, they do not qualitatively change the results.

To represent the fermionic path integral we introduce 4 Grassmann number variables, $d_1(t)$, $\bar{d}_1(t)$, $d_2(t)$ and $\bar{d}_2(t)$, to represent the localised states and a pair of Grassmann fields $\psi(y,t)$ and $\bar{\psi}(y,t)$ to represent the fermions in the continuum. With this in mind the action for this system is given by

$$S[\bar{\psi}, \bar{d}_1, \bar{d}_2, \psi, d_1, d_2] = S_e[\bar{\psi}, \psi] + \sum_{i=\pm 1} S_i[\bar{d}_i, d_i] + S_{\text{imp}}[\bar{\psi}, \bar{d}_1, \bar{d}_2, \psi, d_1, d_2] + S_{\text{pump}}[\bar{\psi}, \bar{d}_1, \bar{d}_2, \psi, d_1, d_2] \,, \tag{4.235}$$

where

$$S_e[\bar{\psi}, \psi] = \int_{\mathcal{K}} \mathrm{d}t \int \mathrm{d}y \, \mathrm{d}y' \, \bar{\psi}(y', t) \left[\imath \delta(y - y') \partial_t - H_0 \right] \psi(y, t) \,, \tag{4.236}$$

$$S_i[\bar{d}_i, d_i] = \int_{\mathcal{K}} \mathrm{d}t \, \bar{d}_i(t) (\imath \partial_t - E_i) d_i(t) \,, \tag{4.237}$$

$$S_{\text{imp}}[\bar{\psi},\bar{d}_1,\bar{d}_2,\psi,d_1,d_2] = -\int_{\mathcal{K}} \mathrm{d}t \int \mathrm{d}y \left[V_1\delta(y)(1-\bar{d}_1(t)d_1(t))\bar{\psi}(y,t)\psi(y,t) + V_2\delta(y-x)\bar{d}_2(t)d_2(t)\bar{\psi}(y,t)\psi(y,t)\right], \tag{4.238}$$

$$S_{\text{pump}}[\bar{\psi},\bar{d}_1,\bar{d}_2,\psi,d_1,d_2] = -\int_{\mathcal{K}} \mathrm{d}t\,\sqrt{\alpha}\Big[W_1(t)\bar{\psi}(0,t)d_1(t) + \bar{W}_1(t)\bar{d}_1(t)\psi(0,t) + W_2(t)\bar{\psi}(x,t)d_2(t) + \bar{W}_2(t)\bar{d}_2(t)\psi(x,t)\Big], \tag{4.239}$$

Here $\int_{\mathcal{K}} \mathrm{d}t$ denotes integration over the Keldysh contour and all t values should be understood to take values on this contour (i.e. they may be on the forward or backward branch of the contour). Since the FES cannot be described by finite order perturbations on an equilibrium theory, we must use non-equilibrium methods and the Keldysh formalism. The action in eq. (4.235) is consistent with the Hamiltonian in section 4.1 and the Keldysh path integral formulation is equivalent to the calculation above. This formalism, however, provides a conceptually clearer way to approach the notion of a time non-local interaction.

To focus on the dynamics of the localised states we will integrate out the wire degrees of freedom, to obtain an effective action. This is analogous to tracing out the wire degrees of freedom above to obtain the reduced density matrix.

$$e^{\imath S_{\text{eff}}[\bar{d}_1,\bar{d}_2,d_1,d_2]} = e^{\imath\sum_{t=\pm1} S_i[\bar{d}_i,d_i]} \int \mathcal{D}[\bar{\psi},\psi] \exp\left[\imath\left(S_{\text{e}} + S_{\text{imp}} + S_{\text{pump}}\right)\right] \tag{4.240}$$

$$= e^{\imath\sum_{t=\pm1} S_i[\bar{d}_i,d_i]} \int \mathcal{D}[\bar{\psi},\psi] \exp\left[\imath\int_{\mathcal{K}} \mathrm{d}t\,\mathrm{d}t' \int \mathrm{d}y\,\mathrm{d}y' \Big(\bar{\psi}(y,t)G^{-1}(y,t,y',t')\psi(y',t') - \sqrt{\alpha}\delta(y-y')\delta(t-t')\Big[W_1(t')\delta(y')\bar{\psi}(y,t)d_1(t') + \bar{W}_1(t)\delta(y)\bar{d}_1(t)\psi(y',t') + W_2(t')\delta(y')\bar{\psi}(y,t)d_2(t') + \bar{W}_2(t)\delta(y)\bar{d}_2(t)\psi(y',t')\Big]\Big)\right], \tag{4.241}$$

where

$$G^{-1}[\bar{d}_1,\bar{d}_2,d_1,d_2](y,t,y',t') = \delta(t-t')\big[\imath\delta(y-y')\partial_t - H_0 - V_1\delta(y)\delta(y')(1-\bar{d}_1(t)d_1(t')) - V_2\delta(y-x)\delta(y-y')\bar{d}_2(t)d_2(t')\big]. \tag{4.242}$$

We can formally evaluate this by the normal rules for a Gaussian fermionic path integral. (Note that the decision to neglect interactions was crucial here.) This results in

$$e^{\imath(S_{\text{eff}} - \sum_{i=\pm1} S_i)} =$$

$$\mathrm{Det}(\imath G^{-1})\exp\left[-\alpha\int \mathrm{d}t\,\mathrm{d}t'\,\mathrm{d}y\,\mathrm{d}y'\left(\bar{W}_1(t)\delta(y)\bar{d}_1(t)+\bar{W}_2(t)\delta(y-x)\bar{d}_2(t)\right)\right.$$
$$\left.\times\, G[\bar{d}_1,\bar{d}_2,d_1,d_2](y,t,y',t')\big(W_1(t')\delta(y')d_1(t')+W_2(t')\delta(y'-x)d_2(t')\big)\right]. \tag{4.243}$$

If we write

$$G^{-1}=G_0^{-1}-V\ , \tag{4.244}$$
$$G_0^{-1}=\delta(t-t')\left[\imath\delta(y-y')\partial_t-H_0\right]\ , \tag{4.245}$$
$$V=\delta(t-t')\left(V_1\delta(y)\delta(y')(1-\bar{d}_1(t)d_1(t')-V_2\delta(y-x)\delta(y-y')\bar{d}_2(t)d_2(t')\right)\ , \tag{4.246}$$

we can factor the determinant in eq. (4.243) to give

$$\mathrm{Det}\left(\imath G^{-1}\right)=\mathrm{Det}\left(\imath G_0^{-1}\right)\mathrm{Det}\left(1+\imath G_0V\right)\ . \tag{4.247}$$

The term $\mathrm{Det}\left(\imath G_0^{-1}\right)$ is a constant, independent of any of the d_is so it can be absorbed into the normalisation of the path integral. Using the determinant-trace identity we can write

$$\mathrm{Det}\left(1+\imath G_0V\right)=\exp\left[\mathrm{Tr}\ln\left(1+\imath G_0V\right)\right]\ . \tag{4.248}$$

This is analogous to the closed loop term in the Nozières-De Dominicis paper [3], that is it is the renormalisation of the vacuum by the interaction. This can be seen by direct diagrammatic expansion of the term or by noting that it is independent of the pump terms, which add fermions to the wire and so give an "open-line" contribution.

The term

$$\big(\bar{W}_1(t)\delta(y)\bar{d}_1(t)+\bar{W}_2(t)\delta(y-x)\bar{d}_2(t)\big)G[\bar{d}_1,\bar{d}_2,d_1,d_2](y,t,y',t')$$
$$\times\left(W_1(t')\delta(y')d_1(t')+W_2(t')\delta(y'-x)d_2(t')\right) \tag{4.249}$$

in eq. (4.243) can be interpreted as an interaction between the two localised states. As it involves two different time indices, however, it is, as we mentioned above, a time non-local interaction. This gives a very different perspective on the system to the one given in the preceding sections.

We can connect these two perspectives by considering the Feynman-Vernon influence functional. If we write the localised state degrees of freedom together as $\vec{d}$ and the wire degrees of freedom as simply ψ then the Feynman-Vernon influence functional, $\mathcal{F}$, can be defined by

$$\langle\vec{d}_f|\rho(t)|\vec{d}'_f\rangle=\int \mathrm{d}\vec{d}_i\,\mathrm{d}\vec{d}'_i\int \mathrm{d}\psi_f\,\mathrm{d}\psi_i\,\mathrm{d}\psi'_i\int_{(\vec{d}_i,\psi_i)}^{(\vec{d}_f,\psi_f)}\mathcal{D}[\vec{d},\psi]e^{-\imath S[\vec{d},\psi]}$$
$$\int_{(\vec{d}'_i,\psi'_i)}^{(\vec{d}'_f,\psi_f)}\mathcal{D}[\vec{d}',\psi']e^{\imath S[\vec{d}',\psi']}\langle\vec{d}_i,\psi_i|\rho(0)\otimes\rho_T|\vec{d}_i,\psi'_i\rangle \tag{4.250}$$

$$= \int \mathrm{d}\vec{d}_i \, \mathrm{d}\vec{d}'_i \, \langle \vec{d}_i | \rho(0) | \vec{d}'_i \rangle \int_{\vec{d}_i}^{\vec{d}_f} \mathcal{D}[\vec{d}] \int_{\vec{d}'_i}^{\vec{d}_f} \mathcal{D}[\vec{d}'] e^{\imath \sum_i (S_i[\vec{d}'] - S_i[\vec{d}])} \mathcal{F}[\vec{d}, \vec{d}'] \, , \tag{4.251}$$

with

$$\mathcal{F}[\vec{d}, \vec{d}'] = \int \mathrm{d}\psi_f \, \mathrm{d}\psi_i \, \mathrm{d}\psi'_i \, \langle \psi_i | \rho_T | \psi'_i \rangle$$
$$\times \int_{\psi_i}^{\psi_f} \mathcal{D}[\psi] \int_{\psi'_i}^{\psi_f} \mathcal{D}[\psi'] e^{\imath (S_e[\psi'] + S_{\mathrm{imp}}[\psi', \vec{d}'] + S_{\mathrm{pump}}[\psi', \vec{d}'] - S_e[\psi] - S_{\mathrm{imp}}[\psi, \vec{d}] - S_{\mathrm{pump}}[\psi, \vec{d}])} \tag{4.252}$$

$$= \mathrm{Tr} \left[U^\dagger[\vec{d}] U[\vec{d}'] \rho_T \right] \, , \tag{4.253}$$

where $\int_\alpha^\beta \mathcal{D}[f]$ denotes the path integral over f with boundary conditions given by α and β respectively and $U[\vec{d}]$ denotes the evolution operator for the wire, given that the localised states follow a fixed path $\vec{d}(t)$. The Feynman-Vernon influence functional encapsulates the full information about the wire and its interaction with the localised states and so if we can calculate it we can, in principle, use it to calculate the evolution of the density matrix.

It can be seen that the double path integral (together with the integral over ψ_f) in eq. (4.252) is identical to the path integral along the Keldysh contour given in eq. (4.240), with the path integral over ψ' corresponding to the forward branch of the contour, the path integral over ψ corresponding to the backward branch of the contour and ψ_f giving the integral over the final state at the very end of the contour. This connection is even more apparent in eq. (4.253), which strongly resembles the form of the Keldysh partition function. The fact that there is only a single integral over the fianl states, thereby closing the contour, is due to our tracing out the state of the wire to obtain the reduced density matrix forcing the final state of the wire at the end of the forward and backward time evolutions to be equal. By contrast, we do not trace out the state of the impurities and so eq. (4.250) contains two distinct final states for the impurites and the corresponding evolution contours would not be closed.

The perturbative expansion of the time evolution operator can be seen as an explicit summing over the possible paths of the system, with all possible sequences of interactions occurring. (This approach of explicit resummation was famously used by Anderson, Yuval and Hamann [52, 54, 58, 59] to analyse the Kondo problem, treating each possible path as a series of Fermi edge like events and resumming the result.)

The formalism developed in this section is, however, cumbersome for practical calculations. This is due to the non-linearity of the interaction term. The interaction coefficient $G[\bar{d}_1, \bar{d}_2, d_1, d_2]$ is itself a complex functional of d_1 and d_2. This means that directly evaluating the functional integral for S_{eff} is not practical (if indeed it is possible). Therefore, whilst the path integral provides an elegant tool to understand earlier results conceptually, for practical calcula-

tions the methods employed above in determining the density matrix, $\rho(t)$, are preferable.

4.12 Further speculation

4.12.1 Finite Temperature

We will briefly discuss the effect of the wire initially being in a finite temperature state as there is little new ground conceptually in doing so, but it is of obvious importance for experimental realisations. To introduce a finite temperature wire we replace the initial zero temperature density matrix for the wire degrees of freedom, which we had suggestively named $\rho_{T=0}$, with a finite temperature density matrix

$$\rho_T = \frac{e^{-(H_0+H_{\rm ee})/T}}{\mathrm{Tr}\left[e^{-(H_0+H_{\rm ee})/T}\right]} \,. \tag{4.254}$$

The change in the continuum density matrix carries through the calculation in a straightforward manner. The partial traces over the wire degrees of freedom are now performed with the new density matrix and the zero temperature wire expectations are now replaced with finite temperature expectations. The evaluation of these types of expectation has been studied extensively, for example in [24, 93]. Explicitly reproducing the results above for the finite temperature case would be a routine, but not terribly enlightening calculation. To understand the essential physics we can employ a rule of thumb, attributed to Yuval and Anderson [54], and subsequently shown to be rigorous [84], that to obtain the finite temperature expectation values in a Luttinger Liquid we can simply take the characteristic power law correlators and replace them with powers of sinh functions

$$\left(\imath\eta + \frac{x}{u} - t\right)^{-\alpha} \to \left[\frac{\sinh\left(\pi k_B T(\frac{x}{u} - t + \imath\eta)\right)}{\pi k_B T}\right]^{-\alpha} \,. \tag{4.255}$$

With this rule we can see the effect of temperature on the correlation functions. For $\left|\frac{x}{u} - t\right| \ll \frac{1}{k_B T}$ we recover the zero temperature result. For $\left|\frac{x}{u} - t\right| \gg \frac{1}{k_B T}$ the temperature provides an exponential cut off on the correlation function.

We therefore have a qualitative picture of the spatial spread of the FES at finite temperature. The phenomenology follows the same basic outline as the zero temperature case described above, but temperature acts as a cut off, limiting the range of the range of the travelling signal and the time after the pulses that it can be detected.

If we assume a Fermi velocity $u \sim v_F \sim 10^5 \mathrm{ms}^{-1}$ and a separation between the impurities $x \sim 1\mu\mathrm{m}$ this gives $T_{\max} = \frac{\hbar u}{k_B x} \sim 0.75\mathrm{K}$, which is experimentally obtainable.

4.12.2 Backscattering impurities

We will now return to consider the effect of backscattering interactions. As mentioned above in section 4.5 the inclusion of backscattering from the impurity results in transcendental terms in the Hamiltonian which cannot be treated analytically. A full evaluation of the resulting correlation functions would require either sophisticated non-perturbative approaches or the use of renormalisation group methods.

We will not explore the renormalisation group approach to this problem here for two reasons. Firstly, standard RG methods typically focus on the static or constant frequency cases and are not well suited to the study of transient behaviour as we are here. Secondly, as discussed in section 4.5 and in [77], whilst the backscattering term may be a relevant perturbation, the many-body correlations that result in renormalisation take time to build up and so are unlikely to contribute strongly on the short time scales $\sim \frac{x}{v_F}$ we are considering. We will, therefore, instead employ a perturbative approach, which should be able to, at the very least, give a qualitative indication of the new physics introduced by the backscattering impurity and should be accurate at sufficiently short times.

We will focus on the F_1 term, because, as discussed above, this give a representative example of the majority of the interesting physics. For the sake of simplicity we will also limit our attention to the case that $t_f = t$, as this both removes the effect of the FES due to the second localised state and simplifies time ordering considerations. We will observe, however, that the A and D_2 terms will remain independent of FES physics even after backscattering is included.

As stated in eq. (4.69), the backscattering potential is given by

$$h_{\text{back}}(\tau) = \sum_{i\in\{1,2\}} \frac{V_{ib}(\tau)}{2\pi\alpha} \sum_{\sigma=\pm1} e^{-\imath\sigma(\tilde{\varphi}_+(0,\tau)+\tilde{\varphi}_-(0,\tau))} , \tag{4.256}$$

where we have included a time evolution under the Hamiltonian $h_{1,0}$ in anticipation of the perturbative expansion.

We can now write F_1 in the interaction picture of this new perturbation

$$F_1 = e^{-\imath\Delta E_1 t} \left\langle T\psi(x,t)R_1^\dagger(t) \exp\left[-\imath\int_0^t \mathrm{d}\tau\, h_{\text{back}}(\tau)\right] R_1(0)\psi^\dagger(0,0)\right\rangle . \tag{4.257}$$

Expanding the exponential perturbatively we obtain

$$\begin{aligned} F_1 &= e^{-\imath\Delta E_1 t} \sum_{n=0}^{\infty} \left[\frac{1}{n!}\left(\prod_{1=1}^{n} \frac{-\imath V_{1b}}{2\pi\alpha}\int_0^t \mathrm{d}\tau_i \sum_{\sigma_1=\pm1}\right)\right. \\ &\qquad \left.\left\langle T\psi(x,t)R_1^\dagger(t)\left[\prod_{i=1}^{n} e^{-\imath\sigma_i(\tilde{\varphi}_+(0,\tau_1)+\tilde{\varphi}_-(0,\tau_i))}\right] R_1(0)\psi^\dagger(0,0)\right\rangle\right] \\ &= e^{-\imath\Delta E_1 t} \sum_{n=0}^{\infty} \left[\frac{1}{n!}\left(\prod_{1=1}^{n} \frac{-\imath V_{1b}}{2\pi\alpha}\int_0^t \mathrm{d}\tau_i \sum_{\sigma_1=\pm1}\right) \sum_{r,r'=\pm1}\right. \end{aligned} \tag{4.258}$$

$$\left\langle T\psi_r(x,t)R_1^\dagger(t)\left[\prod_{i=1}^{n}e^{-\imath\sigma_i(\tilde{\varphi}_+(0,\tau_1)+\tilde{\varphi}_-(0,\tau_i))}\right]R_1(0)\psi_{r'}^\dagger(0,0)\right\rangle\right] . \tag{4.259}$$

We now consider the constraint in eq. (4.86), which states that the overall expectation of a product of exponentials of bosonised fields vanishes unless the sum the coefficients of the fields in the exponentials is zero. When this condition is applied to eq. (4.259) we find, if the expectation value is to be non-zero we must have

$$r - r' + 2\sum_{i=1}^{n}\sigma_i = 0 . \tag{4.260}$$

If n is even, then, as $\sigma_1 = \pm 1$, we have that $\sum_{i=1}^{n}\sigma_i$ is also even, giving us

$$2\sum_{i=1}^{n}\sigma_i \equiv 0 \mod 4 . \tag{4.261}$$

This implies that, if eq. (4.260) is to be satisfied,

$$r - r' \equiv 0 \mod 4 , \tag{4.262}$$

$$\Rightarrow r = r' , \tag{4.263}$$

as $r, r' = \pm 1$. Conversely if n is odd, $\sum_{i=1}^{n}\sigma_i$ is odd, implying that

$$2\sum_{i=1}^{n}\sigma_i \equiv 2 \mod 4 . \tag{4.264}$$

Imposing eq. (4.260) then gives us

$$r - r' \equiv -2 \mod 4 , \tag{4.265}$$

$$\Rightarrow r = -r' . \tag{4.266}$$

This can be interpreted as saying that if we put in a right mover, and there are an even number of backscattering events we will take out a right mover and if there are an odd number of backscattering events we will take out a left mover.

We can evaluate each term in eq. (4.259) using eq. (4.95). After doing so we can factor out the terms that do not depend on σ_i. For the even order terms this must give the zeroth order term F_1^r, for the odd terms it will give a slightly modified expression, due to the change in chirality of one of the fermion operators.

$$F_1 = \sum_{r=\pm 1}\left[F_1^r\sum_{n=0}^{\infty}D_{2n}^r + \tilde{F}_1^r\sum_{n=0}^{\infty}D_{2n+1}^r\right] , \tag{4.267}$$

where

$$\tilde{F}_1^r = \frac{1}{2\pi}\alpha^{-\frac{1}{K}\frac{\delta_1}{\pi}\left(3-2\frac{\delta_1}{\pi}\right)-\frac{K^2-1}{2K}}e^{\Delta E_1 t}e^{\imath r k_F x}\left(\eta+\imath u t\right)^{\frac{1}{K}\frac{\delta_1}{\pi}\left(1-2\frac{\delta_1}{\pi}\right)}$$

$$\prod_{\nu=\pm1}(\eta-\nu\imath x)^{-\frac{\delta_1}{\pi}\frac{(1+\nu rK)}{2K}}(\eta-\nu\imath(x-\nu ut))^{\frac{K^2-1}{4K}+\frac{\delta_1}{\pi}\frac{(1+r\nu K)}{2K}}\,, \tag{4.268}$$

$$\begin{aligned}D_n^r=\frac{1}{n!}\left(\frac{-\imath V_{1b}}{2}\right)^n\int_0^t \mathrm{d}\tau_1\,\ldots\mathrm{d}\tau_n\sum_{\sigma_1\ldots\sigma_n=\pm1}\delta\left(r\left(1-(-1)^n\right)+2\sum_{i=1}^n\sigma_i\right)\\ \times\prod_{i=1}^n\left[\left(\frac{\eta-\imath(x-u(t-\tau_i))}{\alpha}\right)^{\sigma_i\frac{rK+1}{2}}\left(\frac{\eta+\imath(x+u(t-\tau_i))}{\alpha}\right)^{\sigma_i\frac{rK-1}{2}}\right.\\ \left.\times\left(\frac{\eta+u\tau_i}{\alpha}\right)^{(-1)^{n+1}r\sigma_iK}\prod_{j=1}^{i}\left(\frac{\eta+u|\tau_i-\tau_j|}{\alpha}\right)^{2K\sigma_i\sigma_j}\right],\end{aligned} \tag{4.269}$$

where, in the interests of readability, we have slightly abused notation in writing the δ-function, which should be 1 rather than infinite when its argument vanishes and D_0^r is understood to be 1. Interestingly F_1^r and $\tilde{F}_1^r$ are entirely independent of V_{1b} and the D_n^r are independent of V_{1f}, that is the contributions from the forward and backward scattering completely factorise. This significantly simplifies the calculations by allowing us to treat the two contributions separately.

We see that $\tilde{F}_1^r$ has the same general form as F_1^r (given that we are considering the case that $t_f=t$), with only a slight change to the power law exponents. In particular it shows the same propagating signal.

Evaluating the D_n^rs in a closed form is, in general, impossible and the convergence properties of the series in eq. (4.267) have not been determined. We can see, however, that they are explicitly functions of $x\pm ut$ and so they should show the same travelling signal as the other terms.

The first order term, however, can be explicitly evaluated to give

$$\begin{aligned}D_1^r=\frac{2^{\frac{1+K}{2}}}{1+K}\alpha^{-2K}V_{1b}\frac{rx\left(2\eta+\imath(ut+rx)\right)^K}{(ut-rx-\imath\eta)(rx+\imath\eta)}\Bigg[\\ \alpha^{\frac{K-1}{2}}(ut-rx-\imath\eta)(\eta+\imath rx)^{\frac{K-1}{2}}(x^2+\eta^2)^{\frac{1+K}{2}}\\ \times\mathfrak{F}_1\left(\frac{1+K}{2},-K,-\frac{1+K}{2},\frac{3+K}{2},\frac{rx-\imath\eta}{ut+rx-2\imath\eta},\frac{rx-\imath\eta}{2rx}\right)\\ +(rx+\imath\eta)(rx-ut+\imath\alpha)^{\frac{1-K}{2}}(rx)^{\frac{K-1}{2}}(\eta+\imath(ut-rx))^{\frac{1+K}{2}}(\eta+\imath(ut+rx))^{\frac{1+K}{2}}\\ \times\mathfrak{F}_1\left(\frac{1+K}{2},-K,-\frac{1+K}{2},\frac{3+K}{2},\frac{ut+rx-\imath\eta}{ut+rx-2\imath\eta},\frac{ut+rx-\imath\eta}{2rx}\right)\Bigg],\end{aligned} \tag{4.270}$$

where $\mathfrak{F}_1$ is Appell's hypergeometric function. If we plot the first order term as a function of t for fixed x we find that it diverges for both large t and large $|x|$. The divergence of D_1^r with x is clearly shown in Fig. 4.6 for a range of values of K. This suggests that the perturbative approach outlined here is valid only for a small range of these parameters and we probably cannot rely on the quantitative results it produces except for extremely small values

of V_{1b}. It should be possible to extend this region, at least up to a point, by considering higher order terms in eq. (4.267), but these would have to be computed numerically. These higher order terms should become larger at later times, so extending the time over which we are interested should require the inclusion of progressively more terms in eq. (4.267). Moving beyond this region would take us into the strong coupling regime indicated by the relevance (for repulsive interactions) of the backscattering term under renormalisation group flow. Standard renormalisation approaches, however, are poorly suited to the current problem, as discussed above.

Whilst the quantitative range of validity of of these results, we can examine the perturbative result for qualitative suggestions of what the full result may contain. For $K = 0.7$, Fig. 4.6(a) shows there is a kink the real part of D_1^r propagating in the opposite direction to the main signal in F_1 (i.e. if $r = 1$ the singularity in D_1^r is propagating to the left). This is what we might have expected from a backscattered signal. For $K \geq 1$, however, there are some unexpected features. Both Figs. 4.6(b) and 4.6(c) show a minimum in $|D_1^1|$ at around $x = \frac{u}{3}t$. Further numerical investigations suggest that this minimum propagates in the usual r direction (to the left for $r = 1$) with a constant speed of $\frac{u}{3}$, independent of K. It appears to be due to an approximate cancellation of the two bracketed terms in eq. (4.270). The physical origin of this feature, if it is physical at all, are not clear.

If we combine D_1^r with $\tilde{F}_1^r$ to get the full first order response, as shown in Fig. 4.7, then the features in Fig. 4.6 are superimposed with those which can be read off eq. (4.268). In particular we have a pronounced singularity propagating in the backscattered direction (left for $r = 1$). We can, however still see the features of D_1^1, most notably the divergence at large x and the minimum propagating at $\frac{u}{3}$ in the case that $K \geq 1$.

Our perturbative analysis gives us some suggestion of what may happen when backscattering is included fully, including the suggestion of novel physics by a feature propagating at a one third the speed of the excitations in the Luttinger Liquid. A more sophisticated approach is, however, required to give a real picture of how backscattering will change the spatio-temporal FES, and whether the features seen here have a physical basis.

4.12.3 Spinful Fermions

Luttinger liquids exhibit spin-charge separation: The spin and charge degrees of freedom are able to propagate independently of each other. The excitations of these separate degrees of freedom are charge and spin density waves respectively. Both sectors independently obey decoupled Luttinger liquid Hamiltonians, with different charge and spin velocities u_ρ and u_σ.

With this in mind we can fairly easily see the qualitative effect of adding spin to the model above, as the result will essentially be two decoupled copies of the original model with different propagation velocities. We would expect, therefore, for each of the propagating $x \pm ut$ terms in our expressions above to split into two terms travelling with spin and charge velocities respectively.

Figure 4.6: The real and imaginary parts of the FES independent part of the first order backscattering response $\frac{D_1^1}{V_{1b}}$ as a function of x for a range of different fermion-fermion interactions.

(a) Repulsive fermion-fermion interactions, $K = 0.7$

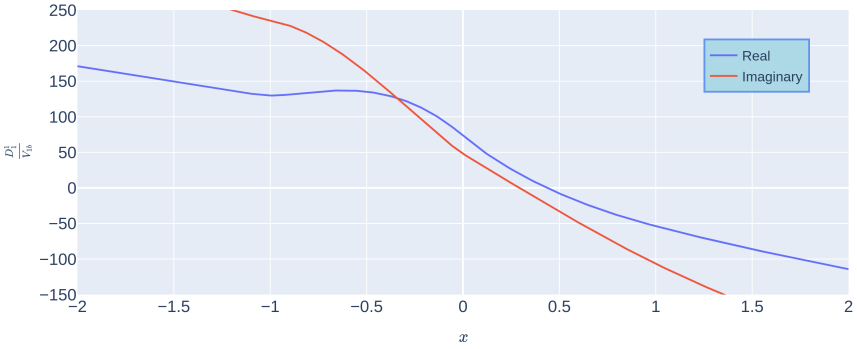

(b) Free Fermions, $K = 1$

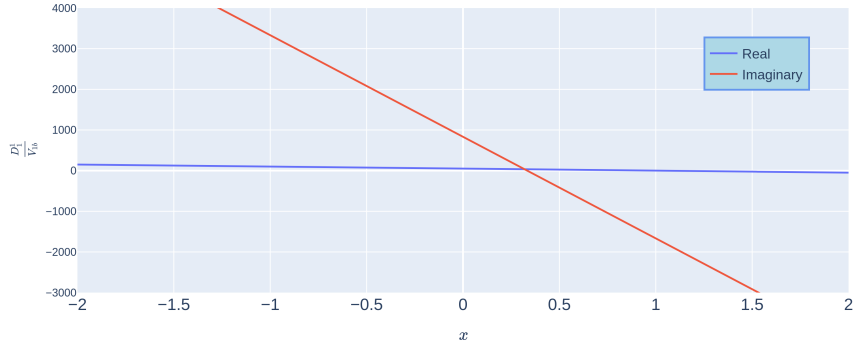

(c) Attractive fermion-fermion interactions, $K = 1.3$

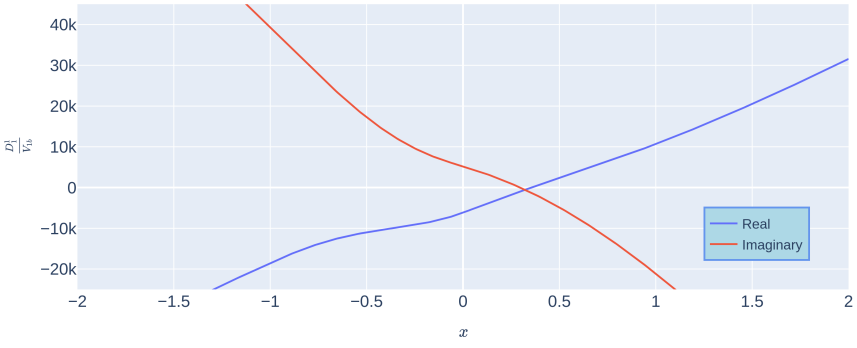

Figure 4.7: The magnitude of the first order backscattering response $\left|\frac{\tilde{F}_1^1 D_1^1}{V_{1b}}\right|$ as a function of x for a range of different fermion-fermion interactions. All values are calculated with $ut = 1$, $\delta_1 = 0.4\pi$ and $\alpha = \eta = 0.01$ in arbitrary units. The singular features propagating at $\pm u$ can be clearly seen, as can the minimum propagating at $\frac{u}{3}$ for attractive interactions.

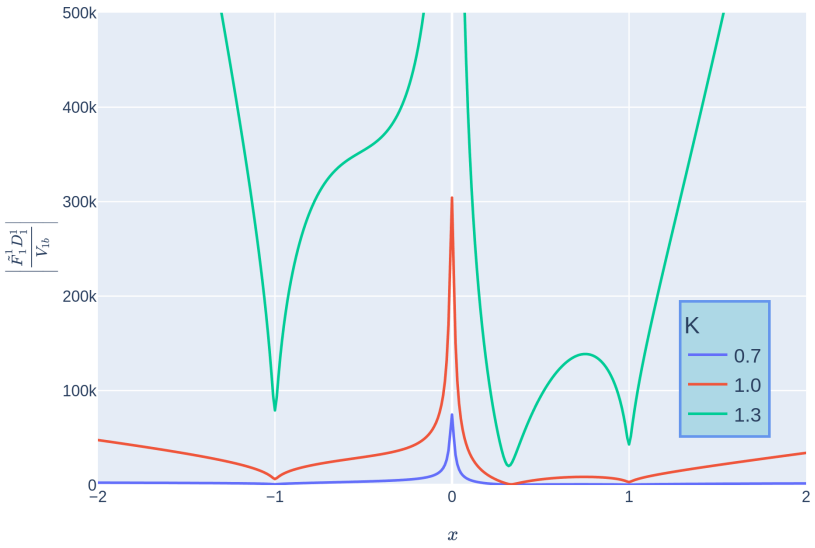

This will result in multiple peaks in, for example F_1^r, but each peak will have its height suppressed by the other terms which are not on resonance. This suppression of the peak represents the fact that the fractionalised spin and charge of the injected fermion have become separated in the wire, but we must remove a full fermion with both components.

We have chosen not to pursue explicitly calculating results in the spinful case. Although conceptually the calculation should be straightforward, the result would be even more cumbersome to work with and analyse than the already complex expressions obtained above. It seems more informative to work with the simpler model that we believe captures the essential physics. Experimental realisations of this model may require the spinful case to be calculated explicitly, in which case it should be a routine, if lengthy calculation.

4.12.4 Higher dimensional systems

One of the most striking features of the standard FES is that it is largely independent of dimension of the system. This feature cannot be reasonably expected

when considering the spatial FES, however some features of the calculation done here may carry over into the two or higher dimensional case.

If we consider only low energy scattering of the impurity, so that only the s-wave channel is available, we would expect recover quasi-1D behaviour. The spherical symmetry of the system means that we are left with only the radial coordinate. This suggests that the broad qualitative features of our calculation may still hold in this case. There should be some sort of propagating signal that decays with distance and with time. What's more in this low energy quasi-1D regime we would expect these decays to follow power laws similar to those we have calculated here. We would expect, however, that there would be an additional decay with the separation of the impurities $\sim \frac{1}{x}$ due to the spreading out of the signal.

Performing a detailed calculation in higher dimensions, however, may be non-trivial. Our results in one dimension gave rise to some lengthy expressions and it is reasonable to expect things to be at least as complicated in higher dimensions. A certain amount of care would have to be taken to ensure the methods used were not simply capable of computing the desired result, but were able to do so with reasonable efficiency and whilst making the underlying physics reasonably transparent.

To give an example of the type of concerns that may arise, consider the case of 2 point like impurities, in a 3D bath. We would expect turning on each of these impurities to result in a signal propagating out from the respective impurities in a spherical shell. The system as a whole, however, has a cylindrical symmetry. The representation of the spherically propagating signal in a cylindrical coordinate system will be somewhat complex, as would representing the dynamics driven by one impurity in a spherical coordinate system centred on the other. Reconciling these mismatched symmetries and finding a representation in which balances the needs of efficiently performing the required calculations whilst also allowing the physics of the result to be understood would require careful consideration.

4.13 Summary

We have investigated how the OC spreads out in space and time, with particular interest in the implications for quantum information processing technology. We considered a model of two impurities, the state of which can be changed by applying a pulse at fixed times, and were able to solve this model exactly, calculating the reduced density matrix for the impurity states. The most important result was calculating F, the off diagonal elements of this density matrix, which provide an upper bound on the transfer of quantum information between the localised states. The full form of F proved to be extremely complicated, however the FES physics turned out to be captured by the leading order term F_1^r.

Examining F_1^r we found that the term had the form of a generalised Loschmidt echo. It displayed power law decays with both the distance between the impu-

rities and the time between pulses. It also shows a peak propagating out from where the impurity was first introduced, indicating a signal carrying information about the OC travelling through the system. In addition, there is an 'echo peak' travelling back from the second impurity to the first, which can be detected in the coherence, despite being unable to alter the state of the impurities.

With regard to quantum information applications, we found that at long times the OC reasserted itself, with F_1^r decaying to zero, unless the system was finely tuned to $\delta_1 = -\delta_2$. This may represent a significant consideration for the design of quantum information processing systems based on many-fermion systems.

As an alternative perspective, we considered whether the OC could be viewed as a time delayed interaction between the localised states. To flesh out this idea we considered a path integral formulation and showed that the effective action for the localised states could indeed be viewed as having an interaction mediated by the OC in the wire. This approach provides interesting conceptual insights, but is less well suited to practical calculations than the operator formalism used to obtain the reduced density matrix.

Chapter 5

Shallow Bands and the Strong Potential Limit

This section is embargoed until February 2025

Chapter 6

Conclusions

This section is embargoed until February 2025

Acknowledgements

Funding

This work was supported by EPSRC [grant number EP/L015110/1]

Bibliography

[1]T. W. Kibble, "Topology of cosmic domains and strings", Journal of Physics A: Mathematical and General **9**, 1387 (1976).

[2]W. H. Zurek, "Cosmological experiments in superfluid helium?", Nature **317**, 505–508 (1985).

[3]P. Nozières and C. T. De Dominicis, "Singularities in the X-Ray Absorption and Emission of Metals. III. One-Body Theory Exact Solution", Physical Review **178**, 1097–1107 (1969).

[4]P. W. Anderson, "Infrared Catastrophe in Fermi Gases with Local Scattering Potentials", Physical Review Letters **18**, 1049–1051 (1967).

[5]Y. Adamov and B. Muzykantskii, "Fermi gas response to the nonadiabatic switching of an external potential", Physical Review B - Condensed Matter and Materials Physics **64**, 2453181–2453189 (2001).

[6]M. Knap, A. Shashi, Y. Nishida, A. Imambekov, A. A. Abanin, and E. Demler, "Time-dependent impurity in ultracold fermions: Orthogonality catastrophe and beyond", Physical Review X **2**, 041020 (2012).

[7]A. S. Plastina, J Goold, N. L. Gullo, F, A Sindona, J Goold, N. L. Gullo, and F Plastina, "Statistics of the work distribution for a quenched Fermi gas", New Journal of Physics **16**, 45013 (2014).

[8]I. Snyman, "Linear response of a one-dimensional conductor coupled to a dynamical impurity with a Fermi edge singularity", Physical Review B - Condensed Matter and Materials Physics Rev. B **89**, 85118 (2014).

[9]A Sheikhan and I. Snyman, "Fermi edge singularity and finite-frequency spectral features in a semi-infinite one-dimensional wire", Physical Review B - Condensed Matter and Materials Physics **86**, 85122 (2012).

[10]J. M. Zhang and Y. Liu, "Dynamical Friedel oscillation of a Fermi sea", (2018).

[11]D. Loss and D. P. DiVincenzo, "Quantum computation with quantum dots", Physical Review A - Atomic, Molecular, and Optical Physics **57**, 120–126 (1998).

[12]G. D. Mahan, "Excitons in degenerate semiconductors", Phys. Rev. **153**, 882–889 (1967).

[13]T. A. Callcott, E. T. Arakawa, and D. L. Ederer, "L23 soft-x-ray emission and absorption spectra of Na", Phys. Rev. B **18**, 6622–6630 (1978).

[14]A. K. Geim, P. C. Main, N. La Scala, L. Eaves, T. J. Foster, P. H. Beton, J. W. Sakai, F. W. Sheard, M. Henini, G. Hill, M. A. Pate, N. L. Scala, L. Eaves, T. J. Foster, P. H. Beton, J. W. Sakai, F. W. Sheard, M. Henini, G. Hill, and M. A. Pate, "Fermi-Edge Singularity in Resonant Tunneling", Physical Review Letters **72**, 2061–2064 (1994).

[15]I Itskevich, T Ihn, A Thornton, M Henini, T Foster, P Moriarty, A Nogaret, P Beton, L Eaves, and P Main, "Resonant magnetotunneling through individual self-assembled InAs quantum dots", Phys. Rev. B **54**, 16401–16404 (1996).

[16]K. A. Benedict, A. S. G. Thornton, T Ihn, P. C. Main, L Eaves, and M Henini, "Fermi edge singularities in high magnetic fields", Physica B: Cond. Mat. **256-258**, 519–522 (1998).

[17]I Hapke-Wurst, U Zeitler, H Frahm, A. G. M. Jansen, R. J. Haug, and K Pierz, "Magnetic-field-induced singularities in spin-dependent tunneling through InAs quantum dots", Phys. Rev. B **62**, 12621–12624 (2000).

[18]E. E. Vdovin, Y. N. Khanin, O. Makarovsky, Y. V. Dubrovskii, A. Patanè, L. Eaves, M. Henini, C. J. Mellor, K. A. Benedict, and R. Airey, "Magnetoanisotropy of electron-correlation-enhanced tunneling through a quantum dot", Physical Review B - Condensed Matter and Materials Physics (2007) 10.1103/PhysRevB.75.115315.

[19]N. Maire, F. Hohls, T. Lüdtke, K. Pierz, and R. J. Haug, "Noise at a Fermi-edge singularity in self-assembled InAs quantum dots", Physical Review B - Condensed Matter and Materials Physics (2007) 10.1103/PhysRevB.75.233304.

[20]M Rüth, T Slobodskyy, C Gould, G Schmidt, and L. W. Molenkamp, "Fermi edge singularity in II-VI semiconductor resonant tunneling structures", Appl. Phys. Lett. **93**, 182104 (2008).

[21]T. Krahenmann, L. Ciorciaro, C. Reichl, W. Wegscheider, L. Glazman, T. Ihn, K. Ensslin, T. Krähenmann, L. Ciorciaro, C. Reichl, W. Wegscheider, L. Glazman, T. Ihn, and K. Ensslin, "Fermi edge singularities in transport through lateral GaAs quantum dots", New J. Phys. **19**, 23009 (2017).

[22]R. Schmidt, M. Knap, D. A. Ivanov, J. S. You, M. Cetina, and E. Demler, "Universal many-body response of heavy impurities coupled to a Fermi sea: A review of recent progress", Reports on Progress in Physics **81**, 024401 (2018).

[23]M. Cetina, M. Jag, R. S. Lous, I. Fritsche, J. T. M. Walraven, R. Grimm, J. Levinsen, M. M. Parish, R. Schmidt, M. Knap, and E. Demler, "Ultrafast many-body interferometry of impurities coupled to a Fermi sea", Science **354**, 21 (2016).

[24]T. Giamarchi, *Quantum Physics in One Dimension* (2003).

[25]B. Roulet, J. Gavoret, and P. Nozières, "Singularities in the X-Ray Absorption and Emission of Metals. I. First-Order Parquet Calculation", Physical Review **178**, 1072–1083 (1969).

[26]N Rivier and E Simanek, "Exact calculation of the orthogonality catastrophe in metals", Phys. Rev. Lett. **26**, 435–438 (1971).

[27]D. C. Langreth, "Singularities in the X-ray absorption and emission of metals", Phys. Rev. **182**, 973–974 (1969).

[28]D. R. Hamann, "Orthogonality Catastrophe in Metals", Phys. Rev. Lett. **26**, 1030–1032 (1971).

[29]I Affleck and A. W. W. Ludwig, "The Fermi edge singularity and boundary condition changing operators", J. Phys. A. Math. Gen. **27**, 5375–5392 (1994).

[30]F. B. Kugler and J. von Delft, "Fermi-edge singularity and the functional renormalization group", Journal of Physics Condensed Matter **30**, 195501 (2018).

[31]R Haensel, G Keitel, P Schreiber, B Sonntag, and C Kunz, "Measurement of the anomaly at the LII,III edge of sodium", Phys. Rev. Lett. **23**, 528–529 (1969).

[32]T. A. Callcott, E. T. Arakawa, and D. L. Ederer, "Emission and absorption x-ray edges of Li", Phys. Rev. B **16**, 5185–5192 (1977).

[33]T. A. Callcott and E. T. Arakawa, "Temperature dependence of the K X-ray emission edge of Li", Phys. Rev. Lett. **38**, 442–445 (1977).

[34]T. Ishii, Y. Sakisaka, S. Yamaguchi, T. Hanyu, and H. Ishii, "Threshold Singularities of p-shell Absorption in Potassium, Rubidium and Cesium Metals", J. Phys. Soc. Japan **42**, 876–881 (1977).

[35]T. H. Chiu, D. Gibbs, J. E. Cunningham, and C. P. Flynn, "X-ray-edge problem in metals. I. Universal scaling in alkali-alkali alloys", Phys. Rev. B **32**, 588–601 (1985).

[36]D. Gibbs, T. H. Chiu, J. E. Cunningham, and C. P. Flynn, "X-ray-edge problem in metals. II. Alkali-metal atoms adsorbed on alkali and other metal surfaces", Phys. Rev. B **32**, 602–611 (1985).

[37]G. K. Wertheim, D. M. Riffe, and P. H. Citrin, "Bulk and surface singularity indices in the alkali metals", Phys. Rev. B **45**, 8703–8708 (1992).

[38]F. G. Fumi, "CXVI. Vacancies in monovalent metals", The London, Edinburgh, and Dublin Philosophical Magazine and Journal of Science **46**, 1007–1020 (1955).

[39]A. E. Ruckenstein and S. Schmitt-Rink, "Many-body aspects of the optical spectra of bulk and low-dimensional doped semiconductors", Physical Review B **35**, 7551–7557 (1987).

[40]S Jiang, J. M. Zhang, L. J. Zhang, and S. C. Shen, "The Fermi-edge singularity in CdTe/Cd1-xMnxTe:In multiple quantum wells", J. Phys. Condens. Matter **6**, 10391–10396 (1994).

[41]C Latta, F Haupt, M Hanl, A Weichselbaum, M Claassen, W Wuester, P Fallahi, S Faelt, L Glazman, J Von Delft, H. E. Türeci, and A Imamoglu, "Quantum quench of Kondo correlations in optical absorption", Nature **474**, 627–630 (2011).

[42]J. M. Calleja, A. R. Goñi, B. S. Dennis, J. S. Weiner, A Pinczuk, S Schmitt-Rink, L. N. Pfeiffer, K. W. West, J. F. Müller, and A. E. Ruckenstein, "Large optical singularities of the one-dimensional electron gas in semiconductor quantum wires", Solid State Commun. **79**, 911–915 (1991).

[43]X. L. Wang, M. Ogura, T. Guillet, V. Voliotis, and R. Grousson, "Strong Fermi-edge singularity in ultra-high-quality AlGaAs/GaAs quantum wires", Physica E **32**, 329–332 (2006).

[44]K. A. Matveev and A. I. Larkin, "Interaction-induced threshold singularities in tunneling via localized levels", Physical Review B - Condensed Matter and Materials Physics **46**, 15337–15347 (1992).

[45]D. H. Cobden and B. A. Muzykantskii, "Finite-temperature Fermi-edge singularity in tunneling studied using random telegraph signals", Phys. Rev. Lett. **75**, 4274–4277 (1995).

[46]R. A. Jalabert and H. M. Pastawski, "Environment-Independent Decoherence Rate in Classically Chaotic Systems", Physical Review Letters **86**, 2490 (2001).

[47]M. Combescot and P. Nozières, "Infrared catastrophy and excitons in the X-ray spectra of metals", J. Phys. France **32**, 913–929 (1971).

[48]G. Yuval, "X-Ray Edge Problem with Finite Hole Mass", Physical Review B **4**, 4315 (1971).

[49]E. Müller-Hartmann, T. V. Ramakrishnan, and G. Toulouse, "Localized Dynamic Perturbations in Metals", Physical Review B **3**, 1102 (1971).

[50]J. Kondo, "Resistance Minimum in Dilute Magnetic Alloys", Progress of Theoretical Physics **32**, 37–49 (1964).

[51]J. R. Schrieffer and P. A. Wolff, "Relation between the Anderson and Kondo Hamiltonians", Physical Review **149**, 491–492 (1966).

[52]P. W. Anderson and G. Yuval, "Exact results in the kondo problem: Equivalence to a classical one-dimensional coulomb gas", Physical Review Letters **23** (1969) 10.1103/PhysRevLett.23.89.

[53]P. W. Anderson, "A poor man's derivation of scaling laws for the Kondo problem", Journal of Physics C: Solid State Physics **3**, 2436–2441 (1970).

[54]G. Yuval and P. W. Anderson, "Exact Results for the Kondo Problem: One-Body Theory and Extension to Finite Temperature", Physical Review B **1**, 1522–1528 (1970).

[55]K. G. Wilson, "The renormalization group: Critical phenomena and the Kondo problem", Reviews of Modern Physics **47**, 773–840 (1975).

[56]N. Andrei, K. Furuya, and J. H. Lowenstein, "Solution of the Kondo problem", Reviews of Modern Physics **55**, 331–402 (1983).

[57]A. C. Hewson, *The Kondo Problem to Heavy Fermions* (Cambridge University Press, 1993).

[58]P. W. Anderson, G. Yuval, and D. R. Hamann, "Exact Results in the Kondo Problem. II. Scaling Theory, Qualitatively Correct Solution, and Some New Results on One-Dimensional Classical Statistical Models", Physical Review B **1**, 4464 (1970).

[59]P. W. Anderson, G. Yuval, and D. R. Hamann, "Scaling theory for the Kondo and one-dimensional Ising models", Solid State Communications **8**, 1033–1037 (1970).

[60]K. Ohtaka and Y. Tanabe, "Golden-rule approach to the soft-x-ray-absorption problem", Physical Review B **28**, 6833–6846 (1983).

[61]I. Klich, "Full Counting Statistics: An elementary derivation of Levitov's formula", (2002) 10.1007/978-94-010-0089-5.

[62]P. Deift, A. Its, and I. Krasovsky, "Asymptotics of Toeplitz, Hankel, and Toeplitz+Hankel determinants with Fisher-Hartwig singularities", Annals of Mathematics **174**, 1243–1299 (2011).

[63]D. B. Gutman, Y. Gefen, and A. D. Mirlin, "Bosonization out of equilibrium", EPL **90**, 37003 (2010).

[64]D. B. Gutman, Y. Gefen, and A. D. Mirlin, "Non-equilibrium 1D many-body problems and asymptotic properties of Toeplitz determinants", Journal of Physics A: Mathematical and Theoretical **44**, 165003 (2011).

[65]K. D. Schotte and U. Schotte, "Tomonaga's model and the threshold singularity of x-ray spectra of metals", Physical Review **182**, 479–482 (1969).

[66]A. Peres, "Stability of quantum motion in chaotic and regular systems", Physical Review A **30**, 1610–1615 (1984).

[67]J. J. Loschmidt, "Über den Zustand des Wärmegleichgewichts eines Systems von Körpern mit Rücksicht auf die Schwerkraft", Sitzungsberichte der Akademie der Wissenschaften, Wien **II**, 128–142 (1876).

[68]J. Watrous, *The Theory of Quantum Information* (Cambridge University Press, 2018), p. 590.

[69]P. Talkner, E. Lutz, and P. Hänggi, "Fluctuation theorems: Work is not an observable", Physical Review E - Statistical, Nonlinear, and Soft Matter Physics **75** (2007) 10.1103/PhysRevE.75.050102.

[70]F. M. Cucchietti, D. A. R. Dalvit, J. P. Paz, and W. H. Zurek, "Decoherence and the loschmidt echo", Physical Review Letters **91**, 210403 (2003).

[71]F. D. M. Haldane, "'Luttinger liquid theory' of one-dimensional quantum fluids. I. Properties of the Luttinger model and their extension to the general 1D interacting spinless Fermi gas", Journal of Physics C: Solid State Physics **14**, 2585–2609 (1981).

[72]R. Shankar, "Quantum field theory and condensed matter: An introduction", Quantum Field Theory and Condensed Matter: An Introduction, 1–439 (2017).

[73]D. K. Lee and Y. Chen, "X-ray response of the Luttinger model", Physical Review Letters **69**, 1399–1402 (1992).

[74]C. L. Kane and M. P. Fisher, "Transmission through barriers and resonant tunneling in an interacting one-dimensional electron gas", Physical Review B **46**, 15233–15262 (1992).

[75]C. L. Kane and M. P. Fisher, "Transport in a one-channel Luttinger liquid", Physical Review Letters **68**, 1220–1223 (1992).

[76]A. Komnik, R. Egger, and A. O. Gogolin, "Exact Fermi-edge singularity exponent in a Luttinger liquid", Physical Review B **56**, 1153 (1997).

[77]A. O. Gogolin, "Local time-dependent perturbation in Luttinger liquid", Physical Review Letters **71**, 2995–2998 (1993).

[78]C. L. Kane, K. A. Matveev, and L. I. Glazman, "Fermi-edge singularities and backscattering in a weakly interacting one-dimensional electron gas", Physical Review B **49**, 2253 (1994).

[79]A. Imambekov and L. I. Glazman, "Universal theory of nonlinear luttinger liquids", Science **323**, 228–231 (2009).

[80]M. Khodas, M. Pustilnik, A. Kamenev, and L. I. Glazman, "Fermi-Luttinger liquid: Spectral function of interacting one-dimensional fermions", Physical Review B - Condensed Matter and Materials Physics **76**, 155402 (2007).

[81]M. Pustilnik, M. Khodas, A. Kamenev, and L. I. Glazman, "Dynamic response of one-dimensional interacting fermions", Physical Review Letters **96**, 196405 (2006).

[82]N. D'Ambrumenil and B. Muzykantskii, "Fermi gas response to time-dependent perturbations", Physical Review B - Condensed Matter and Materials Physics **71**, 1–14 (2005).

[83]N. I. Muskhelishvili, *Singular Integral Equations* (Springer Netherlands, Dordrecht, 1977).

[84]B. Braunecker, "Response of a Fermi gas to time-dependent perturbations: Riemann-Hilbert approach at nonzero temperatures", Physical Review B - Condensed Matter and Materials Physics **73**, 75122 (2006).

[85]B. Muzykantskii, N D'Ambrumenil, and B. Braunecker, "Fermi-Edge Singularity in a Nonequilibrium System", Physical Review Letters **91**, 266602 (2003).

[86]W. Pauli, "General Principles of Quantum Mechanics", General Principles of Quantum Mechanics (1980) 10.1007/978-3-642-61840-6.

[87]D. A. Abanin and L. S. Levitov, "Fermi-edge resonance and tunneling in nonequilibrium electron gas", Physical Review Letters **94**, 186803 (2005).

[88]M. Gebert, H. Küttler, and P. Müller, "Anderson's Orthogonality Catastrophe", Commun. Math. Phys. **329**, 979–998 (2014).

[89]W. E. Liu, J. Levinsen, and M. M. Parish, "Variational Approach for Impurity Dynamics at Finite Temperature", Phys. Rev. Lett. **122**, 205301 (2019).

[90]I. Snyman and S. Florens, "Microscopic bosonization of band structures: x-ray processes beyond the Fermi edge", New J. Phys. **19**, 113031 (2017).

[91]I. Snyman, "Electron-electron correlations in a dynamical impurity system with a Fermi edge singularity", Physical Review B - Condensed Matter and Materials Physics **87**, 165135 (2013).

[92]S. Campbell, M. Á.M. A. García-March, T. Fogarty, and T. Busch, "Quenching small quantum gases: Genesis of the orthogonality catastrophe", Phys. Rev. A **90**, 13617 (2014).

[93]J. Von Delft and H. Schoeller, "Bosonization for Beginners Refermionization for Experts", Annalen der Physik Ann. Physik **9805275**, 225305 (1998).

[94]J. Sólyom, "The Fermi gas model of one-dimensional conductors", Advances in Physics **28**, 201–303 (1979).

[95]H. Steinberg, G. Barak, A. Yacoby, L. N. Pfeiffer, K. W. West, B. I. Halperin, and K. Le Hur, "Charge fractionalization in quantum wires", Nature Physics **4**, 116–119 (2008).

[96]K. Le Hur, B. I. Halperin, and A. Yacoby, "Charge fractionalization in nonchiral Luttinger systems", Annals of Physics **323**, 3037–3058 (2008).

[97]C. A. De Carvalho and H. M. Nussenzveig, "Time delay", Physics Report **364**, 83–174 (2002).

[98]C. Jackson and B. Braunecker, "Spatio-temporal Spread of Fermi-edge Singularity as Time Delayed Interaction and Impact on Time-dependent RKKY Type Coupling", Physical Review Research **4**, 013119 (2022).

[99]Z. Wang, Y. He, Q. Wang, Y. Zhang, B. Hu, and Z. Liu, "The application of double side Feynman diagram in strong-pump strong-probe spectroscopy", The 9th International Symposium on Ultrafast Phenomena and Terahertz Waves (2018), paper WI39, WI39 (2018).

[100]T. L. C. Jansen, S. Saito, J. Jeon, and M. Cho, "Theory of coherent two-dimensional vibrational spectroscopy", Journal of Chemical Physics **150**, 100901 (2019).

[101]W. P. Aue, E. Bartholdi, and R. R. Ernst, "Two-dimensional spectroscopy. Application to nuclear magnetic resonance", The Journal of Chemical Physics **64**, 2229–2246 (1976).

[102]W. Kuehn, K. Reimann, M. Woerner, T. Elsaesser, and R. Hey, "Two-dimensional terahertz correlation spectra of electronic excitations in semiconductor quantum wells", Journal of Physical Chemistry B **115**, 5448–5455 (2011).

[103]F. Mahmood, D. Chaudhuri, S. Gopalakrishnan, R. Nandkishore, and N. P. Armitage, "Observation of a marginal Fermi glass", Nature Physics **17**, 627–631 (2021).

[104]P. C. Chen, "An Introduction to Coherent Multidimensional Spectroscopy", Applied Spectroscopy **70**, 1937–1951 (2016).

[105]P. W. Anderson, "Ground state of a magnetic impurity in a metal", Phys. Rev. **164**, 352–359 (1967).

[106]W. K. Wootters, "Entanglement of formation of an arbitrary state of two qubits", Phys. Rev. Lett. **80**, 2245–2248 (1998).